

# Anatomy of New Physics in $B-\bar{B}$ mixing

A. Lenz<sup>a,b</sup>, U. Nierste<sup>c</sup>

and

J. Charles<sup>d</sup>, S. Descotes-Genon<sup>e</sup>, A. Jantsch<sup>f</sup>, C. Kaufhold<sup>g</sup>, H. Lacker<sup>h</sup>,  
S. Monteil<sup>i</sup>, V. Niess<sup>i</sup>

[CKMfitter Group]

<sup>a</sup>*Institut für Physik, Technische Universität Dortmund, D-44221 Dortmund, Germany*

<sup>b</sup>*Institut für Theoretische Physik, Universität Regensburg, D-93949 Regensburg, Germany, e-mail: Alexander.Lenz@physik.uni-regensburg.de*

<sup>c</sup>*Institut für Theoretische Teilchenphysik, Universität Karlsruhe, Karlsruhe Institute of Technology, D-76128 Karlsruhe, Germany, e-mail: nierste@particle.uni-karlsruhe.de*

<sup>d</sup>*Centre de Physique Théorique, Campus de Luminy, Case 907, F-13288 Marseille Cedex 9, France (UMR 6207 du CNRS associée aux Universités d'Aix-Marseille I et II et Université du Sud Toulon-Var; laboratoire affilié à la FRUMAM-FR2291), e-mail: charles@cpt.univ-mrs.fr*

<sup>e</sup>*Laboratoire de Physique Théorique d'Orsay, UMR8627, CNRS/Univ. Paris-Sud 11, 91405 Orsay Cedex, France, email: sebastien.descotes-genon@th.u-psud.fr*

<sup>f</sup>*Max-Planck-Institut für Physik (Werner-Heisenberg-Institut), Föhringer Ring 6, 80805 München, Germany, e-mail: jantsch@mppmu.mpg.de*

<sup>g</sup>*Laboratoire d'Annecy-Le-Vieux de Physique des Particules, 9 Chemin de Bellevue, BP 110, F-74941 Annecy-le-Vieux Cedex, France (UMR 5814 du CNRS-IN2P3 associée à l'Université de Savoie), e-mail: kaufhold@lapp.in2p3.fr*

<sup>h</sup>*Humboldt-Universität zu Berlin, Institut für Physik, Newtonstr. 15, D-12489 Berlin, Germany, e-mail: lacker@physik.hu-berlin.de*

<sup>i</sup>*Laboratoire de Physique Corpusculaire de Clermont-Ferrand, Université Blaise Pascal, 24 Avenue des Landais F-63177 Aubiere Cedex, (UMR 6533 du CNRS-IN2P3 associée à l'Université Blaise Pascal), e-mail: monteil@clermont.in2p3.fr, niess@clermont.in2p3.fr*

# Abstract

We analyse three different New Physics scenarios for  $\Delta F = 2$  flavour-changing neutral currents in the quark sector in the light of recent data on neutral-meson mixing. We parametrise generic New Physics contributions to  $B_q - \bar{B}_q$  mixing,  $q = d, s$ , in terms of one complex quantity  $\Delta_q$ , while three parameters  $\Delta_K^{tt}$ ,  $\Delta_K^{ct}$  and  $\Delta_K^{cc}$  are needed to describe  $K - \bar{K}$  mixing. In Scenario I, we consider uncorrelated New Physics contributions in the  $B_d$ ,  $B_s$ , and  $K$  sectors. In this scenario, it is only possible to constrain the parameters  $\Delta_d$  and  $\Delta_s$  whereas there are no non-trivial constraints on the kaon parameters. In Scenario II, we study the case of Minimal Flavour Violation (MFV) and small bottom Yukawa coupling, where  $\Delta \equiv \Delta_d = \Delta_s = \Delta_K^{tt}$ . We show that  $\Delta$  must then be real, so that no new CP phases can be accommodated, and express the remaining parameters  $\Delta_K^{cc}$  and  $\Delta_K^{ct}$  in terms of  $\Delta$  in this scenario. Scenario III is the generic MFV case with large bottom Yukawa couplings. In this case, the Kaon sector is uncorrelated to the  $B_d$  and  $B_s$  sectors. As in the second scenario one has  $\Delta_d = \Delta_s \equiv \Delta$ , however, now with a complex parameter  $\Delta$ . Our quantitative analyses consist of global CKM fits within the Rfit frequentist statistical approach, determining the Standard Model parameters and the new physics parameters of the studied scenarios simultaneously. We find that the recent measurements indicating discrepancies with the Standard Model are well accommodated in Scenarios I and III with new mixing phases, with a slight preference for Scenario I that permits different new CP phases in the  $B_d$  and  $B_s$  systems. Within our statistical framework, we find that the Standard-Model hypothesis  $\Delta_d = \Delta_s = 1$  is disfavoured with p-values of  $3.4\sigma$  and  $3.1\sigma$  in Scenarios I and III respectively.

# Contents

|          |   |           |
|----------|---|-----------|
| <b>1</b> | <b>Introduction</b>   | <b>4</b>  |
| <b>2</b> | <b>Setting the scene</b>  | <b>6</b>  |
| 2.1      | $B - \bar{B}$ mixing basics . . . . .   | 6         |
| 2.2      | $K - \bar{K}$ mixing basics . . . . .   | 9         |
| 2.3      | Master formulae . . . . .   | 12        |
| 2.4      | Three scenarios . . . . .   | 14        |
| 2.4.1    | Scenario I: Non-MFV . . . . .   | 15        |
| 2.4.2    | Scenario II: MFV with small bottom Yukawa coupling . . . . .                            | 15        |
| 2.4.3    | Scenario III: MFV with a large bottom Yukawa coupling . . . . .                         | 19        |
| 2.4.4    | Testing the Standard Model . . . . .  | 20        |
| <b>3</b> | <b>Inputs</b>   | <b>20</b> |
| 3.1      | Hadronic parameters and method of averaging . . . . .                                   | 20        |
| 3.2      | Observables not affected by New Physics in mixing . . . . .                             | 21        |
| 3.3      | Observables in the $B_d - \bar{B}_d$ system affected by New Physics in mixing . . . . . | 26        |
| 3.4      | Observables in the $B_s - \bar{B}_s$ system affected by New Physics in mixing . . . . . | 29        |
| 3.5      | The neutral kaon system . . . . .   | 33        |
| <b>4</b> | <b>Quantitative Studies</b>   | <b>35</b> |
| 4.1      | Standard Model fit . . . . .  | 35        |
| 4.2      | Scenario I . . . . .  | 41        |
| 4.3      | Scenario II . . . . .   | 50        |
| 4.4      | Scenario III . . . . .  | 53        |
| <b>5</b> | <b>Conclusions</b>  | <b>57</b> |
| <b>A</b> | <b>Relationship between <math>\epsilon_K</math> and <math>K - \bar{K}</math> mixing</b> | <b>59</b> |
| A.1      | Corrections to the usual $\epsilon_K$ formula . . . . .                                 | 59        |
| A.2      | Error budget for $\epsilon_K$ . . . . .   | 61        |

# 1 Introduction

Considerations of the stability of the electroweak scale lead to the general belief that there is new physics with particle masses below 1 TeV. While the high- $p_T$  experiments at the LHC should produce these new particles directly, one can study their dynamics also indirectly, through their impact on precision measurements at lower energies. To this end flavour-changing neutral current (FCNC) processes are extremely useful. On one hand they are highly suppressed in the Standard Model and are therefore very sensitive to new physics. On the other hand FCNC processes of  $K$ ,  $B_d$  and  $B_s$  mesons are still large enough to be studied with high statistics in dedicated experiments. Here meson–antimeson mixing plays an outstanding role. First, meson–antimeson oscillations occur at time scales which are sufficiently close to the meson lifetimes to permit their experimental investigation. Second, the Standard Model contribution to meson–antimeson mixing is loop-suppressed and comes with two or more small elements of the Cabibbo-Kobayashi-Maskawa (CKM) matrix [1]. Third, the decays of oscillating mesons give access to many mixing-induced  $CP$  asymmetries through the time-dependent study of decays into  $CP$ -eigenstates, which in some cases one can relate to the parameters of the underlying theory with negligible hadronic uncertainties.

The  $B$ -factories have revealed that the dominant  $b \rightarrow d$  and  $b \rightarrow u$  transitions fit into the pattern of the CKM mechanism and are in agreement with the information on  $s \rightarrow d$  transitions gained in more than forty years of kaon physics. The success of the CKM picture is evident from the many different measurements combining into a consistent and precise determination of the apex  $(\bar{\rho}, \bar{\eta})$  of the  $B$ -meson unitarity triangle (in terms of the Wolfenstein parameterization of the CKM matrix [2, 3]). As a consequence, any contribution from the expected new TeV-scale physics to the measured flavour-changing processes must be suppressed compared to the established CKM mechanism.

Models with only CKM-like flavour violation are said to respect the principle of *minimal flavour violation* (MFV) [4]. The overall picture of experimental data does not require sizable corrections to MFV. Still it is difficult to probe the CKM picture with a better accuracy than, say, 30%, because most quantities entering the global fit of the unitarity triangle suffer from sizable hadronic uncertainties. It should also be stressed that the accuracy of the determination of the CKM parameters decreases notably when one assumes that one or several crucial input(s) could be affected by New Physics contributions. Interestingly, several authors have detected possible hints of new physics in the data. For example it has been argued in the literature that one starts to see a discrepancy between the measurement of  $\sin 2\beta$  and the region preferred by  $|V_{ub}|$  from semileptonic decays on one hand, and  $|\varepsilon_K|$  on the other hand [5, 6]. Also the recently improved measurement of the  $B \rightarrow \tau\nu$  branching ratio deviates from its indirect CKM fit prediction [7]. In addition there are anomalies in the data on  $b \rightarrow s$  transitions. The latter processes do not involve  $\bar{\rho}$  and  $\bar{\eta}$  (to a good accuracy) and therefore directly probe the CKM mechanism. An ongoing debate addresses an extra contribution to  $b \rightarrow s\bar{q}q$ ,  $q = u, d, s$ , decay amplitudes with a  $CP$  phase different from  $\arg(V_{ts}^*V_{tb})$  that can alleviate the pattern of shifts between the measured  $CP$  asymmetries in these  $b \rightarrow s$  penguin modes and the Standard Model predictions (see e.g. [8]).

However, the first place to look for new physics in  $b \rightarrow s$  transitions is  $B_s - \bar{B}_s$  mixing,

where new physics can be parameterised in terms of just two parameters in a model-independent way, as we will discuss in great detail below. A combined analysis of several observables has pointed at the end of 2006 at the possibility of a new-physics contribution with a  $CP$  phase different from that of the Standard-Model box diagram [9]. Models of supersymmetric grand unification can naturally accommodate new contributions to  $b \rightarrow s$  transitions [10]: right-handed quarks reside in the same quintuplets of  $SU(5)$  as left-handed neutrinos, so that the large atmospheric neutrino mixing angle could well affect squark-gluino mediated  $b \rightarrow s$  transitions. At the same time the GUT models of Refs. [10] do not induce too dangerous contributions to the well-measured rare decay  $B \rightarrow X_s \gamma$ .  $B_s - \bar{B}_s$  mixing has been further investigated in other supersymmetric scenarios with [11] and without [12, 13] GUT boundary conditions, in unparticle physics scenarios in Ref. [14], in multi-Higgs-doublet models [15], in models with extra gauge bosons  $Z'$  [16], warped extra dimensions [17], left-right symmetry [18], anomalous  $tWb$ -couplings [19], additional quark families [20] or an additional singlet quark [21], and in a little-Higgs model [23]. On the experimental side, the understanding of  $b \rightarrow s$  transitions has made a tremendous progress in the past years. The Tevatron experiments have discovered and precisely quantified  $B_s - \bar{B}_s$  mixing oscillations [24, 25] whose frequency is in good agreement with the SM prediction, and presented first determinations of the associated  $CP$ -violating phase from tagged analyses of  $B_s \rightarrow J/\psi \phi$  decays [26–30]. Recently, possible new physics in the  $CP$  phase of the  $B_s - \bar{B}_s$  mixing amplitude has received new attention: The DØ collaboration has reported a measurement of the dimuon charge asymmetry which disagrees with the SM prediction by 3.2 standard deviations [31]. The  $CP$  asymmetry in semileptonic or, more generally, any flavour-specific decays, involves the  $B_s - \bar{B}_s$  mixing phase just as  $B_s \rightarrow J/\psi \phi$ , so that both pieces of experimental information can be combined to constrain this phase. The new measurement of the dimuon charge asymmetry has already triggered considerable theoretical interest. Besides predictions for the  $CP$  phase of  $B_s - \bar{B}_s$  mixing in specific models, as quoted above, also model-independent analyses of new physics effects have appeared [32]. Due to the large size of the dimuon asymmetry it was also investigated whether sizeable new physics contributions to the decay of  $B_s$  mesons are possible. This alternative is however strongly constrained by the lifetime ratios of  $B$ -mesons (see e.g. [33]) as well as the semileptonic branching ratios and the the average number of charm quarks per  $b$ -decays (see e.g. [34]).

In this paper we analyse generic scenarios of New Physics which are compatible (at different levels) with the experimental picture sketched above. We set up our notation and define our theoretical framework in Sect. 2, the relevant updated experimental and theoretical inputs to our global analysis are presented in Sect. 3. In Sect. 4.1 we first present the current status of the Standard Model fit. In Sect. 4.2 we perform a fit in which we allow for New Physics in the  $B_d - \bar{B}_d$  mixing and the  $B_s - \bar{B}_s$  mixing system and we project the results onto the New Physics parameters that describe the  $B_d - \bar{B}_d$  mixing and the  $B_s - \bar{B}_s$  mixing system. Sects. 4.3 and 4.4 are dedicated to two MFV scenarios with correlated effects in all meson–antimeson mixing amplitudes. Finally we conclude and list a few perspectives for the close future.

## 2 Setting the scene

### 2.1 $B - \bar{B}$ mixing basics

$B_q - \bar{B}_q$  oscillations (with  $q = d$  or  $q = s$ ) are described by a Schrödinger equation:

$$i \frac{d}{dt} \begin{pmatrix} |B_q(t)\rangle \\ |\bar{B}_q(t)\rangle \end{pmatrix} = \left( M^q - \frac{i}{2} \Gamma^q \right) \begin{pmatrix} |B_q(t)\rangle \\ |\bar{B}_q(t)\rangle \end{pmatrix} \quad (1)$$

with the mass matrix  $M^q = M^{q\dagger}$  and the decay matrix  $\Gamma^q = \Gamma^{q\dagger}$ . The physical eigenstates  $|B_H^q\rangle$  and  $|B_L^q\rangle$  with masses  $M_H^q$ ,  $M_L^q$  and decay rates  $\Gamma_H^q$ ,  $\Gamma_L^q$  are obtained by diagonalizing  $M^q - i\Gamma^q/2$ . The  $B_q - \bar{B}_q$  oscillations in Eq. (1) involve the three physical quantities  $|M_{12}^q|$ ,  $|\Gamma_{12}^q|$  and the  $CP$  phase

$$\phi_q = \arg(-M_{12}^q/\Gamma_{12}^q). \quad (2)$$

We denote the average  $B_q$  mass and width by  $M_{B_q}$  and  $\Gamma_{B_q}$ , respectively. The mass and width differences between  $B_L^q$  and  $B_H^q$  are related to them as

$$\Delta M_q = M_H^q - M_L^q = 2|M_{12}^q|, \quad \Delta \Gamma_q = \Gamma_L^q - \Gamma_H^q = 2|\Gamma_{12}^q| \cos \phi_q, \quad (3)$$

up to numerically irrelevant corrections of order  $m_b^2/M_W^2$ .  $\Delta M_q$  simply equals the frequency of the  $B_q - \bar{B}_q$  oscillations (for details see e.g. [35]). A third quantity probing mixing is

$$a_{\text{fs}}^q = 2 \left( 1 - \left| \frac{q}{p} \right| \right) = \text{Im} \frac{\Gamma_{12}^q}{M_{12}^q} = \frac{|\Gamma_{12}^q|}{|M_{12}^q|} \sin \phi_q = \frac{\Delta \Gamma_q}{\Delta M_q} \tan \phi_q. \quad (4)$$

$a_{\text{fs}}^q$  is the  $CP$  asymmetry in *flavour-specific*  $B_q \rightarrow f$  decays, i.e., the decays  $\bar{B}_q \rightarrow f$  and  $B_q \rightarrow \bar{f}$  are forbidden. The standard way to measure  $a_{\text{fs}}^q$  uses  $B_q \rightarrow X \ell^+ \nu_\ell$  decays, which explains the common name *semileptonic CP asymmetry* for  $a_{\text{fs}}^q$  (for more details see e.g. [36]). Further

$$\frac{q}{p} = -\sqrt{\frac{2M_{12}^* - i\Gamma_{12}^*}{2M_{12} - i\Gamma_{12}}}. \quad (5)$$

Let us now discuss our theoretical understanding of the off-diagonal terms of the evolution matrix, which are responsible for  $B_q - \bar{B}_q$  mixing. The dispersive term  $M_{12}^q$  is completely dominated by box diagrams involving virtual top quarks, and it is related to the effective  $|\Delta B| = 2$  hamiltonian  $H_q^{|\Delta B|=2}$  as

$$M_{12}^q = \frac{\langle B_q | H_q^{|\Delta B|=2} | \bar{B}_q \rangle}{2M_{B_q}}. \quad (6)$$

The Standard Model expression for  $H_q^{|\Delta B|=2}$  is [37]

$$H_q^{|\Delta B|=2} = (V_{tq}^* V_{tb})^2 C Q + \text{h.c.} \quad (7)$$

with the four-quark operator

$$Q = \bar{q}_L \gamma_\mu b_L \bar{q}_L \gamma^\mu b_L, \quad (8)$$

$$q_L = \frac{1}{2} (1 - \gamma_5) q \quad (9)$$

and the Wilson coefficient  $C$ , which depends on the heavy mass scales of the theory. In a wider class of models  $H_q^{|\Delta B|=2}$  maintains the form of Eq. (7) (meaning that there is no other operator than  $Q$  involved), but with a value of  $C$  different from the value in the SM:

$$C^{\text{SM}} = \frac{G_F^2}{4\pi^2} M_W^2 \hat{\eta}_B S \left( \frac{\bar{m}_t^2}{M_W^2} \right). \quad (10)$$

Here  $\bar{m}_t$  is the top quark mass defined in the  $\overline{\text{MS}}$  scheme, related to the pole mass  $m_t^{\text{pole}}$  determined at the Tevatron as  $\bar{m}_t(\bar{m}_t) = 0.957 m_t^{\text{pole}}$  (at next-to-leading order of QCD). The Inami-Lim function  $S$  [38] is calculated from the box diagram with two internal top quarks and evaluates to  $S(\bar{m}_t^2/M_W^2) = 2.35$  for the central value of  $\bar{m}_t$  listed in Tab. 7. QCD corrections are comprised in [39, 40]

$$\hat{\eta}_B = 0.8393 \pm 0.0034. \quad (11)$$

The hadronic matrix element involved is usually parameterised as

$$\langle B_q | Q(\mu_B) | \bar{B}_q \rangle = \frac{2}{3} M_{B_q}^2 f_{B_q}^2 \mathcal{B}_{B_q}(\mu_B), \quad (12)$$

with the decay constant  $f_{B_q}$  and the ‘bag’ factor  $\mathcal{B}_{B_q}$ . The product  $\hat{\eta}_B \mathcal{B}_{B_q}$  is scale and scheme invariant. Our convention in Eq. (11) corresponds to a scale dependent bag parameter with  $\mathcal{B}_{B_q} = 1$  in vacuum insertion approximation. Typical values for the bag parameter obtained on the lattice are e.g.  $\mathcal{B}_{B_s} \approx 0.81$ , see Sec. 3.1. Sometimes a different normalisation with a scale independent bag parameter  $\hat{\mathcal{B}}_{B_q} = b_B(\mu_B) \mathcal{B}_{B_q}(\mu_B)$  is used. The corresponding quantities  $\eta_B = \hat{\eta}_B(\mu_B)/b_B(\mu_B) = 0.551$  and  $\hat{\mathcal{B}}_{B_s} \approx 1.23$  satisfy obviously  $\eta_B \hat{\mathcal{B}}_{B_s} = \hat{\eta}_B \mathcal{B}_{B_s}$ . The analytic formula for  $b_B(\mu_B)$  can be found e.g. in Eq. (XIII.5) of [41].

The absorptive term  $\Gamma_{12}^q$  is dominated by on-shell charmed intermediate states, and it can be expressed as a two-point correlator of the  $|\Delta B| = 1$  Hamiltonian  $H_q^{|\Delta B|=1}$ . By performing a  $1/m_b$ -expansion of this two-point correlator, one can express  $\Gamma_{12}^q$  in terms of  $Q$  and another four-quark operator

$$\tilde{Q}_S = \bar{q}_L^\alpha b_R^\beta \bar{q}_L^\beta b_R^\alpha, \quad (13)$$

where  $S$  stands for ‘‘scalar’’ and  $\alpha, \beta = 1, 2, 3$  are colour indices, see [9]. The matrix element is expressed as

$$\langle B_q | \tilde{Q}_S | \bar{B}_q \rangle = \frac{1}{12} M_{B_q}^2 f_{B_q}^2 \tilde{\mathcal{B}}_{S, B_q} \left( \frac{M_{B_q}}{\bar{m}_b + \bar{m}_q} \right)^2 =: \frac{1}{12} M_{B_q}^2 f_{B_q}^2 \tilde{\mathcal{B}}'_{S, B_q}. \quad (14)$$

The prediction of  $\Gamma_{12}^q$  involves also operators which are subleading in the heavy quark expansion, the matrix elements of which are parameterised by the ‘bag’ factors  $\mathcal{B}_{R, B_q}$  [9].

Finally, we discuss the relative phase  $\phi_q$  between the two off-diagonal terms. In contrast to  $M_{12}^q$ ,  $\Gamma_{12}^q$  receives non-negligible contributions from subleading  $u$  and  $c$  CKM couplings, which implies that  $\phi_q$  is not a pure CKM phase in the Standard Model. The Standard Model contribution to  $\phi_q$  reads [9, 42], with our updated inputs (see Table 9)

$$\begin{aligned}\phi_d^{\text{SM}} &= (-9.6_{-5.8}^{+4.4}) \cdot 10^{-2}, \\ \phi_s^{\text{SM}} &= (+4.7_{-3.1}^{+3.5}) \cdot 10^{-3},\end{aligned}\tag{15}$$

and thus in  $\phi_s$  the SM contribution is clearly subleading in the presence of generic New Physics effects.

The previous quantities are expected to be affected by New Physics in different ways. While  $M_{12}^q$  coming from box diagrams is very sensitive to new physics both for  $B_d$  and  $B_s$ ,  $\Gamma_{12}^s$  stems from Cabibbo-favoured tree-level decays and possible new physics effects are expected to be smaller than the hadronic uncertainties. In the case of  $\Gamma_{12}^d$  though, the contributing decays are Cabibbo-suppressed. In this paper we only consider scenarios where New Physics does not enter tree-level decays. More specifically, we assume that  $B$  decays proceeding through a four-flavour change (*i.e.*,  $b \rightarrow q_1 \bar{q}_2 q_3$ ,  $q_1 \neq q_2 \neq q_3$ ) obtain only SM contributions (*SM4FC*) [43, 44]. This assumption is better defined than just the neglect of NP contributions to tree-mediated decays since on the non-perturbative level tree and penguin amplitudes can not be well separated. Our class of four-flavour-change decays includes  $b \rightarrow d$  decays in which the strong isospin changes by 3/2 units, *i.e.* we use strong isospin as the flavour quantum number of the first quark generation. Then the following inputs used in the fit are considered to be free from NP contributions in their extraction from data:  $|V_{ud}|$ ,  $|V_{us}|$ ,  $|V_{ub}|$ ,  $|V_{cb}|$  and  $\gamma$ . Also the leptonic decays  $B \rightarrow \tau\nu$  (or  $D_s \rightarrow \tau\nu$  and  $D_s \rightarrow \mu\nu$ ), which could be significantly affected by charged Higgs exchange contributions, are assumed to be SM-like. Using these inputs a reference unitarity triangle can be constructed [45], as will be discussed further in Sec. 3.2.

In addition, in order to take advantage of the measurement of the width differences  $\Delta\Gamma_q$ , and of the time-dependent CP-asymmetries in dominant  $b \rightarrow c$  decays, we neglect possible non standard contributions to the  $b \rightarrow c\bar{c}q$  ( $q = d, s$ ) transitions, although they do not strictly enter the SM4FC family. Finally, we assume that the unitarity of the  $3 \times 3$ -CKM matrix still holds in the presence of NP, which ensures that the SM contribution to the neutral meson mixing keeps its usual expression as a function of  $(\bar{\rho}, \bar{\eta})$  and other parameters. Hence, our discussion would not hold in the case of an additional sequential fourth fermion family, which however is not excluded yet by experimental constraints (see Refs. [20] or [46] and references therein).

Thus, New Physics can find its way into the quantities studied in this paper only by changing magnitude and/or phase of  $M_{12}^q$ . It is convenient to define the NP complex parameters  $\Delta_q$  and  $\phi_q^\Delta$  ( $q = d, s$ ) through

$$M_{12}^q \equiv M_{12}^{\text{SM},q} \cdot \Delta_q, \quad \Delta_q \equiv |\Delta_q| e^{i\phi_q^\Delta},\tag{16}$$

see e.g. [9]. With the definition in Eq. (16) the *CP* phase of Eq. (2) reads

$$\phi_q = \phi_q^{\text{SM}} + \phi_q^\Delta.\tag{17}$$

As discussed in Sec. 3, New Physics in  $M_{12}^q$  will not only affect the neutral-meson mixing parameters, but also the time-dependent analyses of decays corresponding to an interference between mixing and decay.

The relation of  $\Delta_q$  to the parameters used e.g. in [47–49] is  $|\Delta_q| = r_q^2$ ,  $\phi_q^\Delta = 2\theta_q$ , and the Standard Model is of course located at  $\Delta_q = 1$ . It is more transparent to look at the cartesian  $\text{Im } \Delta_q$  vs.  $\text{Re } \Delta_q$  plot than the polar  $2\theta_q$  vs.  $r_q^2$  one, because it visualizes the New Physics contribution more clearly and it allows a simple geometrical interpretation of the shape of each individual constraint. For completeness, we note that some authors (e.g. [50–52], see also [43]) prefer to split the SM contribution from the pure NP one in a polar parametrization. The two NP parameters  $h_q$  and  $2\sigma_q$  introduced in this way are defined by

$$\frac{M_{12}^q}{M_{12}^{\text{SM},q}} = 1 + \frac{M_{12}^{\text{NP},q}}{M_{12}^{\text{SM},q}} = \Delta_q = 1 + h_q e^{i2\sigma_q}. \quad (18)$$

We will study the case of the neutral kaon system in the following section, defining analogous parameters  $\Delta_K^{tt}$ ,  $\Delta_K^{ct}$  and  $\Delta_K^{cc}$ . But in this paper, we will not consider the neutral  $D$  meson system. Indeed, in the scenarios we consider here  $D - \bar{D}$  mixing is severely GIM-suppressed and gives no useful constraint, as is already the case within the Standard Model, see e.g. [53].

## 2.2 $K - \bar{K}$ mixing basics

The effective  $|\Delta S| = 2$  hamiltonian describing  $K - \bar{K}$  mixing resembles the  $|\Delta B| = 2$  hamiltonian of Eq. (7), with the important distinction that now also contributions from internal charm quarks are important:

$$H^{|\Delta S|=2} = [(V_{ts}V_{td}^*)^2 C_{tt} + 2V_{ts}V_{td}^*V_{cs}V_{cd}^* C_{ct} + (V_{cs}V_{cd}^*)^2 C_{cc}] Q + h.c. \quad (19)$$

with the operator  $Q = \bar{d}_L \gamma_\mu s_L \bar{d}_L \gamma^\mu s_L$ . As to the case of the  $B_d$  and  $B_s$  mesons, the contribution from  $H^{|\Delta S|=2}$  to  $M_{12}^K$  is found from Eq. (6). A new feature is an additive poorly calculable long-distance contribution involving  $H^{|\Delta S|=1}$  (see e.g. [35, 54]). The Wilson coefficients  $C_{ij}$ ,  $i, j = c, t$ , and the operator  $Q$  depend on the renormalisation scale  $\mu_K$  at which we evaluate these coefficients and the hadronic matrix element  $\langle K|Q|\bar{K} \rangle$ . We parameterise the hadronic matrix element

$$\langle K|Q(\mu_K)|\bar{K} \rangle = \frac{2}{3} m_K^2 f_K^2 \frac{\hat{\mathcal{B}}_K}{b_K(\mu_K)}. \quad (20)$$

Here  $f_K \simeq 156$  MeV and  $m_K$  are the decay constant and mass of the Kaon, respectively, and  $\hat{\mathcal{B}}_K$  is the bag parameter, from which a factor  $b_K(\mu_K)$  is stripped off. Analog to the case of  $B$  mixing  $b_K(\mu_K)$  contains the dependence of  $\langle K|Q(\mu_K)|\bar{K} \rangle$  on the renormalisation

---

\*We use the same notation for operators in the  $B$  and  $K$  systems (cf. Eq. (8)), implying the corresponding flavours ( $b$ ,  $s$  or  $d$ ) of the quark fields.

scheme and the renormalisation scale  $\mu_K$ . The SM values of the Wilson coefficients are

$$\begin{aligned} C_{tt}^{\text{SM}} &= \frac{G_F^2}{4\pi^2} M_W^2 S\left(\frac{\overline{m}_t^2}{M_W^2}\right) \eta_{tt} b_K(\mu_K), \\ C_{ct}^{\text{SM}} &= \frac{G_F^2}{4\pi^2} M_W^2 S\left(\frac{\overline{m}_c^2}{M_W^2}, \frac{\overline{m}_t^2}{M_W^2}\right) \eta_{ct} b_K(\mu_K), \\ C_{cc}^{\text{SM}} &= \frac{G_F^2}{4\pi^2} M_W^2 S\left(\frac{\overline{m}_c^2}{M_W^2}\right) \eta_{cc} b_K(\mu_K), \end{aligned} \quad (21)$$

with the Inami-Lim functions  $S$  calculated from the usual box diagrams. By comparing Eqs. (10) and (21) we verify the MFV feature of the Standard Model  $C^{\text{SM}} = C_{tt}^{\text{SM}}$ . In  $C_{cc}^{\text{SM}}$  the Inami-Lim function can be expanded in terms of the tiny quantity  $\overline{m}_c^2/M_W^2$  to find  $S(x_c) = x_c + O(x_c^2)$ . Likewise  $S(x_c, x_t) \simeq -x_c \log x_c + x_c F(x_t)$  with  $F(\overline{m}_t^2/M_W^2) = 0.56$ . From Eqs. (20) and (21),  $b_K(\mu_K)$  drops out if  $\langle K|H^{|\Delta S|=2}|\overline{K}\rangle$  is expressed in terms of  $\widehat{\mathcal{B}}_K$ . The QCD correction factors  $\eta_{cc}$  [55],  $\eta_{ct}$  [56] and  $\eta_{tt}$  [39] are listed in Tab. 7. The dominant sources of error in these quantities are higher-order QCD corrections<sup>†</sup> ( $\eta_{cc}$  also depends on  $\alpha_s$  and  $\overline{m}_c$  in a sizable way). The latter dependence is made explicit in Tab. 7.

In analogy to Eq. (16) we introduce complex parameters for new physics in the three different contributions and write

$$\begin{aligned} M_{12}^K &\equiv \frac{\langle K|H^{|\Delta S|=2}|\overline{K}\rangle}{2M_K} = (V_{ts}V_{td}^*)^2 M_{12}^{tt} + 2V_{ts}V_{td}^*V_{cs}V_{cd}^* M_{12}^{ct} + (V_{cs}V_{cd}^*)^2 M_{12}^{cc} \\ M_{12}^{ij} &= M_{12}^{\text{SM},ij} \Delta_K^{ij} \equiv M_{12}^{\text{SM},ij} |\Delta_K^{ij}| e^{i\phi_K^{ij}}. \end{aligned} \quad (22)$$

The physical quantities associated with  $K - \overline{K}$  mixing are the  $K_L - K_S$  mass difference  $\Delta M_K = M_{K_L} - M_{K_S}$  and the  $CP$ -violating quantity  $\epsilon_K$ .  $CP$  violation in  $H^{|\Delta S|=1}$  is characterised by  $\epsilon'_K$ . These quantities are defined as

$$\epsilon_K = \frac{\eta_{00} + 2\eta_{+-}}{3}, \quad \epsilon'_K = \frac{-\eta_{00} + \eta_{+-}}{3} \quad \text{with} \quad \eta_{ab} \equiv \frac{\mathcal{A}(K_L \rightarrow \pi^a \pi^b)}{\mathcal{A}(K_S \rightarrow \pi^a \pi^b)}. \quad (23)$$

Since these two quantities are defined in terms of  $K_L$  and  $K_S$ , they can be expressed in terms of  $K - \overline{K}$  mixing parameters and the isospin decay amplitudes  $A(K_0 \rightarrow (\pi\pi)_I) = A_I e^{i\delta_I} = a_I e^{i\theta_i} e^{i\delta_I}$ , where  $a_I$ ,  $\delta_I$  and  $\theta_I$  denote the modulus, the “strong” (CP-even) phase and the “weak” (CP-odd) phase of the decay amplitude [35, 58, 59].  $\epsilon_K$  is essentially proportional to the CP phase  $\phi_K \equiv \arg(-M_{12}^K/\Gamma_{12}^K)$ . In view of the phenomenological “ $\Delta I = 1/2$  rule”  $a_0/a_2 \approx 22$  (and the fact that all other decay modes come with even smaller amplitudes than  $a_2$ ) one can saturate the inclusive quantity  $\Gamma_{12}^K$  completely by the contribution proportional to  $a_0^2$ . Expanding in various small parameters (see Ref. [35] for an elaborate discussion of the approximations involved) one finds:

$$\epsilon_K = \sin \phi_\epsilon e^{i\phi_\epsilon} \left[ \frac{\text{Im} M_{12}^K}{\Delta M_K} + \xi \right] \quad \text{with} \quad \tan \phi_\epsilon = \frac{2\Delta M_K}{\Delta \Gamma_K} \quad \text{and} \quad \xi = \frac{\text{Im} A_0}{\text{Re} A_0} \quad (24)$$

<sup>†</sup>Very recently a NNLO calculation of  $\eta_{ct}$  was performed [57], leading to a value, which is 5% larger than the value used here. This result is not yet included in our analysis.

The troublesome long-distance contribution to  $M_{12}^K$  mentioned after Eq. (19) is eliminated from Eq. (24) by trading  $2\text{Re}M_{12}^K$  for the experimental value of  $\Delta M_K$ . Long-distance contributions to  $\text{Im}M_{12}^K$  are negligible [60]. In Eq. (24)  $\xi$  comprises the contribution from  $\arg(-\Gamma_{12}^K)$  in the limit of  $A_0$  dominance discussed above. The corrections are of order  $(a_2/a_0)^2$  and therefore negligible. The usual expression for  $\epsilon_K$  is obtained from this expression by taking the following further approximations: i) use  $\phi_\epsilon = 45^\circ$  instead of the measured value  $\phi_\epsilon = 43.5(7)^\circ$ , ii) neglect  $\xi$  and iii) compute  $\text{Im}M_{12}$  using only the lowest-dimension  $d = 6$  operator in the effective Hamiltonian of Eq. (19), which is dominated by top and charm box diagrams. The effect of the three simplifications can be parameterised in terms of the parameter  $\kappa_\epsilon$  [6] entering

$$\begin{aligned} \epsilon_K &= \frac{\kappa_\epsilon}{\sqrt{2}} e^{i\phi_\epsilon} \left[ \frac{\text{Im}M_{12}^{(6)}}{\Delta M} \right] \\ &= C_\epsilon \kappa_\epsilon e^{i\phi_\epsilon} \hat{\mathcal{B}}_K \left[ \text{Im} [(V_{cs}V_{cd}^*)^2 \Delta_K^{cc}] \eta_{cc} S\left(\frac{\bar{m}_c^2}{M_W^2}\right) + \text{Im} [(V_{ts}V_{td}^*)^2 \Delta_K^{tt}] \eta_{tt} S\left(\frac{\bar{m}_t^2}{M_W^2}\right) \right. \\ &\quad \left. + 2 \text{Im} (V_{ts}V_{td}^*V_{cs}V_{cd}^* \Delta_K^{ct}) \eta_{ct} S\left(\frac{\bar{m}_c^2}{M_W^2}, \frac{\bar{m}_t^2}{M_W^2}\right) \right]. \end{aligned} \quad (25)$$

The value  $\kappa_\epsilon = 1$  corresponds to the approximations i)–iii) outlined above. The normalisation reads

$$C_\epsilon = \frac{G_F^2 F_K^2 m_K M_W^2}{12\sqrt{2}\pi^2 \Delta M_K}. \quad (27)$$

When expressed in terms of Wolfenstein parameters to lowest order in  $\lambda$ , Eq. (25) defines the familiar hyperbola in the  $\bar{\rho}-\bar{\eta}$  plane.

A series of papers [6, 35, 60, 61] has studied how much the factor  $\kappa_\epsilon$  should deviate from 1 in order to account for the terms neglected by the previous approximations. We recall the different elements in App. A, separating the uncertainties coming from statistic and systematic sources, and we obtain the estimate

$$\kappa_\epsilon = 0.940 \pm 0.013 \pm 0.023, \quad (28)$$

in good agreement with  $\kappa_\epsilon = 0.94 \pm 0.02$  in ref. [60]. We emphasize that the estimate of  $\kappa_\epsilon$  in Eq. (28) relies on the assumption that  $\epsilon'_K$  is unaffected by New Physics (which goes beyond the SM4FC assumption which protects only  $I = 2$  final states). From  $\epsilon_{K,exp} = (2.229 \pm 0.010) \cdot 10^{-3}$  we get the following value for the combination:

$$\epsilon_{K,exp}^{(0)} = \frac{\epsilon_{K,exp}}{\kappa_\epsilon} = (2.367 \pm 0.033 \pm 0.049) \cdot 10^{-3}. \quad (29)$$

In the presence of New Physics, the relationship between the measured  $\epsilon_K$  and the  $\Delta_K^{ij}$ 's is discussed after Eq. (38).

One can also study the semileptonic CP asymmetry

$$A_L \equiv \frac{\Gamma(K_{\text{long}} \rightarrow \ell^+ \nu \pi^-) - \Gamma(K_{\text{long}} \rightarrow \ell^- \bar{\nu} \pi^+)}{\Gamma(K_{\text{long}} \rightarrow \ell^+ \nu \pi^-) + \Gamma(K_{\text{long}} \rightarrow \ell^- \bar{\nu} \pi^+)} = \frac{1 - |q/p|^2}{1 + |q/p|^2},$$

which, however, contains the same information on fundamental parameters as  $\text{Re} \epsilon_K$ .

### 2.3 Master formulae

In this section we provide the master formulae of the theoretical predictions for the observables relevant to the analysis of new physics contributions in mixing. These formulae reflect the dependences on the most important parameters entering the fit and are obtained from the input values as described in Sec. 3. It should be stressed that these numerical equations are shown for illustrative purpose only: the complete formulae are used in the fitting code, which allow to take into account all the contributions computed so far together with the correct treatment of the correlations.

Combining Eqs. (3–12) with Eq. (16) one finds:

$$\begin{aligned}\Delta M_d &= 0.502 \text{ ps}^{-1} \left( \frac{|V_{tb}V_{td}|}{0.0086} \right)^2 \frac{S(\overline{m}_t^2/M_W^2)}{2.35} \frac{f_{B_d}^2 \mathcal{B}_{B_d}}{(0.17 \text{ GeV})^2} \cdot |\Delta_d|, \\ \Delta M_s &= 17.24 \text{ ps}^{-1} \cdot \left( \frac{|V_{tb}V_{ts}^*|}{0.04} \right)^2 \frac{S(\overline{m}_t^2/M_W^2)}{2.35} \frac{f_{B_s}^2 \mathcal{B}_{B_s}}{(0.21 \text{ GeV})^2} \cdot |\Delta_s|. \quad (30)\end{aligned}$$

The remaining uncertainties in the prefactors of the above formulae are due to the choice of the renormalization scale and the values of  $\alpha_s$  and the top quark mass. They are at most 3 % and therefore negligible compared to the theoretical error due to the non-perturbative and CKM parameters.

The derivation of the formulae involving  $\Gamma_{12}^q$  is more complicated [9, 42, 62]. For the  $B_s$  system the dependence on the apex  $(\bar{\rho}, \bar{\eta})$  of the unitarity triangle is strongly suppressed, in contrast to the  $B_d$  system. Furthermore the SM contribution to  $a_{\text{fs}}^s$  is tiny and remains below the present experimental sensitivity, while  $a_{\text{fs}}^d$  is one order of magnitude larger and therefore not completely negligible, see Table 9. Summing up logarithms of the form  $m_c^2/m_b^2 \ln m_c^2/m_b^2$  [63] and using the  $\overline{\text{MS}}$ -scheme for the  $b$  quark mass one finds from Ref. [9] for the decay rate differences:

$$\Delta\Gamma_d = \left( \frac{f_{B_d} \sqrt{\mathcal{B}_{B_d}}}{0.17 \text{ GeV}} \right)^2 \left[ 0.00241 + 0.00056 \frac{\tilde{\mathcal{B}}'_{S,B_d}}{\mathcal{B}_{B_d}} - 0.00047 \frac{\mathcal{B}_{R,B_d}}{\mathcal{B}_{B_d}} \right] \cos(\phi_d^{\text{SM}} + \phi_d^\Delta), \quad (31)$$

$$\Delta\Gamma_s = \left( \frac{f_{B_s} \sqrt{\mathcal{B}_{B_s}}}{0.21 \text{ GeV}} \right)^2 \left[ 0.0797 + 0.0278 \frac{\tilde{\mathcal{B}}'_{S,B_s}}{\mathcal{B}_{B_s}} - 0.0181 \frac{\mathcal{B}_{R,B_s}}{\mathcal{B}_{B_s}} \right] \cos(\phi_s^{\text{SM}} + \phi_s^\Delta). \quad (32)$$

Now the uncertainties in the coefficients are considerably larger than in the the case of the mass differences, but they are still less than about 15 %. The dominant theoretical error of the coefficients comes from the renormalization scale  $\mu_1$  followed by the CKM factors. One encounters matrix elements of higher-dimensional operators in these expressions, denoted by  $\mathcal{B}_R$ , which have a power suppression parametrised by  $m_b^{\text{pow}}$ . The general (assuming unitarity of the  $3 \times 3$  quark mixing matrix) expression for the semileptonic CP asymmetries reads

$$10^4 a_{\text{fs}}^q = \left[ a_q \text{Im} \left( \frac{\lambda_u^q}{\lambda_t^q} \right) + b_q \text{Im} \left( \frac{\lambda_u^q}{\lambda_t^q} \right)^2 \right] \frac{\sin(\phi_q^{\text{SM}} + \phi_q^\Delta)}{|\Delta_q|}, \quad (33)$$

with  $\lambda_x^q = V_{xb}V_{xq}^*$ . The coefficients  $a$ ,  $b$ ,  $c$  read [9, 42]:

$$\begin{aligned}
a_d &= 9.2905 + 0.2973 \frac{\tilde{\mathcal{B}}'_{S,B_d}}{\mathcal{B}_{B_d}} + 0.2830 \frac{\mathcal{B}_{R,B_d}}{\mathcal{B}_{B_d}}, \\
a_s &= 9.4432 + 0.2904 \frac{\tilde{\mathcal{B}}'_{S,B_s}}{\mathcal{B}_{B_s}} + 0.2650 \frac{\mathcal{B}_{R,B_s}}{\mathcal{B}_{B_s}}, \\
b_d &= 0.0720 + 0.0184 \frac{\tilde{\mathcal{B}}'_{S,B_d}}{\mathcal{B}_{B_d}} + 0.0408 \frac{\mathcal{B}_{R,B_d}}{\mathcal{B}_{B_d}}, \\
b_s &= 0.0732 + 0.0180 \frac{\tilde{\mathcal{B}}'_{S,B_s}}{\mathcal{B}_{B_s}} + 0.0395 \frac{\mathcal{B}_{R,B_s}}{\mathcal{B}_{B_s}}, \\
c_d &= -46.8169 - 17.0083 \frac{\tilde{\mathcal{B}}'_{S,B_s}}{\mathcal{B}_{B_s}} + 9.2818 \frac{\mathcal{B}_{R,B_s}}{\mathcal{B}_{B_s}},
\end{aligned} \tag{34}$$

again with uncertainties in the coefficients of less than 15 %. The dominant one comes from the renormalization scheme  $\mu_1$  followed by the CKM factors. For the semileptonic CP asymmetries in the  $B_d$  system we can also write [42]:

$$\begin{aligned}
-10^4 a_{\text{fs}}^d &= \left[ c_d + a_d \left( \frac{\cos \beta}{R_t} - 1 \right) + b_d \left( \frac{\cos 2\beta}{R_t^2} - 2 \frac{\cos \beta}{R_t} + 1 \right) \right] \frac{\sin \phi_d^\Delta}{|\Delta_d|} \\
&+ \left[ a_d \frac{\sin \beta}{R_t} + b_d \left( \frac{\sin 2\beta}{R_t^2} - 2 \frac{\sin \beta}{R_t} \right) \right] \frac{\cos \phi_d^\Delta}{|\Delta_d|},
\end{aligned} \tag{35}$$

where we have written the  $(\bar{\rho}, \bar{\eta})$  dependence in terms of the angle  $\beta$  of the unitarity triangle and the side  $R_t = \sqrt{(1 - \bar{\rho})^2 + \bar{\eta}^2}$ .

The mixing-induced  $CP$  asymmetries in  $B_d \rightarrow J/\psi K_S$  and  $B_s \rightarrow J/\psi \phi$  are very important to constrain  $\phi_d$  and  $\phi_s$ , respectively. For the latter mode an angular analysis is needed to separate the different  $CP$  components [64]. The mixing-induced  $CP$  asymmetries in the two modes determine

$$\sin(\phi_d^\Delta + 2\beta) \quad \text{and} \quad \sin(\phi_s^\Delta - 2\beta_s). \tag{36}$$

Here the angle  $\beta_s$  is defined as positive:

$$\beta_s = -\arg \left( -\frac{V_{ts}^* V_{tb}}{V_{cs}^* V_{cb}} \right) = 0.01811_{-0.00082}^{+0.00085}. \tag{37}$$

(This should be compared with  $\beta = \arg(-V_{td}^* V_{tb}/V_{cd}^* V_{cb}) \approx 0.38$ .)<sup>‡</sup>

<sup>‡</sup>It should be emphasized that the Tevatron experiments, which have presented first determinations of  $\sin(\phi_s^\Delta - 2\beta_s)$  from tagged analyses [26, 27], also use the notation  $\phi_s$  and  $\beta_s$ , but with a slightly different meaning. Comparing the notation of Ref. [26, 27] with our notation one gets

$$\begin{aligned}
\phi_s^{\text{D}\mathcal{O}} &= \phi_s^\Delta - 2\beta_s, \\
-2\beta_s^{\text{CDF}} &= \phi_s^\Delta - 2\beta_s.
\end{aligned}$$

Ref. [26, 27] has neglected  $2\beta_s$  in the relation between  $\Delta\Gamma_s$  and  $\phi_s$  in Eq. (3). This is justified in view of the large experimental errors and the smallness of  $2\beta_s$ .

The measured value  $|\epsilon_K^{\text{exp}}|$  implies the following relation among the CKM elements:

$$1.25 \cdot 10^{-7} = \hat{\mathcal{B}}_K \left[ \text{Im} [(V_{cs}V_{cd}^*)^2 \Delta_K^{cc}] \eta_{cc} S \left( \frac{\overline{m}_c^2}{M_W^2} \right) + \text{Im} [(V_{ts}V_{td}^*)^2 \Delta_K^{tt}] \eta_{tt} S \left( \frac{\overline{m}_t^2}{M_W^2} \right) + 2 \text{Im} (V_{ts}V_{td}^*V_{cs}V_{cd}^* \Delta_K^{ct}) \eta_{ct} S \left( \frac{\overline{m}_c^2}{M_W^2}, \frac{\overline{m}_t^2}{M_W^2} \right) \right]. \quad (38)$$

Here the number on the LHS originates from

$$1.25 \cdot 10^{-7} = \frac{12\sqrt{2}\pi^2 \Delta M_K |\epsilon_K^{\text{exp}}|}{G_F^2 f_K^2 m_K M_W^2 \kappa_\epsilon}, \quad (39)$$

The peculiar hierarchy of the CKM elements in Eq. (38) enhances the sensitivity to the imaginary part of  $\Delta_K^{cc}$ . Expanding to lowest non-vanishing order in the Wolfenstein parameter  $\lambda$  shows

$$\begin{aligned} \text{Im} [(V_{cs}V_{cd}^*)^2 \Delta_K^{cc}] &= -2A^2\lambda^6\overline{\eta} \text{Re} \Delta_K^{cc} + \lambda^2 \text{Im} \Delta_K^{cc}, \\ \text{Im} [(V_{ts}V_{td}^*)^2 \Delta_K^{tt}] &= 2A^4\lambda^{10}(1-\overline{\rho})\overline{\eta} \text{Re} \Delta_K^{tt} + A^4\lambda^{10} [(1-\overline{\rho})^2 - \overline{\eta}^2] \text{Im} \Delta_K^{tt}, \\ 2 \text{Im} (V_{ts}V_{td}^*V_{cs}V_{cd}^* \Delta_K^{ct}) &= 2A^2\lambda^6\overline{\eta} \text{Re} \Delta_K^{ct} + 2A^2\lambda^6(1-\overline{\rho}) \text{Im} \Delta_K^{ct}. \end{aligned} \quad (40)$$

$\Delta M_K$  is dominated by physics from low scales. The short-distance contribution is dominated by the charm-charm contribution involving the QCD coefficient  $\eta_{cc}$  [55]. There is an additional long-distance contribution from box diagrams with two internal up quarks, which cannot be calculated reliably. For instance, one could attribute an uncertainty of order 100% to the theory prediction of  $\Delta M_K$  and try to extract a constraint on  $|\Delta_K^{cc}|$  from  $\Delta M_K$ . While  $\Delta_K^{cc}$  is very sensitive to any kind of new physics which distinguishes between the first and second quark generations, we will see in Sect. 2.4 that in MFV scenarios all effects on  $\Delta_K^{cc}$  are totally negligible. In an unspecified non-MFV scenario both  $\epsilon_K$  and  $\Delta M_K$  are useless, because  $\Delta_K^{cc}$ ,  $\Delta_K^{ct}$  and  $\Delta_K^{tt}$  are uncorrelated with any other observable entering the global fit of the unitarity triangle, while in MFV scenarios  $\Delta M_K$  is Standard-Model-like. Therefore we do not consider  $\Delta M_K$  any further.

## 2.4 Three scenarios

After having introduced our parameterisation of new physics in terms of the  $\Delta$  parameters in Eqs. (16) and (38), we can now discuss the three different physics scenarios which we consider in this article. The common feature of all scenarios is the assumption that all relevant effects of new physics are captured by the  $\Delta$  parameters. As long as one only considers the quantities entering the global fit of the unitarity triangle in conjunction with the observables of  $B_s - \overline{B}_s$  mixing, this property is fulfilled in many realistic extensions of the Standard Model<sup>§</sup>. However, once a specific model is studied, often other quantities (unrelated to the global fit of the unitarity triangle) constrain the parameter space; prominent

<sup>§</sup>A notable exception are models with large couplings of a light charged-Higgs boson to down-type fermion. In such models  $\mathcal{B}(B \rightarrow \tau\nu_\tau)$ , which we assume to be Standard-Model-like, is modified. Another exception are models with a non unitary  $3 \times 3$  CKM matrix, *e.g.* with new fermion generations.

examples are branching ratios of rare decays such as  $\mathcal{B}(B \rightarrow X_s \gamma)$  and  $\mathcal{B}(B_s \rightarrow \mu^+ \mu^-)$ . Such effects cannot be included in a model-independent approach like ours. Still, we will see that interesting bounds on the  $\Delta$  parameters can be found within the broad classes of models defined by our three scenarios. In any specific model covered by our scenarios, the constraints on the  $\Delta$  parameters can only be stronger, but not weaker than those presented in this paper.

Two scenarios involve the MFV hypothesis. The notion of MFV means that all flavour-violation stems from the Yukawa sector. It is usually implied that all flavour-changing transitions in the quark sector are solely governed by the CKM matrix, while flavour-changing transitions in the lepton sector come with elements of the Pontecorvo–Maki–Nakagawa–Sakata (PMNS) matrix. Strictly speaking, this conclusion is only valid if MFV is invoked at or below the GUT scale. If MFV is built into a GUT model at a higher scale, it is well possible that imprints of the PMNS matrix can be found in FCNC processes of quarks. Indeed, the articles in Ref. [10] discuss supersymmetric GUT models with flavour-blind soft SUSY-breaking terms near the Planck scale. The renormalisation group evolution involving the large top Yukawa coupling then induces FCNC transitions between right-handed bottom and strange quarks at low energies. In our analysis this situation is a very special case of the scenario I discussed below.

#### 2.4.1 Scenario I: Non-MFV

In this scenario we do not assume anything about the flavour structure of the New Physics interaction. Since here  $\Delta_K^{cc}$ ,  $\Delta_K^{ct}$  and  $\Delta_K^{tt}$  are unrelated to other parameters, we can neither derive any constraints on these parameters nor use  $\epsilon_K$  in the global fit. While  $\Delta_d$  and  $\Delta_s$  are a-priori independent, the allowed ranges for these parameters are nevertheless correlated through the global fit and the unitarity constraints on the CKM matrix. This can be qualitatively understood as follows. Consider a value for  $|\Delta_s|$  which exhausts the range allowed by the hadronic uncertainties in  $\Delta M_s$ . The good theoretical control over the ratio  $\Delta M_d/\Delta M_s$  then fixes  $|V_{td}|^2 |\Delta_d|$  quite precisely. The global fit of the unitarity triangle further constrains  $|V_{td}| \propto \sqrt{(1 - \bar{\rho})^2 + \bar{\eta}^2}$ , so that a-posteriori the allowed ranges for  $|\Delta_d|$  and  $|\Delta_s|$  become correlated. Also the flavour-mixed CP-asymmetry  $a_{fs}$  measured at the TeVatron experiments correlates the parameters  $\Delta_d$  and  $\Delta_s$ .

#### 2.4.2 Scenario II: MFV with small bottom Yukawa coupling

We adopt the symmetry-based definition of MFV of Ref. [4] to discuss our two other scenarios. Ignoring the lepton sector here, the starting point is the  $[U(3)]^3$  flavour symmetry of the gauge sector of the Standard Model, which entails the flavour-blindness of this sector. The gauge part of the lagrangian is invariant under independent unitary rotations of the left-handed quark doublets  $Q_L^i$  (where  $i = 1, 2, 3$  labels the generation), and the right-handed quark singlets  $d_R^i$  and  $u_R^i$  in flavour space. In the Standard Model the  $[U(3)]^3$  flavour symmetry is broken by the Yukawa interactions. This symmetry breaking permits discriminating flavour quantum numbers, quark masses and flavour-changing transitions. Within the Standard Model only the top Yukawa coupling  $y_t$  is large, all other Yukawa couplings are small or even tiny. These small parameters pose a challenge to generic exten-

sions of the Standard Model. This challenge is met by the MFV hypothesis which extends the Standard Model assuming that the only sources of  $[U(3)]^3$  flavour symmetry breaking remain the Yukawa couplings. Specifying to the familiar basis of mass eigenstates, we list the following consequences of the MFV hypothesis:

- i) Any flavour-changing transition is governed by the same CKM elements as in the Standard Model.
- ii) Any chirality flip  $q_R \rightarrow q_L$  is proportional to the Yukawa coupling  $y_q$  (and, by hermiticity of the lagrangian, any  $q_L \rightarrow q_R$  flip is proportional to  $y_q^*$ ).
- iii) Any flavour-changing transition of a right-handed quark involves a factor of the corresponding Yukawa coupling.
- iv) FCNC transitions have the same pattern of GIM cancellations as in the SM.

For example, property i) and iii) imply that any  $b_R \rightarrow s_R$  transition is of the form  $V_{ts}V_{tb}^*y_b y_s^* f(|y_t|^2, |y_b|^2, |y_s|^2)$ , where  $f$  is some function of  $|y_{t,s,b}|^2$ . The actual power of Yukawa couplings in the contribution from a given Feynman diagram is determined by the number of chirality flips through property ii). Property iv) ensures that any possible contribution proportional to  $V_{cs}V_{cb}^*$  is GIM-suppressed, i.e. proportional to  $|y_c|^2$ , and negligible as in the SM.

However, we deviate in one important aspect from Ref. [4]. We explicitly allow for  $CP$ -violating phases which do not originate from the Yukawa sector.  $CP$  violation is an interference phenomenon and involves the differences from otherwise unphysical phases. In order to avoid new  $CP$  phases one must align the phases of the Yukawa couplings with those of other parameters which are unrelated to the Yukawa sector. For instance, in the context of the Minimal Supersymmetric Standard Model (MSSM) this tuning of phases affects the  $\mu$  term, the gaugino mass terms, and the trilinear soft SUSY-breaking terms. It is difficult to motivate this alignment from symmetries or through a dynamical mechanism. We therefore explicitly permit extra  $CP$  phases outside the Yukawa sector, i.e. we consider effects from flavour-conserving  $CP$  phases. Usually such phases are constrained by experimental bounds on electric dipole moments, in particular for the MSSM, where stringent bounds on flavour-conserving  $CP$  phases can only be avoided with quite heavy superparticles. But in our context of generic MFV sizable flavour-conserving  $CP$  phases cannot be excluded a priori [22].

Ref. [4] considers two possibilities for the dominant flavour-symmetry breaking mechanism. While the large top Yukawa coupling always breaks the flavour symmetries of the gauge sector, one can consider the case that the bottom Yukawa coupling is also large and spoils flavour blindness at an equal level (this occurs in the popular MSSM scenarios with large  $\tan\beta$  [65]). Our scenario II corresponds to the case, where only the top Yukawa coupling is large. That is, in scenario II we neglect all effects from down-type Yukawa couplings. The possible  $|\Delta B| = 2$  operators are discussed in Ref. [4]. Thanks to MFV property iii) four-quark operators with right-handed  $b$  or  $s$  fields are accompanied by small (down-type) Yukawa couplings [4] and no other operator than  $Q$  in Eq. (8) occurs in scenario II. Therefore, the only effect of new physics is to change the coefficient  $C$  in Eq. (7).

An important observation is that  $C$  will always be real, even in the presence of flavour-conserving  $CP$  phases: The MFV hypothesis implies that  $C$  is independent of the flavours of the external quarks. If we interchange  $b_L$  and  $q_L$ , the corresponding four-quark interaction will be governed by the same coefficient  $C$  and the effective hamiltonian will contain the combination

$$(V_{tq}^* V_{tb})^2 C \bar{q}_L \gamma_\mu b_L \bar{q}_L \gamma^\mu b_L + (V_{tb}^* V_{tq})^2 C \bar{b}_L \gamma_\mu q_L \bar{b}_L \gamma^\mu q_L.$$

Now the hermiticity of the hamiltonian implies  $C = C^*$ . (An explicit check is provided by the MSSM, where flavour-conserving  $CP$ -violating parameters enter  $C$  only through their moduli or real parts). Hence our scenario II corresponds to the case

$$\Delta_s = \Delta_d = \Delta_K^{tt} \quad \text{with} \quad \phi_s^\Delta = \phi_d^\Delta = \phi_K^{ij\Delta} = 0. \quad (41)$$

We next discuss an important extension of the MFV analysis of Ref. [4] in the case of  $\epsilon_K$ , where we include effects from the charm Yukawa coupling  $y_c$ . The potential relevance of these effects becomes clear when one notices that the Inami-Lim functions  $S(\bar{m}_c^2/M_W^2, \bar{m}_t^2/M_W^2)$  and  $S(\bar{m}_c^2/M_W^2)$  are proportional to  $\bar{m}_c^2/M_W^2$ . Within the Standard Model a substantial contribution to the  $\epsilon_K$ -hyperbola stems from terms which are quadratic in  $y_c$ , and we have to extend our analysis of MFV New Physics to order  $y_c^2$ . Splitting the Wilson coefficients as:

$$C = C^{\text{SM}} + C^{\text{NP}}, \quad C_{ij} = C_{ij}^{\text{SM}} + C_{ij}^{\text{NP}}, \quad (42)$$

MFV constrains the new contributions  $C^{\text{NP}}, C_{ij}^{\text{NP}}$  to obey the following pattern:

$$C_{ij}^{\text{NP}} = V_{is} V_{id}^* V_{js} V_{jd}^* f(|y_i|^2, |y_j|^2) \quad (43)$$

where  $f$  is a real-valued function with  $f(0, x) = f(x, 0) = 0$  by the GIM mechanism and, of course,  $C^{\text{NP}}(\mu) = C_{it}^{\text{NP}}(\mu)$ . We must now distinguish two cases depending on whether the dominant contributions from new physics affect the diagrams with the light charm or up quarks or rather involve particles with a mass similar to or heavier than the top quark.

In the first case, we have to consider new physics contributions  $C_{ct}^{\text{NP}}$  and  $C_{cc}^{\text{NP}}$  which involve the charm and up quarks on an internal line. Such contributions occur, for example, in box diagrams in which one or both W bosons are replaced by charged Higgs bosons. These diagrams with only light internal quark lines lead to negligible effects, if the new particle exchanged between the quark lines is a scalar (like a Higgs boson), because scalars couple left-handed to right-handed fields and come with the penalty of small Yukawa couplings. The extra helicity flip (if an internal quark is right-handed) or the GIM mechanism (on an internal line with only left-handed quarks) brings in extra Yukawa couplings and the contribution to  $C_{ct}^{\text{NP}}$  and  $C_{cc}^{\text{NP}}$  is of order  $|y_c|^4$  or smaller and negligible compared to SM contributions, which are proportional to  $\bar{m}_c^2 \propto |y_c|^2$ . A scaling like in the SM, with just two powers of  $|y_c|$ , could occur in principle if the new exchanged particle is a heavy gauge boson mimicking the SM couplings to the left-handed quark doublets. We are not aware of a realistic theory with such particles and do not consider this possibility further.

The second case corresponds to new physics contributions which involve heavy particles and directly add to the coefficient  $C$  in Eq. (10). A prominent example for a contribution

of this type are the chargino-squark diagrams in the MSSM and it is worthwhile to discuss this example for illustration, before returning to our generic scenario. The chargino-stop box diagram, which contributes to  $\Delta_K^{tt}$ , is widely discussed in the literature. However, to our knowledge, nobody has studied the corresponding effect in  $\Delta_K^{ct}$  or  $\Delta_K^{cc}$ . The former parameter receives contributions from a box diagram with a scharm on one line and a stop on the other. In the limit  $y_c = 0$  there is an exact GIM cancellation between the contributions from the charm and up squarks, which has been invoked to justify the omission of scharm effects. The first non-vanishing contribution is proportional to  $|y_c|^2$  (corresponding to  $\tilde{c}_L \rightarrow \tilde{c}_R$  and  $\tilde{c}_R \rightarrow \tilde{c}_L$  flips). Since the same flip is needed on the stop line, there is also a factor of  $|y_t|^2$  involved. Clearly, we recognise the pattern of Eq. (43) with the same function  $f$  as in  $\Delta_K^{tt}$ . Extending to the generic MFV situation, it is easy to relate  $\Delta_K^{ct}$  to  $\Delta_K^{tt}$  for theories in which  $y_t$  is small enough that we can expand  $\Delta_K^{ct}$  and  $\Delta_K^{tt}$  to the lowest order in  $y_t$  (like in the MSSM for moderate values of  $\tan\beta$  and not-too-large values of the trilinear breaking term  $A_t$ ).<sup>¶</sup> Then

$$f(|y_i|^2, |y_j|^2) = f_0 |y_i|^2 |y_j|^2 + \mathcal{O}(|y_{i,j}|^6), \quad (44)$$

and up to small corrections one has  $C_{ct}^{\text{NP}} = C_{tt}^{\text{NP}} |y_c|^2 / |y_t|^2$  and  $C_{cc}^{\text{NP}} = C_{tt}^{\text{NP}} |y_c|^4 / |y_t|^4$ . Since  $C_{cc}^{\text{NP}}$  is real in scenario II, we can certainly neglect it and set  $\Delta_K^{cc} = 1$  in Eq. (38). To account for the situation that  $y_t$  is close to one we should vary  $C_{ct}^{\text{NP}}$  around  $C_{tt}^{\text{NP}} |y_c|^2 / |y_t|^2$ . A realistic range for  $C_{ct}^{\text{NP}}$  can be obtained from the SM situation. In  $S(\overline{m}_{c,t}^2 / M_W^2)$  the relevant quantity is  $\overline{m}_{c,t} / M_W \sim 2y_{c,t}$ . However, while  $S(\overline{m}_c^2 / M_W^2) \simeq \overline{m}_c^2 / M_W^2$ ,  $S(\overline{m}_t^2 / M_W^2)$  differs from  $\overline{m}_t^2 / M_W^2$  by a bit less than a factor of 2. We take this as a conservative estimate and choose

$$C_{ct}^{\text{NP}} = \lambda_K \frac{\overline{m}_c^2}{\overline{m}_t^2} C_{tt}^{\text{NP}} \quad \text{with} \quad 0.5 \leq \lambda_K \leq 2, \quad (45)$$

while  $C_{cc}^{\text{NP}} = 0$ .

Since no new operators occur in scenario II, our new physics parameters are related to the Wilson coefficient  $C$  in a simple way:

$$\Delta_K^{ij} = \frac{C_{ij}}{C_{ij}^{\text{SM}}} = 1 + \frac{C_{ij}^{\text{NP}}}{C_{ij}^{\text{SM}}}. \quad (46)$$

Eqs. (45) and (46) imply the relation

$$\begin{aligned} \Delta_K^{ct} &= 1 + \lambda_K \frac{\overline{m}_c^2}{\overline{m}_t^2} \frac{C_{tt}^{\text{SM}}}{C_{ct}^{\text{SM}}} (\Delta_K^{tt} - 1) \\ &= 1 + \lambda_K \frac{\overline{m}_c^2}{\overline{m}_t^2} \frac{S(\overline{m}_t^2 / M_W^2) \eta_{tt}}{S(\overline{m}_c^2 / M_W^2, \overline{m}_t^2 / M_W^2) \eta_{ct}} (\Delta_K^{tt} - 1) \end{aligned} \quad (47)$$

$$= 1 + 0.078 \lambda_K (\Delta_K^{tt} - 1). \quad (48)$$

The numerical value 0.078 is obtained for the central values of Tab. 7. The smallness of this number roots in the enhancement of  $S(\overline{m}_c^2 / M_W^2, \overline{m}_t^2 / M_W^2)$  by the large leading logarithm

<sup>¶</sup>The actual expansion parameter is  $y_t v / M$ , where  $M$  is the mass scale of the new particles in the loop and  $v = 174$  GeV is the Higgs vev.

$\log(\overline{m}_c^2/M_W^2) = -8.3$ , which stems from box diagrams with internal charm and up quarks. This logarithm is absent in the new physics contribution, which is formally of the order of a next-to-leading-order correction. In summary, Eqs. (41) and (47) and  $\Delta_K^{cc} = 1$  define our scenario II.

### 2.4.3 Scenario III: MFV with a large bottom Yukawa coupling

In scenario III we consider a large bottom Yukawa coupling. Then  $H_q^{|\Delta B|=2}$  in Eq. (7) is modified to include operators that are not suppressed anymore

$$H_q^{|\Delta B|=2} = (V_{tq}^* V_{tb})^2 \left[ C Q + C_S Q_S + \tilde{C}_S \tilde{Q}_S \right] + \text{h.c.} \quad (49)$$

Here  $Q_S = \bar{q}_L b_R \bar{q}_L b_R$  and  $\tilde{Q}_S$  is defined in Eq. (13). MFV does not put any constraint on  $C_S$  and  $\tilde{C}_S$  which can be complex (an example of an MSSM scenario with a complex  $C_S$  can be found in Ref. [66], and an up-to-date renormalisation-group analysis of  $C_S$  and  $\tilde{C}_S$  can be found in the appendix of the fifth article in Ref. [13]). In the following, we will assume that the matrix elements of  $Q$ ,  $Q_S$ ,  $\tilde{Q}_S$  are affected in the same way by  $U$ -spin breaking corrections, so that the presence of new operators in  $H_q^{|\Delta B|=2}$  yields a scenario III corresponding to the case  $\Delta_s = \Delta_d$  with generally non-zero  $\phi_s^\Delta = \phi_d^\Delta$ .

$C_S$  and  $\tilde{C}_S$  necessarily involve at least two powers of  $y_b$  because of MFV property iii). In the kaon case, the corresponding contribution to analogous coefficients  $C_S$  and  $\tilde{C}_S$  in  $H^{|\Delta S|=2}$  would involve  $y_s^2$  instead. Clearly, such contributions to  $\Delta_K^{tt}$  and  $\Delta_K^{ct}$  will have a negligible impact on  $\epsilon_K$ , but this need not be the case for  $\Delta_K^{cc}$ , in view of the big lever arm in Eq. (40), meaning that the coefficient of  $\text{Im } \Delta_K^{cc}$  is larger than that of  $\text{Re } \Delta_K^{cc}$  by three orders of magnitude. Contributions to  $\Delta_K^{cc}$  from box diagrams with new heavy particles involve four powers of  $|y_c|$  in addition to the two powers of  $y_s$  and are negligible compared to the SM contribution  $\propto |y_c|^2$  even when multiplied by a factor of 1000. New contributions involving internal charm quarks (or some new neutral scalar particle coupling a  $d_L$  to an  $s_R$ ) can be proportional to  $|y_c|^2$  as in the SM, but the two powers of  $y_s$  are sufficient to suppress the effect below a level which is relevant for  $\epsilon_K$ . In addition, in scenario III,  $C$  will be a function of  $|y_b|^2$ , which complicates the relationship to the corresponding coefficient in  $H^{|\Delta S|=2}$  and even our proof that  $C$  is real does not hold anymore. In summary, our scenario III comes with  $\Delta_s = \Delta_d$  and this parameter is complex. The parameters  $\Delta_K^{ij}$  are as in scenario II (that is, they are real, fulfill Eq. (47), and  $\Delta_K^{cc} = 1$ ), but are now unrelated to  $\Delta_{d,s}$ .

One ought to mention that scenarios II and III do not exhaust the possibilities offered by MFV. For instance, Refs. [13, 65] consider MFV-MSSM scenarios with  $M_{\text{SUSY}} \gg M_{A^0} \gtrsim v$ , where  $M_{\text{SUSY}}$  and  $M_{A^0}$  denote the masses of the superparticles and the  $CP$ -odd Higgs boson, respectively, and  $v = 174 \text{ GeV}$  is the electroweak scale. In the MSSM the coefficient  $C_S$  is highly suppressed [13]<sup>||</sup>, while the operator  $\bar{s}_L b_R \bar{s}_R b_L$  occurs with a sizable coefficient, despite of the suppression with the small strange Yukawa coupling. Its counterpart in the  $B_d$  system comes with the even smaller down Yukawa coupling and is

<sup>||</sup>The vanishing of  $C_S$  in the MFV-MSSM scenario with  $M_{\text{SUSY}} \gg M_{A^0} \gtrsim v$  stems from a softly broken Peccei-Quinn symmetry [4], which we have not built into our scenarios II and III.

negligible. In the scenario of Refs. [13, 65] the connection between  $B_s - \bar{B}_s$  mixing and  $B_d - \bar{B}_d$  mixing is lost. But large effects in  $B_s - \bar{B}_s$  mixing are not allowed, due to the experimental bound on  $\text{BR}(B_s \rightarrow \mu\mu)$  [13] (for up-to-date results, see [67]).

#### 2.4.4 Testing the Standard Model

There are various ways to test the SM. The simplest one is to determine all the relevant parameters from a global fit, and test the fit prediction for a given observable compared with the direct measurement. This kind of test is independent of any underlying New Physics scenario.

The second kind of test addresses a definite New Physics scenario extending the SM, and computes the statistical significance that the parameters take their SM value. In our case it corresponds to testing whether one or several  $\Delta$  parameters are compatible with  $\Delta = 1$ .

In the relevant sections below we will perform both kind of tests, and discuss their interpretation.

## 3 Inputs

In this Section, we discuss all relevant experimental and theoretical inputs entering the fits. The corresponding values and uncertainties are quoted in Tables 6 and 7. In general, if there is only one uncertainty quoted, we understand this error as a statistical one. In case of two error contributions, the first one is taken as a statistical error while the second, theoretical, error is treated as an allowed range for the observable or the parameter under consideration. This kind of uncertainty is treated in the Rfit scheme described in Refs. [44, 68].

### 3.1 Hadronic parameters and method of averaging

Several hadronic inputs are required for the fits presented, and we mostly rely on Lattice QCD (LQCD) simulations to estimate these quantities involving strong interactions at low energies. The presence of results from different lattice QCD collaborations with various statistics and systematics make it all the more necessary to combine them in a careful way. The procedure that we have chosen to determine these lattice averages is as follows: We collect the relevant calculations of the quantity that we are interested in and we take only unquenched results with 2 or 2+1 dynamical fermions, even those from proceedings without a companion article (flagged with a star). In these results, we separate the error estimates into a Gaussian part and a flat part that is treated à la Rfit. The Gaussian part collects the uncertainties from purely statistical origin, but also the systematics that can be controlled and treated in a similar way (e.g., interpolation or fitting in some cases). The remaining systematics constitute the Rfit error. If there are several sources of error in the Rfit category, we add them linearly \*\*. The Rfit model is simple but also very

---

\*\*Keeping in mind that in many papers this combination is done in quadrature and the splitting between different sources is not published.

strict. It amounts to assuming that the theoretical uncertainty is rigorously constrained by a mathematical bound that is our only piece of information. If Rfit is taken *stricto sensu* and the individual likelihoods are combined in the usual way (by multiplication), the final uncertainty can be underestimated, in particular in the case of marginally compatible values. We correct this effect by adopting the following averaging recipe. We first combine the Gaussian uncertainties by combining the likelihoods restricted to their Gaussian part. Then we assign to this combination the smallest of the individual Rfit uncertainties. The underlying idea is twofold:

- the present state of the art cannot allow us to reach a better theoretical accuracy than the best of all estimates.
- this best estimate should not be penalized by less precise methods (as it would happen be the case if one took the dispersion of the individual central values as a guess of the combined theoretical uncertainty).

It should be stressed that the concept of a theoretical uncertainty is ill-defined, and the combination of them even more. Thus our approach is only one among the alternatives that can be found in the literature [69,70]. In contrast to some of the latter, ours is algorithmic and can be reproduced. Moreover, we differ from the PDG-like method advocated in Ref. [70] on two points. We separate systematic and statistic errors, which prevents us from assigning a reduced systematics to a combination of several results suffering from the same systematic uncertainty. We do not attempt at estimating the (partial) correlations between the results from different collaborations, even though we are aware of their existence (results from the same gauge configuration, using the same procedure to determine the lattice spacing...). Whatever the averaging method chosen, one should emphasize that it relies crucially on the quality of the error estimation performed by each collaboration.

The following tables show the inputs used and the average obtained by applying the procedure described above for the following hadronic parameters: the decay constant  $f_{B_s}$  for the  $B_s$  meson (Table 1), the ratio of decay constants  $f_{B_s}/f_{B_d}$  (Table 2), the scheme-invariant bag parameter  $\hat{\mathcal{B}}_{B_s} = 1.523 \mathcal{B}_{B_s}(m_b)$  for the  $B_s$  meson discussed after Eq. 12 (Table 3), the ratio of bag parameters  $\mathcal{B}_{B_s}/\mathcal{B}_{B_d}$  (Table 4), and the bag parameter  $\mathcal{B}_K(2 \text{ GeV})$  for the neutral kaon (Table 5).

We are not aware of lattice estimates for the power-suppressed matrix elements corresponding to  $\mathcal{B}_{\tilde{R}_i}$ . We will assign them a value of  $1 \pm 0.5$ , taking a flat uncertainty for the two bag parameters contributing the most to  $\Delta\Gamma^q$  and  $a_{SL}^q$  ( $\mathcal{B}_{\tilde{R}_2}$  and  $\mathcal{B}_{\tilde{R}_3}$  respectively), and a Gaussian error for the other ones. These bag parameters vary independently for  $B_d$  and  $B_s$  mesons, *i.e.* we do not assume the exact SU(3) symmetry for them.

## 3.2 Observables not affected by New Physics in mixing

In this section, we first discuss the observables allowing us to establish an universal preferred region in the  $\bar{\rho} - \bar{\eta}$  subspace, independent of any NP contributions in mixing.

- The CKM matrix element  $|V_{ud}|$  has been determined from three different methods: superallowed nuclear  $\beta$ -decays, neutron  $\beta$ -decay and pion  $\beta$ -decay. Currently, the

| Reference    | $N_f$ | $f_{B_s} \pm \sigma_{stat} \pm \sigma_{Rfit}$ | Article |
|--------------|-------|---|---------|
| CP-PACS01    | 2     | $242 \pm 9_{-34}^{+53}$                       | [71]    |
| MILC02       | 2     | $217 \pm 6_{-31}^{+58}$                       | [72]    |
| JLQCD03      | 2     | $215 \pm 9_{-15}^{+19}$                       | [73]    |
| HPQCD03      | 2+1   | $260 \pm 7 \pm 39$                            | [74]    |
| FNAL-MILC09* | 2+1   | $243 \pm 6 \pm 22$                            | [75]    |
| HPQCD09      | 2+1   | $231 \pm 5 \pm 30$                            | [76]    |
| Our average  |       | $228 \pm 3 \pm 17$                            |         |

Table 1: Calculations and average used for the decay constant  $f_{B_s}$ .  $N_f$  stands for the number of dynamical flavours used in the simulation. The first uncertainty quotes the statistical uncertainty, the second the Rfit error.

| Reference    | $N_f$ | $f_{B_s}/f_{B_d} \pm \sigma_{stat} \pm \sigma_{Rfit}$ | Article |
|--------------|-------|---|---------|
| CP-PACS01    | 2     | $1.179 \pm 0.018 \pm 0.023$                           | [71]    |
| MILC02       | 2     | $1.16 \pm 0.01_{-0.04}^{+0.08}$                       | [72]    |
| JLQCD03      | 2     | $1.13 \pm 0.03_{-0.02}^{+0.17}$                       | [73]    |
| FNAL-MILC09* | 2+1   | $1.245 \pm 0.028 \pm 0.049$                           | [75]    |
| HPQCD09      | 2+1   | $1.226 \pm 0.020 \pm 0.033$                           | [76]    |
| Our average  |       | $1.199 \pm 0.008 \pm 0.023$                           |         |

Table 2: Calculations and average used for the ratio of decay constants  $f_{B_s}/f_{B_d}$ .  $N_f$  stands for the number of dynamical flavours used in the simulation. The first uncertainty quotes the statistical uncertainty, the second the Rfit error.

| Reference    | $N_f$ | $\hat{\mathcal{B}}_{B_s} \pm \sigma_{stat} \pm \sigma_{Rfit}$ | Article |
|--------------|-------|---|---------|
| JLQCD03      | 2     | $1.299 \pm 0.034_{-0.095}^{+0.122}$                           | [73]    |
| HPQCD06      | 2+1   | $1.168 \pm 0.105 \pm 0.140$                                   | [79]    |
| RBC/UKQCD07* | 2+1   | $1.21 \pm 0.05 \pm 0.05$                                      | [84]    |
| HPQCD09      | 2+1   | $1.326 \pm 0.04 \pm 0.03$                                     | [76]    |
| Our average  |       | $1.28 \pm 0.02 \pm 0.03$                                      |         |

Table 3: Calculations and average used for the bag parameter  $\hat{\mathcal{B}}_{B_s}$ .  $N_f$  stands for the number of dynamical flavours used in the simulation. The first uncertainty quotes the statistical uncertainty, the second the Rfit error.

| Reference   | $N_f$ | $\mathcal{B}_{B_s}/\mathcal{B}_{B_d} \pm \sigma_{stat} \pm \sigma_{Rfit}$ | Article |
|-------------|-------|---|---------|
| JLQCD03     | 2     | $1.017 \pm 0.016^{+0.076}_{-0.017}$                                       | [73]    |
| HPQCD09     | 2+1   | $1.053 \pm 0.020 \pm 0.030$   | [76]    |
| Our average |       | $1.05 \pm 0.01 \pm 0.03$  |         |

Table 4: Calculations and average used for the bag parameter ratio  $\mathcal{B}_{B_s}/\mathcal{B}_{B_d}$ .  $N_f$  stands for the number of dynamical flavours used in the simulation. The first uncertainty quotes the statistical uncertainty, the second the Rfit error.

| Reference     | $N_f$ | $\mathcal{B}_K(2 \text{ GeV}) \pm \sigma_{stat} \pm \sigma_{Rfit}$ | Article |
|---------------|-------|--|---------|
| JLQCD08       | 2     | $0.537 \pm 0.004 \pm 0.072$  | [82]    |
| HPQCD/UKQCD06 | 2+1   | $0.618 \pm 0.018 \pm 0.179$  | [83]    |
| RBC/UKQCD07   | 2+1   | $0.524 \pm 0.010 \pm 0.052$  | [80]    |
| ALVdW09       | 2+1   | $0.527 \pm 0.006 \pm 0.049$  | [81]    |
| Our average   |       | $0.527 \pm 0.0031 \pm 0.049$                                       |         |

Table 5: Calculations and average used for the bag parameter  $\mathcal{B}_K(2 \text{ GeV})$ .  $N_f$  stands for the number of dynamical flavours used in the simulation. The first uncertainty quotes the statistical uncertainty, the second the Rfit error.

best determination of  $|V_{ud}|$  comes from superallowed  $\beta$ -decays where the uncertainty is dominated by the theoretical error, see e.g. Ref. [85, 86]. An analysis by Towner and Hardy [87] focusing on an improvement of the isospin-symmetry-breaking terms finds a central value for  $|V_{ud}|$  which is larger though still compatible when compared to values quoted in the past, with a slightly reduced uncertainty:  $|V_{ud}| = 0.97425 \pm 0.00022$ .

- The matrix element  $|V_{us}|$  can be determined from  $K_{e3}$  decays, from hadronic  $\tau$  decays, and from semileptonic hyperon decays. We are using the  $K_{e3}$  average quoted by Flavianet [88]. The experimental number for  $f_+(q^2 = 0) \cdot |V_{us}|$  obtained by averaging results from ISTRAP, KLOE, KTeV, and NA48(/2), as quoted by Flavianet, is  $f_+(q^2 = 0) \cdot |V_{us}| = 0.21664 \pm 0.00046$  [88]. Taking the Lattice QCD result for the  $K \rightarrow \pi$  form factor  $f_+$  of  $0.964 \pm 0.005$  [89], this translates into  $|V_{us}| = 0.2246 \pm 0.0012$  [88].
- The matrix element  $|V_{cb}|$  is obtained from semileptonic decays  $B \rightarrow X_c \ell \nu$ , where  $X_c$  is either a  $D^*$  meson (exclusive method) or a sum over all hadronic final states containing charm (inclusive method). For several years the most precise value has been provided by the inclusive method where the theoretical uncertainties have been pushed below the 2 % level by determining the relevant non-perturbative Heavy Quark Expansion (HQE) parameters from moment measurements in  $B \rightarrow X_c \ell \nu$  and  $B \rightarrow X_s \gamma$  decays. The inclusive  $|V_{cb}|$  value used in our analysis is taken from the Heavy Flavour Averaging Group (HFAG) [90],  $|V_{cb, \text{incl}}| = (41.85 \pm 0.43 \pm 0.59) \times 10^{-3}$ ,

where the first error contains the experimental and HQE uncertainties and the second reflects the theoretical uncertainty on the total rate prediction for  $B \rightarrow X_c \ell \nu$ .

The theoretical uncertainty on the exclusive  $|V_{cb}|$  determination in the calculation of the form factor value at zero recoil  $F(1)$  has not been competitive so far. A recent calculation provides a significantly smaller error budget:  $F(1) = 0.921 \pm 0.013 \pm 0.020$  [91], although the exclusive  $|V_{cb}|$  determination still gives a larger uncertainty. Using the average value for the product  $F(1)|V_{cb}| = (36.04 \pm 0.52) \times 10^{-3}$  from the Heavy Flavour Averaging Group (HFAG) [90] and applying a 0.7 % QED correction [92], one finds  $|V_{cb,\text{excl}}| = (38.85 \pm 0.56_{\text{exp}} \pm 0.55_{\text{theostat}} \pm 0.84_{\text{theosys}}) \times 10^{-3} = (38.85 \pm 0.77 \pm 0.84) \times 10^{-3}$ , which has a smaller central value than the inclusive result.

We average the two  $|V_{cb}|$  values in such a way that the smallest theoretical uncertainty is preserved similarly to our procedure to average lattice inputs and we obtain  $|V_{cb}| = (40.89 \pm 0.38 \pm 0.59) \times 10^{-3}$ , keeping in mind, however, that the inclusive and exclusive numbers are not in perfect agreement.

- The two methods to extract  $|V_{ub}|$ , the inclusive and the exclusive ones (using the theoretically cleanest  $B \rightarrow \pi \ell \nu$  decays), both suffer from significant theoretical uncertainties. The exclusive measurements prefer values around  $3.5 \times 10^{-3}$  [90]. The numbers quoted are from partial rates measured at large  $q^2$  ( $> 16 \text{ GeV}^2$ ) or at small  $q^2$  ( $< 16 \text{ GeV}^2$ ), using form factor calculations from LQCD [93, 94], or Light Cone Sum Rules (LCSR) [95], respectively. The fit input is the average of these numbers, following the same procedure as for the Lattice QCD parameters:  $|V_{ub,\text{excl}}| = (3.51 \pm 0.10 \pm 0.46) \times 10^{-3}$ .

The average of inclusive results quoted by HFAG using [90] the Shape Function (SF) scheme [96] yields  $(4.32 \pm 0.16_{-0.23}^{+0.22}) \times 10^{-3}$ , where the first uncertainty contains the statistical and experimental systematic uncertainty as well as the modelling errors for  $b \rightarrow u \ell \nu$  and  $b \rightarrow c \ell \nu$  transitions. Compared to HFAG, we modify the assignment of the uncertainties as follows. We add the following uncertainties in quadrature: statistical uncertainty, experimental systematics,  $b \rightarrow c$  and  $b \rightarrow u$  modeling and the error from the HQE parameters ( $b$ -quark mass  $m_b$  and  $\mu_\pi^2$ ). Several theoretical uncertainties can only be guesstimated: the shape function uncertainty, contributions from subleading shape functions, weak annihilations and the procedure of scale matching. We assign an additional uncertainty on  $m_b$ , which reflects higher order corrections not accounted for in the partial rate predictions for  $B \rightarrow X_u \ell \nu$  [97]. We choose 50 MeV as the additional uncertainty. All these uncertainties of a second type are added linearly. As a result, we obtain a significantly larger theoretical uncertainty compared to the uncertainty quoted by the HFAG:  $(4.32_{-0.24}^{+0.21} \pm 0.45) \times 10^{-3}$ .

The exclusive and the inclusive inputs are then averaged using the same recipe as for the Lattice QCD parameters and we obtain:  $|V_{ub}| = (3.92 \pm 0.09 \pm 0.45) \times 10^{-3}$ .

- A measurement of the branching fraction for  $B^+ \rightarrow \tau \nu$  allows one to constrain the product  $|V_{ub}| \cdot f_B$  where  $f_B$  is the decay constant of the charged  $B$  meson. The

theoretical prediction for this branching fraction is given by

$$\mathcal{B}(B \rightarrow \tau\nu) = \frac{G_F^2 m_{B^+} m_\tau^2}{8\pi} \left(1 - \frac{m_\tau^2}{m_{B^+}^2}\right)^2 |V_{ub}|^2 f_B^2 \tau_{B^+}. \quad (50)$$

We use the experimental value  $\tau_{B^+} = 1.639 \cdot 10^{-12} s$  in our analysis.  $\mathcal{B}(B \rightarrow \tau\nu)$  combined with the constraint from the oscillation frequency  $\Delta m_d$  (see Sec. 3.3) removes the dependence on the decay constant  $f_B$  (assuming that the decay constant for the charged and neutral  $B$  meson is the same, i.e., neglecting isospin-breaking effects of order 1%).

First evidence for the decay  $B \rightarrow \tau\nu$  has been made by the Belle collaboration [98] as well as the first observation of this decay [99]. The world average for  $\mathcal{B}(B \rightarrow \tau\nu)$  that is used in the analysis calculated from the measurements performed by *BABAR* and Belle [98–101] is  $\mathcal{B}(B \rightarrow \tau\nu) = (1.73 \pm 0.35) \times 10^{-4}$ .

- The input for the CKM angle  $\gamma$  ( $= \arg[-V_{ud}V_{ub}^*/(V_{cd}V_{cb}^*)]$ ) is taken from a combined full frequentist analysis of the CKMfitter group using  $CP$ -violating asymmetries in charged  $B$  decays to neutral  $D^{(*)}$  mesons plus charged  $K^{(*)}$  mesons. The data are taken from HFAG using the three different methods proposed by Gronau, London, Wyler (GLW) [103], and Atwood, Dunietz, Soni (ADS) [104], and including also the Dalitz plot approach developed by Giri, Grossman, Soffer and Zupan (GGSZ), and independently by the Belle collaboration [105]. At the 68.3 % confidence level (CL), the result of this analysis is  $(70_{-21}^{+14})^\circ$  with a second solution at  $\gamma + \pi$ . The constraint is shown in Figure 1.

The above determination of  $\gamma$  raises interesting statistical issues. The angle  $\gamma$  actually appears as the complex phase of a suppressed ratio  $r_B$  of decay amplitudes (different  $r_B$ 's appear for different final states); in other words in the limit  $r_B \rightarrow 0$  there is no constraint left on the CKM phase, and for finite  $r_B$  the error on  $\gamma$  is roughly inversely proportional to  $r_B$  itself. It turns out that the current data do not exclude tiny values for the  $r_B$ 's, one obtains for the  $DK$  final state  $r_B = 0.104_{-0.025}^{+0.015}$  at 68.3% CL, the  $D^*K$  final state  $r_B = 0.116_{-0.024}^{+0.025}$  at 68.3% CL, and for the final state  $DK^*$  final state  $r_B = 0.113_{-0.047}^{+0.061}$  at 68.3% CL. Because the ratio of amplitudes is related to the bare observables non-linearly, its maximum-likelihood estimate is biased, and it can be shown that this bias overestimates the value of  $r_B$  which in turn implies an underestimate of the uncertainty on  $\gamma$ . In the statistical language, this effect yields a significant *undercoverage* of the naïve 68.3 % CL interval for  $\gamma$  computed from the log-likelihood variation.

A better estimate of the statistical uncertainty on  $\gamma$  can be obtained by inspecting the deviation of the distribution of the log-likelihood among a large number of toy experiments from its asymptotic limit. Problems arise because this distribution is not only non asymptotic, but also depends on *nuisance parameters*, that is other parameters than  $\gamma$  that are necessary to compute the toy experiments. In such a situation the most conservative approach is called the *supremum* one, since it maximizes the uncertainty over all possible values of the nuisance parameters. To date this method which guarantees the coverage properties by construction is the

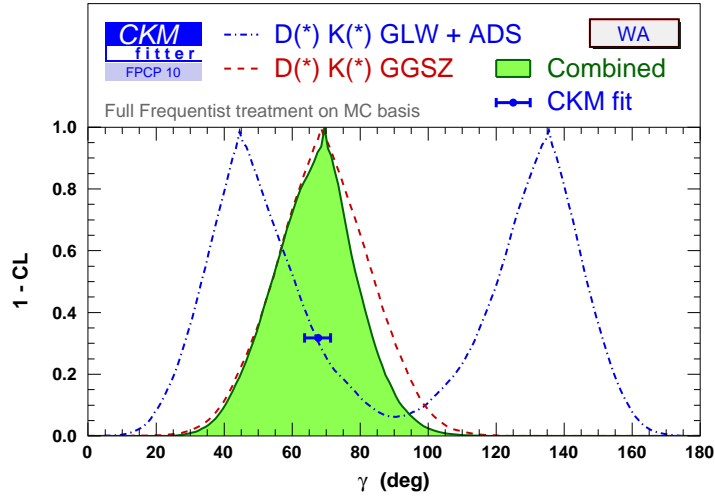


Figure 1: Constraint on the angle  $\gamma$  from a combined analysis of  $B \rightarrow D^{(*)}K^{(*)}$  decays.

default one for the treatment of  $\gamma$  in CKMfitter, but it must be kept in mind that it actually leads to overcoverage in general [106].

Another determination of  $\gamma$  which is unaffected by new physics in  $B-\bar{B}$  mixing is obtained by combining measurements of  $\alpha$  and  $\beta$ : The corresponding quantities are changed into  $\alpha - \phi_d^\Delta/2$  and  $\beta + \phi_d^\Delta/2$  in the presence of a new physics phase  $\phi_d^\Delta$  which therefore drops out of  $\gamma = \pi - (\alpha - \phi_d^\Delta/2) - (\beta + \phi_d^\Delta/2)$ . This procedure leads to a significantly more precise determination of  $\gamma$  than  $B \rightarrow D^{(*)}K^{(*)}$  decays. The individual measurements of  $\alpha - \phi_d^\Delta/2$  and  $\beta + \phi_d^\Delta/2$  are described in the next section.

### 3.3 Observables in the $B_d-\bar{B}_d$ system affected by New Physics in mixing

The following observables can be affected by  $|\Delta F| = 2$  NP contributions in the  $B_d^0 - \bar{B}_d^0$  system:

- The oscillation frequency  $\Delta m_d$  in the  $B_d$  sector has been measured with  $O(1\%)$  precision mainly due to the  $B$ -factory data [123]. The translation of the measured value for  $\Delta m_d$  into constraints on the CKM parameter combination  $|V_{td}V_{tb}^*|^2$  suffers from significant uncertainties in the theoretical calculation of the product  $f_{B_d}\sqrt{\mathcal{B}_{B_d}}$  of hadronic parameters. These hadronic parameters can be obtained from LQCD computation, computing  $f_{B_d}\sqrt{\mathcal{B}_{B_d}}$  from  $f_{B_s}$  and  $\mathcal{B}_{B_s}$ , and the flavour-symmetry breaking ratios  $f_{B_s}/f_{B_d}$  and  $\mathcal{B}_{B_s}/\mathcal{B}_{B_d}$  as quoted in Section 3.1 and summarized in Table 7. The value and uncertainty for the perturbative QCD correction  $\hat{\eta}_B$  has

been originally estimated in Ref. [41]. With up-to-date values and uncertainties for  $\alpha_s$  and the top-quark mass one obtains  $\hat{\eta}_B = 0.8393 \pm 0.0034$ . For the top-quark mass we take the average value of the Tevatron Electroweak Working Group [107],  $m_t = (172.4 \pm 1.2)$  GeV, combining published and also preliminary results from DØ and CDF. This mass, interpreted as a pole mass, is translated into  $\overline{m}_t(\overline{m}_t) = (165.017 \pm 1.156 \pm 0.11)$  GeV in the  $\overline{\text{MS}}$ -scheme at one-loop order. It should be noted, however, that the identification of the measured mass value to the pole mass is under debate (with potential new systematics coming from this identification), see e.g. [108].

- In the SM, the decay width difference  $\Delta\Gamma_d$  is predicted to be small:  $\Delta\Gamma_d = (38_{-12}^{+11}) \times 10^{-4} \text{ ps}^{-1}$  [9] (with our inputs). The average between DELPHI and BABAR measurements of the ratio  $\Delta\Gamma_d/\Gamma_d$  calculated by HFAG [109, 110, 123] is  $0.009 \pm 0.037$ . The experimental uncertainty is much larger than the size of the SM prediction,  $\Delta\Gamma_d/\Gamma_d = (46_{-18}^{+17}) \times 10^{-4}$ , and the measured value is in good agreement with the SM prediction within experimental uncertainties so that stringent constraints on NP contributions cannot be derived at the present stage of precision. Since a huge amount of statistics will be needed to measure  $\Delta\Gamma_d$  at the level predicted by the Standard Model, this situation will probably not change for quite a long time. Even then if a deviation from the Standard Model value were observed due to NP contributions in mixing it would show up beforehand in other observables like  $a_{\text{fs}}^d$  or  $\sin 2\beta$ . As a consequence,  $\Delta\Gamma_d$  has no visible impact in our discussion and it is not used as an input to the fits presented here.
- $CP$  violation in  $B_d$  mixing (i.e.,  $|q/p| \neq 1$ , with  $q/p$  defined in Eq. (5)) can be measured from the untagged dilepton rate asymmetry

$$a_{\text{fs}}^d = \frac{N_{\ell^+\ell^+} - N_{\ell^-\ell^-}}{N_{\ell^+\ell^+} + N_{\ell^-\ell^-}} = 2(1 - |q/p|). \quad (51)$$

With a tagged time-dependent decay asymmetry, one measures

$$A_{\text{SL}}^q(t) \equiv \frac{\Gamma(\bar{B}_q^0(t) \rightarrow l^+ X) - \Gamma(B_q^0(t) \rightarrow l^- X)}{\Gamma(\bar{B}_q^0(t) \rightarrow l^+ X) + \Gamma(B_q^0(t) \rightarrow l^- X)} \quad (52)$$

$$= \frac{1 - |q/p|^4}{1 + |q/p|^4} = 2(1 - |q/p|) + \mathcal{O}((|q/p| - 1)^2), \quad (53)$$

with the time-dependence dropping out. A weighted average of BABAR, Belle and CLEO measurements [111] results in  $A_{\text{SL}}^d = -(47 \pm 46) \times 10^{-4}$  [123], which is about one standard deviation below the SM prediction of  $a_{\text{fs}}^d = (-6.4_{-1.8}^{+1.6}) \times 10^{-4}$  [9, 42, 62] (with our inputs).

- Within the SM the measurement of the  $S$  coefficient in the time-dependent  $CP$  asymmetry  $A_{CP}(t) = S \sin(\Delta m_d \cdot t) + C \cos(\Delta m_d \cdot t)$  in decays of neutral  $B_d$  mesons to final states  $(c\bar{c})K^0$  provides a measurement of the parameter  $\sin 2\beta$ , where  $\beta = \arg[-V_{td}V_{tb}^*/(V_{cd}V_{cb}^*)]$ , to a very good approximation. The current uncertainty of

0.023 on  $S$  is still dominated by statistics [123]. The difference between the measured  $S$  coefficient and  $\sin 2\beta$  due to penguin contributions has been theoretically estimated in Ref. [112] to be below the  $10^{-3}$  level, while phenomenologically less stringent constraints on this difference are quoted in Refs. [113–116].

When interpreting the measured  $S$  coefficient as  $\sin(2\beta + \phi_d^\Delta)$  the  $SM_4FC$  hypothesis does not rigorously apply. However, the gluonic penguin is  $OZI$ -suppressed and the  $Z$ -penguin is estimated to be small so that NP in decay is assumed to be negligible with respect to the leading tree amplitude. We neglect the effect from possible NP in  $K - \bar{K}$  mixing on  $\sin(2\beta + \phi_d^\Delta)$ , which is justified given the small value of the well-measured  $CP$ -violating parameter  $\epsilon_K$ .

- The measurement of  $\sin(2\beta + \phi_d^\Delta)$  results in two solutions for  $2\beta + \phi_d^\Delta$  (in  $[0, \pi]$ ). One of these solutions can be excluded by measuring the sign of  $\cos(2\beta + \phi_d^\Delta)$ . For a recent review of *BABAR* and Belle measurements see e.g. Ref. [117]. The current experimental results from *BABAR* and Belle using a time- and angular-dependent analysis of  $B^0 \rightarrow J/\psi K^{*0}$  decays, a time-dependent Dalitz-plot analysis in  $B^0/\bar{B}^0 \rightarrow D^{(*)0}/\bar{D}^{(*)0}h^0$  with  $B^0/\bar{B}^0 \rightarrow D^{(*)0}/\bar{D}^{(*)0}h^0$ , and  $B^0/\bar{B}^0 \rightarrow D^{*+}D^{*-}K_S^0$ , disfavour negative  $\cos(2\beta + \phi_d^\Delta)$  values but HFAG deems it difficult to average the different measurements or to determine a reliable confidence level as a function of  $\cos(2\beta + \phi_d^\Delta)$  [123]. Here, as a simplification, it is only assumed that  $\cos(2\beta + \phi_d^\Delta) > 0$ .
- The constraint on the CKM angle  $\alpha = \pi - \beta - \gamma$  is obtained from time-dependent and time-independent measurements in the decays  $B \rightarrow \pi\pi$ ,  $B \rightarrow \rho\rho$ , and  $B \rightarrow \rho\pi$ . The time-dependent  $CP$  asymmetries measured in  $B \rightarrow \pi\pi$  provide information on the effective parameter  $\sin(2\alpha_{\text{eff}})$  (which is a function of  $\alpha$  and the penguin-to-tree ratio [102]). It is possible to translate this measurement into a constraint on  $\alpha$  by exploiting isospin symmetry which allows to pin down the penguin-to-tree ratio and thus to determine the difference  $\alpha - \alpha_{\text{eff}}$  from data [118]. Under the assumption of exact isospin symmetry the amplitudes  $A^{+-} \equiv A(B^0 \rightarrow \pi^+\pi^-)$ ,  $A^{00} \equiv A(B^0 \rightarrow \pi^0\pi^0)$ , and  $A^{+0} \equiv A(B^+ \rightarrow \pi^+\pi^0)$  satisfy a triangular relationship:  $\sqrt{2}A^{+0} - \sqrt{2}A^{00} = A^{+-}$ . A corresponding relationship holds for the  $CP$  conjugated decays:  $\sqrt{2}\bar{A}^{+0} - \sqrt{2}\bar{A}^{00} = \bar{A}^{+-}$ . These isospin triangles can be reconstructed by measuring the branching fractions and direct  $CP$  asymmetries for the final states  $B^0 \rightarrow \pi^+\pi^-$ ,  $B^0 \rightarrow \pi^0\pi^0$ , and  $B^+ \rightarrow \pi^+\pi^0$ . Since one measures  $\sin(2\alpha_{\text{eff}})$  and since the triangle has a twofold ambiguity for its apex in the complex plane, there is an eightfold ambiguity for  $\alpha$  in  $[0, \pi]$ . The extraction of  $\alpha$  from the isospin analysis is independent of any possible NP contributions in the  $\Delta I = 1/2$  decay amplitude except for the singular point  $\alpha = 0$  [119]. If there is no NP contribution in the  $\Delta I = 3/2$  decay amplitude (as assumed here), the extraction provides  $\alpha = \pi - \gamma - \beta - \phi_d^\Delta/2$ . As a consequence,  $\alpha$  is equivalent to  $\gamma$  if  $\beta + \phi_d^\Delta$  is measured e.g. from  $B \rightarrow J/\psi K_S$  as already pointed out above.

Similar in line an isospin analysis can be performed for the  $B \rightarrow \rho\rho$  system. In this case the analysis needs to take into account the measured longitudinal polarisation of the  $\rho$  mesons in the different final states  $B^0 \rightarrow \rho^+\rho^-$ ,  $B^0 \rightarrow \rho^0\rho^0$ , and  $B^+ \rightarrow \rho^+\rho^0$ .

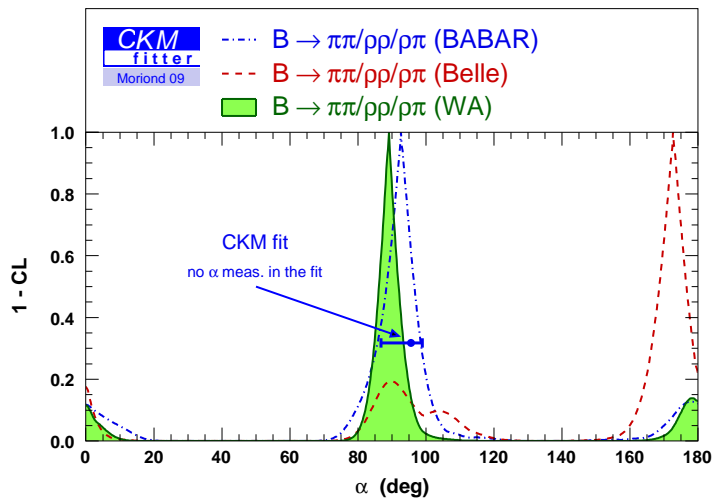


Figure 2: Constraint on the angle  $\alpha$  from the isospin analyses of  $B \rightarrow \pi\pi$  and  $B \rightarrow \rho\rho$  decays and a Dalitz plot analysis of  $B \rightarrow \rho\pi$  decays. In the presence of new physics in  $B_d$  mixing, the quantity shown is  $\pi - \gamma - \beta - \phi_d^\Delta$ .

Finally, the  $\rho\pi$  modes provides another crucial input for  $\alpha$ , by using a model for the Dalitz decay into three pions in addition to the isospin symmetry [120]. The results of these analyses that are based on the world averages of the various *BABAR* and Belle measurements for the CP asymmetries and branching fractions determined by the Heavy Flavour Averaging Group [123] are displayed in Figure 2. The combined analysis results in  $\alpha = (89.0^{+4.4}_{-4.2})^\circ$  at 68.3 % CL.

The most stringent constraint on  $\alpha$  comes currently from the  $B^0 \rightarrow \rho\rho$  channel. The uncertainty is driven by the rather large branching fraction  $BF(B^+ \rightarrow \rho^+\rho^0)$ . The input value for  $BF(B^+ \rightarrow \rho^+\rho^0)$  has changed recently when the *BABAR* collaboration presented a new analysis on the final data set [121]. The large branching fraction value leads to an isospin triangle that just closes. The measurement uncertainty is smaller than the expected uncertainty. As a consequence, the current uncertainty quoted for  $\alpha$  might be on the optimistic side. It should also be stressed that at this level of precision so-far neglected uncertainties (electroweak penguins,  $\pi-\eta^{(\prime)}$  mixing,  $\rho-\omega$  mixing, other isospin violations, finite  $\rho$ -width, etc.) should be considered in more detail.

### 3.4 Observables in the $B_s - \bar{B}_s$ system affected by New Physics in mixing

Observables which can be possibly affected by  $|\Delta F| = 2$  NP contributions in the  $B_s - \bar{B}_s$  system are:

| Observable  | Value and uncertainties                                 | Reference              |
|---|---|------------------------|
| $ V_{ud} $  | $0.97425 \pm 0.00022$                                   | [87]                   |
| $ V_{us} $  | $0.2246 \pm 0.0012$                                     | [88]                   |
| $m_K$   | $(497.614 \pm 0.024)$ MeV                               | [86]                   |
| $G_F$   | $(1.16637 \pm 0.00001) \times 10^{-5}$ GeV <sup>2</sup> | [86]                   |
| $m_W$   | $(80.398 \pm 0.025)$ GeV                                | [86]                   |
| $m_{B_d}$   | $(5.27917 \pm 0.00029)$ GeV                             | [86]                   |
| $m_{B^+}$   | $(5.27953 \pm 0.00033)$ GeV                             | [86]                   |
| $m_{B_s}$   | $(5.3663 \pm 0.0006)$ GeV                               | [86]                   |
| $ V_{cb} $  | $(40.89 \pm 0.38 \pm 0.59) \times 10^{-3}$              | see text               |
| $ V_{ub} $  | $(3.92 \pm 0.09 \pm 0.45) \times 10^{-3}$               | see text               |
| $\mathcal{B}(B \rightarrow \tau \nu_\tau)$        | $(1.73 \pm 0.35) \times 10^{-4}$                        | see text               |
| $\gamma$  | $73^{+19^\circ}_{-24}$                                  | see text               |
| $\Delta m_d$                                      | $(0.507 \pm 0.005)$ ps <sup>-1</sup>                    | [86]                   |
| $a_{\text{fs}}^d$                                 | $(-47 \pm 46) \times 10^{-4}$                           | [123]                  |
| $\sin(2\beta + \phi_d^\Delta)$                    | $0.673 \pm 0.023$                                       | [122]                  |
| $\cos(2\beta + \phi_d^\Delta)$                    | positive  | see text               |
| $\alpha$  | $89.0^{+4.4^\circ}_{-4.2}$                              | see text               |
| $\Delta m_s$                                      | $(17.77 \pm 0.12)$ ps <sup>-1</sup>                     | [25]                   |
| $a_{\text{fs}}$                                   | $(-85 \pm 28) \times 10^{-4}$                           | see text and [31, 124] |
| $a_{\text{fs}}^s$                                 | $(-17 \pm 93) \times 10^{-4}$                           | [125]                  |
| $(\phi_s^\Delta - 2\beta_s)$ vs. $\Delta\Gamma_s$ | see text  | [27, 28, 134]          |
| $\epsilon_K$                                      | $(2.229 \pm 0.010) \times 10^{-3}$                      | [86]                   |
| $\Delta m_K$                                      | $(3.483 \pm 0.006) \times 10^{-12}$ MeV                 | [86]                   |

Table 6: Experimental inputs used in the fits.

| Theoretical Parameter                                     | Value and uncertainties   | Reference                    |
|---|---|------------------------------|
| $f_{B_s}$   | $(228 \pm 3 \pm 17)$ MeV  | see Section 3.1              |
| $\mathcal{B}_{B_s}(m_b)$                                  | $0.846 \pm 0.013 \pm 0.020$   | see Section 3.1              |
| $f_{B_s}/f_{B_d}$   | $1.199 \pm 0.008 \pm 0.023$   | see Section 3.1              |
| $\mathcal{B}_{B_s}/\mathcal{B}_{B_d}$                     | $1.05 \pm 0.01 \pm 0.03$  | see Section 3.1              |
| $\hat{\eta}_B$  | $0.8393 \pm 0.0034$   | see text                     |
| $\bar{m}_t(\bar{m}_t)$                                    | $(165.017 \pm 1.156 \pm 0.11)$ GeV                                      | see text and [107]           |
| $\tilde{\mathcal{B}}_K$                                   | $(0.724 \pm 0.004 \pm 0.067)$   | see Section 3.1              |
| $f_K$   | 156.1 MeV   | see text                     |
| $\kappa_\epsilon$   | $0.940 \pm 0.013 \pm 0.023$   | see text                     |
| $\eta_{tt}$   | $0.5765 \pm 0.0065$   | [39]                         |
| $\eta_{ct}$   | $0.47 \pm 0.04$   | [56]                         |
| $\eta_{cc}$   | $(1.39 \pm 0.35) \left(\frac{1.29 \text{ GeV}}{\bar{m}_c}\right)^{1.1}$ | [55]                         |
| $\lambda_K$   | $(1.25 \pm 0.00 \pm 0.75)$ GeV  | see text                     |
| $\bar{m}_c(\bar{m}_c)$                                    | $(1.286 \pm 0.013 \pm 0.040)$ GeV                                       | see text                     |
| $\tilde{\mathcal{B}}_{S,B_s}/\tilde{\mathcal{B}}_{S,B_d}$ | $1.01 \pm 0 \pm 0.03$   | [126]                        |
| $\tilde{\mathcal{B}}_{S,B_s}(m_b)$                        | $0.91 \pm 0.03 \pm 0.12$  | [126]                        |
| $\Lambda_{\overline{\text{MS}}}^{(5)}$                    | $(0.222 \pm 0.027)$ GeV   | from $\alpha_s(M_Z)$ in [86] |
| $\bar{m}_s(\bar{m}_b)$                                    | $(0.085 \pm 0.017)$ GeV   | [9]                          |
| $\bar{m}_b(\bar{m}_b)$                                    | $(4.248 \pm 0.051)$ GeV   | [90]                         |
| $m_b^{pow}$   | $(4.7 \pm 0 \pm 0.1)$ GeV   | [9]                          |
| $\mathcal{B}_{R_0}$                                       | $1.0 \pm 0.5$   | [9]                          |
| $\mathcal{B}_{\tilde{R}_1}$                               | $1.0 \pm 0.5$   | [9]                          |
| $\mathcal{B}_{R_1}$                                       | $1.0 \pm 0.5$   | [9]                          |
| $\mathcal{B}_{R_2}$                                       | $1.0 \pm 0.5$   | [9]                          |
| $\mathcal{B}_{\tilde{R}_2}$                               | $1.0 \pm 0 \pm 0.5$   | [9]                          |
| $\mathcal{B}_{R_3}$                                       | $1.0 \pm 0.5$   | [9]                          |
| $\mathcal{B}_{\tilde{R}_3}$                               | $1.0 \pm 0 \pm 0.5$   | [9]                          |

Table 7: Theoretical inputs used in the fits.

- The experimental input for the mass difference  $\Delta m_s$  taken from HFAG is dominated by the measurement of CDF [25]. The dependence of the SM prediction  $\Delta m_s^{\text{SM}}$  on  $\bar{\rho} - \bar{\eta}$  coordinates appears very weak through the relevant CKM matrix elements term  $|V_{ts}^* V_{tb}|^2$ , but the physical  $\Delta m_s$  gives a direct constraint in the  $\Delta_s$  plane, by computing  $f_{B_s} \sqrt{\hat{\mathcal{B}}_{B_s}}$  from  $f_{B_s}$  and  $\mathcal{B}_{B_s}$ , given in Table 7. The hadronic matrix element for the  $B_s$  system can be related to the  $B_d$  one via the flavour- $SU(3)$  breaking correction parameter  $\xi$  defined through  $f_{B_s}^2 \mathcal{B}_{B_s} = \xi^2 f_{B_d}^2 \mathcal{B}_{B_d}$ . Measurements of  $\Delta m_s$  thus reduce the uncertainties on  $f_{B_d}^2 \mathcal{B}_{B_d}$  since  $\xi$  is better known from lattice QCD than  $f_{B_d}^2 \mathcal{B}_{B_d}$ . This relation also generates a strong correlation between the NP parameters  $|\Delta_d|$  and  $|\Delta_s|$  when allowing for new physics contributions to mixing.
- The SM prediction [9] for  $a_{\text{fs}}^s$  is at least one order of magnitude smaller than the one for  $a_{\text{fs}}^d$ , see Table 8. Compared to the SM prediction the measurement from DØ has a quite large uncertainty,  $a_{\text{fs}}^s = (-17 \pm 91_{-23}^{+12}) \times 10^{-4}$  [125], and hence does not have a strong impact on the NP constraints in the  $B_s$  sector. It is nevertheless included in our analysis.
- DØ [127] using  $1 \text{ fb}^{-1}$  and CDF [124] have measured inclusive dimuon CP asymmetries. The DØ result corresponding to the measurement quoted in Ref. [127] presented as  $a_{\text{fs}}^d + \frac{f_s Z_s}{f_d Z_d} a_{\text{fs}}^s = -0.0028 \pm 0.0013 \pm 0.0009$  is provided in [128] whereas CDF [124] quotes the result as

$$a_{\text{fs}} = \frac{f_d Z_d a_{\text{fs}}^d + f_s Z_s a_{\text{fs}}^s}{f_d Z_d + f_s Z_s} = 0.0080 \pm 0.0090 \pm 0.0068, \quad (54)$$

where  $f_{d(s)}$  is the fraction of neutral  $B_{d(s)}$  mesons in the fragmentation and  $Z_{d(s)}$  is given by

$$Z_q = \frac{1}{1 - y_q^2} - \frac{1}{1 + x_q^2} \quad (55)$$

with  $y_q = \Delta\Gamma_q/2\Gamma_q$  and  $x_q = \Delta m_q/\Gamma_q$  (see also Ref. [48]). Very recently DØ has presented a new measurement of  $a_{\text{fs}}$  [31] using  $6.1 \text{ fb}^{-1}$  integrated luminosity which shows a  $3.2\sigma$  deviation from the (almost zero) SM prediction, and is the first direct evidence against the SM in  $B$  meson observables:  $a_{\text{fs}} = -0.00957 \pm 0.00251 \pm 0.00146$ . This result supersedes the former result in Ref. [128]. The average between the new DØ result and the CDF result reads

$$a_{\text{fs}} = -0.0085 \pm 0.0028, \quad (56)$$

which is 3.0 standard deviations away from the SM prediction.

For the interpretation of the measured observables we use the following values and uncertainties for  $f_{d(s)}$ ,  $y_q$  and  $x_q$ :  $f_d = 0.333 \pm 0.030$ ,  $f_s = 0.121 \pm 0.015$  with a correlation coefficient of +0.439 are taken from Ref. [90],  $x_d$  is calculated from  $\Delta m_d = (0.507 \pm 0.005) \cdot 10^{12} \text{ s}^{-1}$  [86] and  $\tau_{B_d} = (1.525 \pm 0.009) \cdot 10^{-12} \text{ s}$  [129],  $y_d$  is set to zero since  $\Delta\Gamma_d$  is expected to be very small in the Standard Model and is hardly affected by New Physics,  $x_s$  is calculated from  $\Delta m_s = (17.77 \pm 0.12) \cdot 10^{12} \text{ s}^{-1}$  [86] and  $y_s$  from  $\tau_{B_s} = (1.515 \pm 0.034) \cdot 10^{-12} \text{ s}$  [129], the measurement of  $\Delta\Gamma_s$  in  $B_s \rightarrow J/\psi \phi$

(see below) and the flavour-specific  $B_s$  lifetime  $\tau_{B_s}^{FS} = (1.417 \pm 0.042) \cdot 10^{-12} s$  [129]. This results in  $Z_d = 0.3741 \pm 0.0054$  and  $Z_s = 1.0044^{+0.0058}_{-0.0032}$  hence actually the error on  $Z_{d,s}$  has negligible impact on our global fits.

- CDF and DØ have presented time-dependent tagged analyses [26,27] of  $B_s \rightarrow J/\psi \phi$  decays which provide information on  $\Delta_s$  through  $\Delta\Gamma_s$  and  $\phi_s^\Delta - 2\beta_s$ . These analyses supersede the previous untagged studies of Refs. [130,131] (which use the same data sample, but without the tagging information) and we will not use the untagged results in our analysis. These time-dependent tagged analyses have raised a lot of attention recently, in particular when the UTfit collaboration claimed an evidence of New Physics of at least  $3\sigma$  based on a global fit where these measurements played a central role [132]. It has been later shown, though, that this conclusion came from an overinterpretation of the data [133]. In the framework of the HFAG [123] the CDF and DØ have determined a combined constraint based on the measurements in Refs. [26,27]. In 2009 CDF has updated the analysis on a larger dataset using  $2.8 fb^{-1}$  of data [28]. The new average between DØ [27] and CDF [28] has been presented in Summer 2009 [134]. Using this new average the deviation of the measured value for  $\beta_s$  with respect to the SM value is essentially unchanged and reads 2.3 standard deviations. This average is our default input for the corresponding observables, supplemented by the constraint on the flavour-specific  $B_s$  lifetime  $\tau_{B_s}^{FS} = (1.417 \pm 0.042) \cdot 10^{-12}$  [129] which can be viewed as an independent measurement of  $\Delta\Gamma_s$ . New results for  $B_s \rightarrow J/\psi \phi$  have been presented in Summer 2010 by CDF (with  $5.2 fb^{-1}$ ) [29] and DØ (with  $6.1 fb^{-1}$ ) [27] collaborations, in closer agreement to the Standard Model expectations, but these measurements have not been combined together yet. They have not been included in the present analysis, but are briefly discussed together with the SM significance tests below.

### 3.5 The neutral kaon system

The master formula for  $\epsilon_K$  has been given in Eq. (38), from the relation between  $\epsilon_K$  and  $M_{12}^s$ . The translation of  $\epsilon_K$  into a constraint on  $\bar{\rho}$  and  $\bar{\eta}$  suffers from sizeable uncertainties in the Wolfenstein parameter  $A$  (the determination of which being driven by  $|V_{cb}|^4$ ),  $\hat{\mathcal{B}}_K$  (see Table 7 and Section 3.1), from the long-distance corrections to the relation between  $M_{12}^K$  and  $\epsilon_K$  encoded in  $\kappa_\epsilon$ , and, though of less importance, from uncertainties in the QCD corrections coming from  $\eta_{cc}$  [55], from the charm quark mass  $\bar{m}_c(\bar{m}_c)$  in the  $\overline{\text{MS}}$  scheme, from  $m_t$  and the perturbative QCD corrections  $\eta_{tt}$  [55] and  $\eta_{ct}$  [55].

- From the experimental point of view, the number on the LHS of Eq. 38 has shifted substantially over time. For instance in 1995 the corresponding number was  $1.21 \cdot 10^{-7}$  [56]. More recently, the numerical value for  $\epsilon_K$  has shifted by about 2.3 % (a  $3.7 \sigma$  effect) between the 2004 and 2006 edition of the Particle Data Group (PDG) from  $(2.284 \pm 0.014) \times 10^{-3}$  [135] down to  $(2.232 \pm 0.007) \times 10^{-3}$  [86]. This shift has been mainly driven by improved measurements of the branching fraction  $BF(K_L \rightarrow \pi^+ \pi^-)$  performed by the KTeV, KLOE and NA48 collaborations leading to a reduction of 5.5 % of the semileptonic branching fraction values.

- As discussed in sec. 2.2, the relation between  $\epsilon_K$  and  $K - \bar{K}$  mixing is affected by several corrections encoded in  $\kappa_\epsilon$ . We have combined them with the experimental result for  $\epsilon_K$  as indicated in this section.
- The kaon decay constant  $f_K$  is taken from the review on pseudoscalar decay constants in Ref. [86] which is calculated from the measured branching fraction  $BF(K^+ \rightarrow \mu^+ \nu_\mu(\gamma))$  and the measured charged kaon decay time using an external input for  $|V_{us}|$ . In Ref. [86]  $|V_{us}| = 0.2255 \pm 0.0019$  from  $K_{\ell 3}$  decays is used as external input which leads to  $f_K = 155.5 \pm 0.2 \pm 0.8 \pm 0.2$  MeV where the first error is due to the experimental uncertainties, the second due to the uncertainty from  $|V_{us}|$  and the third due to higher order corrections [86]. With our input of  $|V_{us}| = 0.2246 \pm 0.0012$  this translates into  $f_K = 156.1 \pm 0.2 \pm 0.6 \pm 0.2$  MeV. In the fit, we do not consider the uncertainties on  $f_K$  at this point since they are currently negligible with respect to the other uncertainties. Since the  $f_K$  value obtained in this way is anticorrelated with our  $|V_{us}|$  input a consistent treatment would require including the leptonic kaon decay in the fit and constrain  $f_K$  simultaneously. This would then lead to an even smaller uncertainty on  $f_K$  given the improved uncertainty on  $|V_{us}|$  imposed by the global fit. Such a fit is technically possible but has not been performed here since the error from  $f_K$  on  $\epsilon_K$  does not play an important role.
- Various determinations of the charm quark mass are available. For instance, the charm quark mass in the kinetic mass scheme can be obtained from fits to data from lepton energy and hadronic mass moments in  $B \rightarrow X_c \ell \nu$  decays combined with photon energy moments measured in  $B \rightarrow X_s \gamma$  decays, see e.g. Refs. [123, 136]. The most recent value for the kinetic mass quoted by HFAG is  $m_c^{kin} = (1.165 \pm 0.050)$  GeV [123], corresponding to a value in the  $\overline{\text{MS}}$  scheme:  $\overline{m}_c(\overline{m}_c) = (1.265 \pm 0.060 \pm 0.050)$  GeV. The first uncertainty on the charm quark mass is correlated with the b-quark mass uncertainty obtained from the same fits quoted in Table 6 with a linear correlation coefficient of order 98 %. A second uncertainty of 50 MeV has been added following the discussion in Ref. [136], to take into account the low renormalisation scale and the size of higher-order perturbative corrections when translating the mass from one scheme to another.

As an alternative, the charm quark mass can also be determined from  $e^+e^-$  annihilation data into hadrons created from quark-antiquark pairs. The OPE-based method consists in writing sum rules for moments of the cross section  $\sigma(e^+e^- \rightarrow c\bar{c})$ , which are dominated by the perturbative term and the contribution proportional to the gluon condensate. An older analysis of Steinhauser and Kühn based on a three-loop calculation finds  $\overline{m}_c(\overline{m}_c) = (1.304 \pm 0.027)$  GeV with a small uncertainty [137]. A similar analysis by Jamin and Hoang [138] obtains a consistent result,  $\overline{m}_c(\overline{m}_c) = (1.290 \pm 0.070)$  GeV, but quotes a significantly larger uncertainty. This can be ascribed to the choice of the OPE scale separating short- and long-distance physics and it can be viewed as the impact of (neglected) higher order terms in perturbation theory on the determination of  $m_c$  through such moments. In a more recent calculation at four loops for the perturbative contribution, the uncer-

tainty has been further reduced:  $\overline{m}_c(\overline{m}_c) = (1.286 \pm 0.013)$  GeV [139]<sup>††</sup>. However, in this reference, there is only a limited discussion of the freedom in the choice of the renormalisation scale for the perturbative series and the gluon condensate is varied only in a limited range, even though these two effects were seen as bringing significant systematics in Ref. [138]. In the absence of further studies on the systematics discussed above in the case of the four-loop analysis of ref. [139], we assign an additional theoretical uncertainty of 0.040 GeV and use as our input value:  $\overline{m}_c(\overline{m}_c) = (1.286 \pm 0.013 \pm 0.040)$  GeV which is consistent with the values from the moment fits but has smaller uncertainties.

## 4 Quantitative Studies

### 4.1 Standard Model fit

In this section we present the current status of the Standard Model CKM fit. Fig. 3 shows the fit results in the  $\bar{\rho} - \bar{\eta}$  plane. Table 8 shows the fit results for various parameters. In Tables 8 and 9 we also show the result of the fit for observables that have been individually excluded from the fit in order to quantify possible deviations between the individual input values and their fit predictions. The  $\chi^2/N_{\text{dof}}$  of the combined Standard Model fit is approximately 7.2/7 and hence corresponds to a good overall agreement. However this global minimum  $\chi^2$  mixes quantities that are in perfect agreement with their fit prediction, with others that are individually at odds. Possible deviations between a selection of measured observables and their Standard Model predictions are discussed in more detail in the following.

One observes a sizeable discrepancy between the input value of  $\mathcal{B}(B \rightarrow \tau\nu)$  (see Table 6) and its fit prediction (see Table 9) which is mainly driven by the measured value of  $\sin 2\beta$ , and was first discussed in Ref. [7]. Removing either  $\mathcal{B}(B \rightarrow \tau\nu)$  or  $\sin 2\beta$  from the list of inputs results in a  $\chi^2$  change that corresponds to 2.6 standard deviations. This discrepancy could arise either from a statistical fluctuation in the measured  $\mathcal{B}(B \rightarrow \tau\nu)$  value, from too small (large) a value of  $f_{B_d}$  ( $\hat{\mathcal{B}}_{B_d}$ ), or from NP in  $B \rightarrow \tau\nu$  and/or the  $\sin 2\beta$  measurements in  $B \rightarrow J/\psi K_S$ . There is a specific correlation between the  $\sin 2\beta$  and  $\mathcal{B}(B \rightarrow \tau\nu)$  in the global fit that is a bit at odds with the direct experimental determination. This is best viewed in the  $(\sin 2\beta, \mathcal{B}(B \rightarrow \tau\nu))$  plane (see Fig. 4), regarding the prediction from the global fit without using these measurements. The shape of the correlation can be understood more deeply by considering the ratio  $\mathcal{B}(B \rightarrow \tau\nu)/\Delta m_d$ , where the decay constant  $f_{B_d}$  cancels, leaving limited theoretical uncertainties restricted to the bag parameter  $\hat{\mathcal{B}}_{B_d}$ . The formula for the ratio displays explicitly that the correlation between  $\mathcal{B}(B \rightarrow \tau\nu)$  and the angle  $\beta$  is controlled by the values of  $\hat{\mathcal{B}}_{B_d}$ , and the angles  $\gamma$  and  $\alpha = \pi - \beta - \gamma$ :

$$\frac{\mathcal{B}(B \rightarrow \tau\nu)}{\Delta m_d} = \frac{3\pi}{4} \frac{m_\tau^2}{m_W^2 S(x_t)} \left(1 - \frac{m_\tau^2}{m_{B^+}^2}\right)^2 \tau_{B^+} \frac{1}{\hat{\mathcal{B}}_{B_d} \eta_B} \frac{1}{|V_{ud}|^2} \left(\frac{\sin \beta}{\sin \gamma}\right)^2. \quad (57)$$

<sup>††</sup>Using an improved routine for the renormalisation group evolution of the computed value  $m_c(3\text{GeV}) = (0.986 \pm 0.013)$  GeV the same group finds a slightly shifted central value  $\overline{m}_c(\overline{m}_c) = 1.268$  GeV [140].

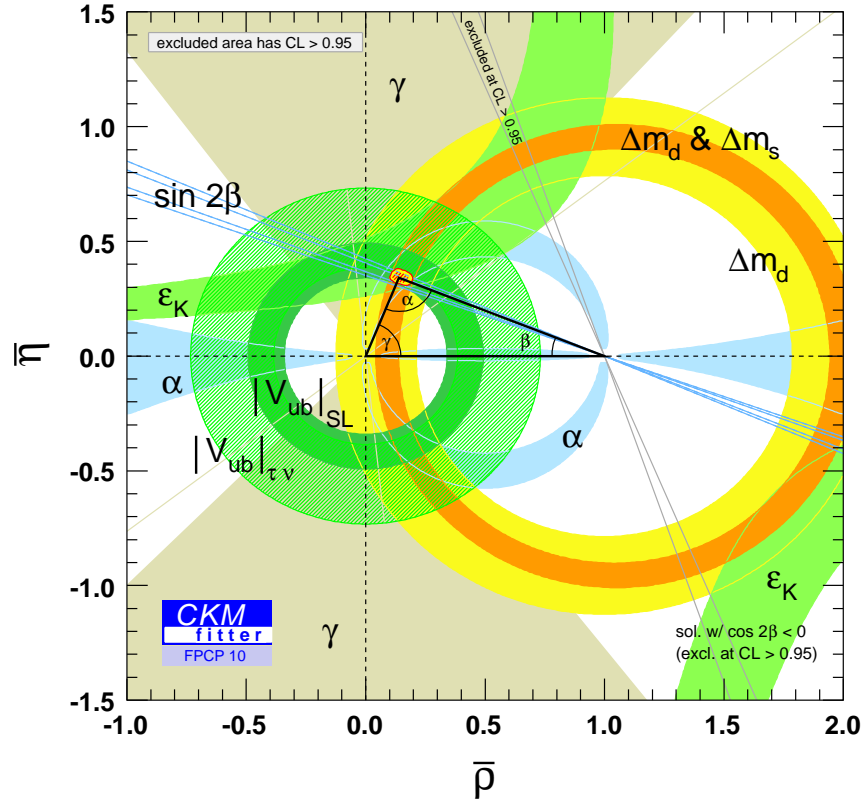


Figure 3: Constraint on the CKM  $(\bar{\rho}, \bar{\eta})$  coordinates from the global Standard Model CKM-fit. Regions outside the coloured areas have CL > 95.45 %. For the combined fit the yellow area inscribed by the contour line represents points with CL < 95.45 %. The shaded area inside this region represents points with CL < 68.3 %.

The comparison of the indirect prediction of  $\hat{\mathcal{B}}_{B_d}$  from the above analytical formula (having only  $\mathcal{B}(B \rightarrow \tau\nu)$ ,  $\Delta m_d$ ,  $\sin 2\beta$ ,  $\alpha$ ,  $\gamma$  and  $|V_{ud}|$  as inputs, that is an almost completely theory-free determination of  $\hat{\mathcal{B}}_{B_d}$ ) with the current direct lattice determination  $\hat{\mathcal{B}}_{B_d} = 1.221_{-0.085}^{+0.087}$  is given in Fig. 5. For this test the deviation is  $2.7 \sigma$ , dominated first by the experimental error on  $\mathcal{B}(B \rightarrow \tau\nu)$ ,  $\alpha$ ,  $\gamma$  and second by the theoretical uncertainty on  $\hat{\mathcal{B}}_{B_d}$ . This tests clearly shows that the semileptonic extraction of  $|V_{ub}|$  has little to do with the  $\mathcal{B}(B \rightarrow \tau\nu)$  anomaly. Further insight is provided by Fig. 6 where the constraints on the decay constant  $f_{B_d}$  and  $f_{B_d}\sqrt{\hat{\mathcal{B}}_{B_d}}$  are shown. We compare the fit inputs  $f_{B_d}$  and  $f_{B_d}\sqrt{\hat{\mathcal{B}}_{B_d}}$  taken from LQCD calculations with their predictions from the fit. The measured  $\mathcal{B}(B \rightarrow \tau\nu)$  value leads to the constraint on  $f_{B_d}$  represented by the green band. The orange band represents the constraint on  $f_{B_d}\sqrt{\hat{\mathcal{B}}_{B_d}}$  thanks to the  $\Delta m_d$  measurement. The combined prediction for both quantities (red and yellow regions) reveals that the

| Quantity                                  | central $\pm$ CL $\equiv$ $1\sigma$ | $\pm$ CL $\equiv$ $2\sigma$  | $\pm$ CL $\equiv$ $3\sigma$  |
|---|-------------------------------------|------------------------------|------------------------------|
| $A$                                       | $0.8184^{+0.0094}_{-0.0311}$        | $0.818^{+0.019}_{-0.040}$    | $0.818^{+0.028}_{-0.048}$    |
| $\lambda$                                 | $0.22512^{+0.00075}_{-0.00075}$     | $0.2251^{+0.0015}_{-0.0015}$ | $0.2251^{+0.0022}_{-0.0022}$ |
| $\bar{\rho}$                              | $0.139^{+0.027}_{-0.023}$           | $0.139^{+0.051}_{-0.033}$    | $0.139^{+0.063}_{-0.042}$    |
| $\bar{\eta}$                              | $0.342^{+0.016}_{-0.015}$           | $0.342^{+0.031}_{-0.027}$    | $0.342^{+0.046}_{-0.037}$    |
| $\widehat{B}_K$ (!)                       | $0.82^{+0.26}_{-0.14}$              | $0.82^{+0.33}_{-0.18}$       | $0.82^{+0.40}_{-0.21}$       |
| $f_{B_s}$ [MeV] (!)                       | $234.7^{+9.8}_{-8.3}$               | $235^{+13}_{-12}$            | $235^{+16}_{-15}$            |
| $\widehat{\mathcal{B}}_{B_s}$ (!)         | $1.136^{+0.103}_{-0.043}$           | $1.136^{+0.457}_{-0.081}$    | $1.14^{+0.61}_{-0.11}$       |
| $f_{B_s}/f_{B_d}$ (!)                     | $1.199^{+0.058}_{-0.044}$           | $1.199^{+0.109}_{-0.096}$    | $1.20^{+0.15}_{-0.14}$       |
| $\mathcal{B}_{B_s}/\mathcal{B}_{B_d}$ (!) | $1.156^{+0.075}_{-0.104}$           | $1.16^{+0.15}_{-0.21}$       | $1.16^{+0.23}_{-0.30}$       |
| $m_c$ [GeV] (!)                           | $1.49^{+0.56}_{-0.52}$              | $1.49^{+0.64}_{-0.68}$       | $1.49^{+0.70}_{-0.85}$       |
| $m_t$ [GeV] (!)                           | $153.5^{+10.5}_{-6.9}$              | $154^{+40}_{-10}$            | $154^{+53}_{-13}$            |
| $J$ [ $10^{-5}$ ]                         | $2.98^{+0.15}_{-0.19}$              | $2.98^{+0.30}_{-0.23}$       | $2.98^{+0.45}_{-0.28}$       |
| $\alpha$ [deg] (!)                        | $97.4^{+1.5}_{-9.5}$                | $97.4^{+2.9}_{-12.1}$        | $97.4^{+4.3}_{-13.9}$        |
| $\beta$ [deg] (!)                         | $28.11^{+0.69}_{-1.84}$             | $28.1^{+1.4}_{-5.0}$         | $28.1^{+2.1}_{-7.7}$         |
| $\gamma$ [deg] (!)                        | $67.7^{+3.6}_{-4.1}$                | $67.7^{+5.2}_{-7.7}$         | $67.7^{+6.7}_{-9.5}$         |
| $\beta_s$ [deg]                           | $1.038^{+0.048}_{-0.047}$           | $1.038^{+0.097}_{-0.080}$    | $1.04^{+0.14}_{-0.11}$       |

Table 8: Fit results of the Standard Model fit. The notation ‘(!)’ means that the fit output represents the indirect constraint, *i.e.* the corresponding direct input has been removed from the analysis.

predicted value for  $f_{B_d}\sqrt{\widehat{\mathcal{B}}_{B_d}}$  is in very good agreement with the LQCD input. Therefore, if the discrepancy is driven by too small a  $f_{B_d}$  value, the lattice artefact responsible for this underestimation should not affect the more complicated determination of the  $\Delta B = 2$  matrix element proportional to  $f_{B_d}\sqrt{\widehat{\mathcal{B}}_{B_d}}$ , as already demonstrated in Fig. 5 in order to preserve the good agreement between the predicted and calculated values for  $f_{B_d}\sqrt{\widehat{\mathcal{B}}_{B_d}}$ .

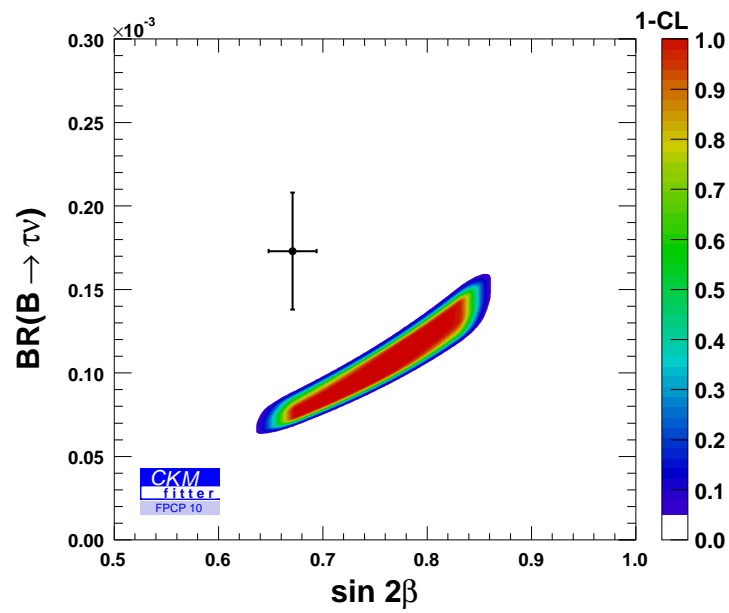


Figure 4: Constraint in the  $(\sin 2\beta, \mathcal{B}(B \rightarrow \tau\nu))$  plane. The coloured constraint represents the prediction for these quantities from the global fit when these inputs are removed while the cross represents the measurements with the corresponding  $1\sigma$  uncertainty.

| Quantity   | central $\pm$ CL $\equiv$ $1\sigma$ | $\pm$ CL $\equiv$ $2\sigma$        | $\pm$ CL $\equiv$ $3\sigma$        |
|--|-------------------------------------|------------------------------------|------------------------------------|
| $ V_{ud} $ (!)   | $0.97444^{+0.00028}_{-0.00028}$     | $0.97444^{+0.00055}_{-0.00056}$    | $0.97444^{+0.00082}_{-0.00084}$    |
| $ V_{us} $ (!)   | $0.22544^{+0.00095}_{-0.00095}$     | $0.2254^{+0.0019}_{-0.0019}$       | $0.2254^{+0.0028}_{-0.0029}$       |
| $ V_{ub} $ (!)   | $0.00353^{+0.00015}_{-0.00021}$     | $0.00353^{+0.00030}_{-0.00032}$    | $0.00353^{+0.00045}_{-0.00042}$    |
| $ V_{cd} $   | $0.22498^{+0.00075}_{-0.00075}$     | $0.2250^{+0.0015}_{-0.0015}$       | $0.2250^{+0.0022}_{-0.0022}$       |
| $ V_{cs} $   | $0.97348^{+0.00021}_{-0.00017}$     | $0.97348^{+0.00038}_{-0.00035}$    | $0.97348^{+0.00055}_{-0.00052}$    |
| $ V_{cb} $ (!)   | $0.04548^{+0.00078}_{-0.00574}$     | $0.0455^{+0.0014}_{-0.0062}$       | $0.0455^{+0.0020}_{-0.0067}$       |
| $ V_{td} $   | $0.00865^{+0.00024}_{-0.00039}$     | $0.00865^{+0.00036}_{-0.00056}$    | $0.00865^{+0.00048}_{-0.00069}$    |
| $ V_{ts} $   | $0.04072^{+0.00038}_{-0.00146}$     | $0.04072^{+0.00076}_{-0.00180}$    | $0.0407^{+0.0011}_{-0.0021}$       |
| $ V_{tb} $   | $0.999133^{+0.000060}_{-0.000016}$  | $0.999133^{+0.000074}_{-0.000032}$ | $0.999133^{+0.000086}_{-0.000048}$ |
| $\phi_d$ [deg]   | $-5.5^{+2.5}_{-3.3}$                | $-5.5^{+2.7}_{-4.3}$               | $-5.5^{+2.9}_{-5.6}$               |
| $\phi_s$ [deg]   | $0.27^{+0.20}_{-0.18}$              | $0.27^{+0.28}_{-0.25}$             | $0.27^{+0.35}_{-0.31}$             |
| $ \epsilon_K $ [ $10^{-3}$ ] (!)                       | $2.01^{+0.58}_{-0.66}$              | $2.01^{+0.73}_{-0.74}$             | $2.01^{+0.88}_{-0.81}$             |
| $\Delta m_d$ [ $\text{ps}^{-1}$ ] (!)                  | $0.558^{+0.053}_{-0.065}$           | $0.558^{+0.091}_{-0.116}$          | $0.56^{+0.13}_{-0.16}$             |
| $\Delta m_s$ [ $\text{ps}^{-1}$ ] (!)                  | $17.8^{+2.0}_{-2.2}$                | $17.8^{+3.3}_{-3.4}$               | $17.8^{+4.5}_{-4.3}$               |
| $a_{\text{fs}}$ [ $10^{-4}$ ] (!)                      | $-3.10^{+0.83}_{-0.98}$             | $-3.1^{+1.1}_{-1.4}$               | $-3.1^{+1.2}_{-1.9}$               |
| $a_{\text{fs}}^d$ [ $10^{-4}$ ] (!)                    | $-6.4^{+1.6}_{-1.8}$                | $-6.4^{+1.9}_{-2.4}$               | $-6.4^{+2.2}_{-3.1}$               |
| $a_{\text{fs}}^s$ [ $10^{-4}$ ] (!)                    | $0.30^{+0.12}_{-0.13}$              | $0.30^{+0.19}_{-0.20}$             | $0.30^{+0.24}_{-0.27}$             |
| $\Delta\Gamma_d$ [ $\text{ps}^{-1}$ ] (!)              | $0.0038^{+0.0011}_{-0.0012}$        | $0.0038^{+0.0013}_{-0.0014}$       | $0.0038^{+0.0014}_{-0.0016}$       |
| $\Delta\Gamma_s$ [ $\text{ps}^{-1}$ ] (!)              | $0.124^{+0.038}_{-0.042}$           | $0.124^{+0.044}_{-0.050}$          | $0.124^{+0.049}_{-0.058}$          |
| $\mathcal{B}(B \rightarrow \tau\nu)$ [ $10^{-4}$ ] (!) | $0.763^{+0.113}_{-0.061}$           | $0.763^{+0.214}_{-0.097}$          | $0.76^{+0.30}_{-0.13}$             |
| $\mathcal{B}(B \rightarrow \mu\nu)$ [ $10^{-6}$ ]      | $0.380^{+0.046}_{-0.043}$           | $0.380^{+0.085}_{-0.071}$          | $0.380^{+0.123}_{-0.088}$          |
| $\mathcal{B}(B \rightarrow e\nu)$ [ $10^{-11}$ ]       | $0.89^{+0.11}_{-0.10}$              | $0.89^{+0.20}_{-0.17}$             | $0.89^{+0.29}_{-0.21}$             |

Table 9: Fit results of the Standard Model fit. The notation ‘(!)’ means that the fit output represents the indirect constraint, *i.e.* the corresponding direct input has been removed from the analysis.

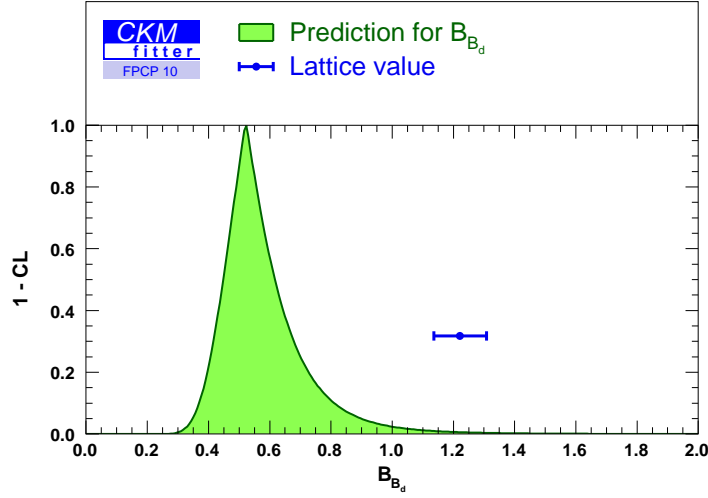


Figure 5: Comparison between the  $\hat{\mathcal{B}}_{B_d}$  parameter used in the global fit and its prediction. The coloured constraint represents the prediction of  $\hat{\mathcal{B}}_{B_d}$  quantities from the global fit while the blue point represents the input value with the corresponding  $1\sigma$  uncertainty as used in the global fit.

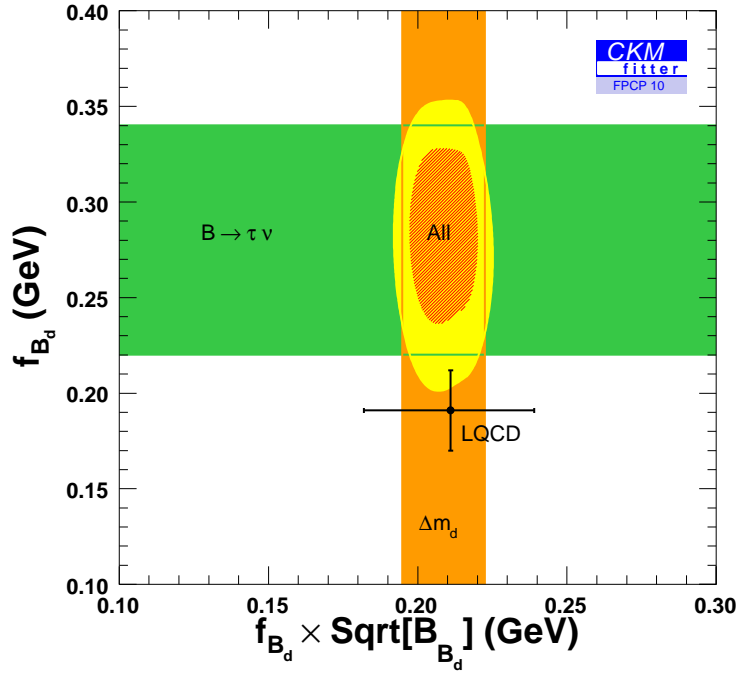


Figure 6: Constraint on  $f_{B_d}$  and  $f_{B_d}\sqrt{\hat{\mathcal{B}}_{B_d}}$ . The green band shows the 95.45% CL constraint on  $f_{B_d}$  when  $\mathcal{B}(B \rightarrow \tau\nu)$  is included in the fit. The orange band represents the 95.45% CL constraint on  $f_{B_d}\sqrt{\hat{\mathcal{B}}_{B_d}}$  thanks to the  $\Delta m_d$  measurement. The combined 68.3% CL and 95.45% CL constraint is shown in red, respectively, in yellow. The black point shows the  $1\sigma$  uncertainty on  $f_{B_d}$  and  $f_{B_d}\sqrt{\hat{\mathcal{B}}_{B_d}}$  as used in the fit.

| Observable   | deviation<br>wrt the SM fit |
|--|-----------------------------|
| $\mathcal{B}(B \rightarrow \tau\nu)$                                   | 2.6 $\sigma$                |
| $-2\beta_s$  | 2.1 $\sigma$                |
| $a_{\text{fs}}$  | 3.0 $\sigma$                |
| $-2\beta_s$ and $a_{\text{fs}}$  | 3.1 $\sigma$                |
| $\mathcal{B}(B \rightarrow \tau\nu)$ , $-2\beta_s$ and $a_{\text{fs}}$ | 3.7 $\sigma$                |

Table 10: Pull values for the most anomalous observables in the SM global fit, in terms of the number of equivalent standard deviations between the direct measurement (Table 6) and the full indirect fit prediction (Table 9). These numbers are computed from the  $\chi^2$  difference with and without the input, interpreted with the appropriate number of degrees of freedom.

Another potential anomaly related to the  $|\epsilon_K|$  asymmetry has been widely discussed in the literature [5, 6], but does not show up with our choice of inputs and statistical treatment. More details can be found in the Appendix. Other interesting outcomes of the SM global fit concern the prediction of the recently measured CP-asymmetries by the TeVatron experiments, namely in  $B_s \rightarrow J/\psi\phi$  and in dimuonic inclusive decays (see Section 3). The discrepancy of these measurements with respect to their SM fit prediction, together with the  $\mathcal{B}(B \rightarrow \tau\nu)$  anomaly, are summarized in Table 10. It is worth noting that the SM does not correlate these anomalies between each other, because the standard prediction for CP-violation ( $-2\beta_s$  and  $a_{\text{fs}}$ ) in the  $B_s$  system is essentially zero, and hence at leading order has no common parameter with the  $\mathcal{B}(B \rightarrow \tau\nu)$  anomaly.

## 4.2 Scenario I: New Physics in $B_d - \bar{B}_d$ mixing and $B_s - \bar{B}_s$ mixing

In this section we present the CKM fit for scenario I where New Physics in mixing is independently allowed in the  $B_d$  and  $B_s$  system (*i.e.*  $\Delta_d$  and  $\Delta_s$  are independent). These fits exclude the constraint from  $\epsilon_K$  since it is not possible to obtain non-trivial constraints for the three NP parameters in the  $K$  sector. The first study of this kind using only  $B$ -factory data has been performed in [49] followed by a complete quantitative analysis [44] profiting from the large data sets of *BABAR* and *Belle*. Analyses taking also into account the  $B_s$  system have been performed by the UTfit collaboration [141, 142].

In Fig. 7 we show the  $\bar{\rho} - \bar{\eta}$  plane for this fit, allowing us to constrain the parameters of the CKM matrix using observables not affected by New Physics according to our hypothesis. There are two allowed solutions in  $\bar{\rho} - \bar{\eta}$  which can not be distinguished when using only  $|V_{ud}|$ ,  $|V_{us}|$ ,  $|V_{cb}|$ ,  $|V_{ub}|$  from semileptonic decays and from  $B \rightarrow \tau\nu$ ,  $\gamma$  and  $\alpha - \phi_d^\Delta/2$  and  $\beta + \phi_d^\Delta/2$ . Once  $a_{\text{fs}}^d$  is added, the second solution at negative  $\bar{\rho}$  and  $\bar{\eta}$  values is clearly disfavoured leaving as the only solution the one with positive  $\bar{\rho}$  and  $\bar{\eta}$  values. Figures 8

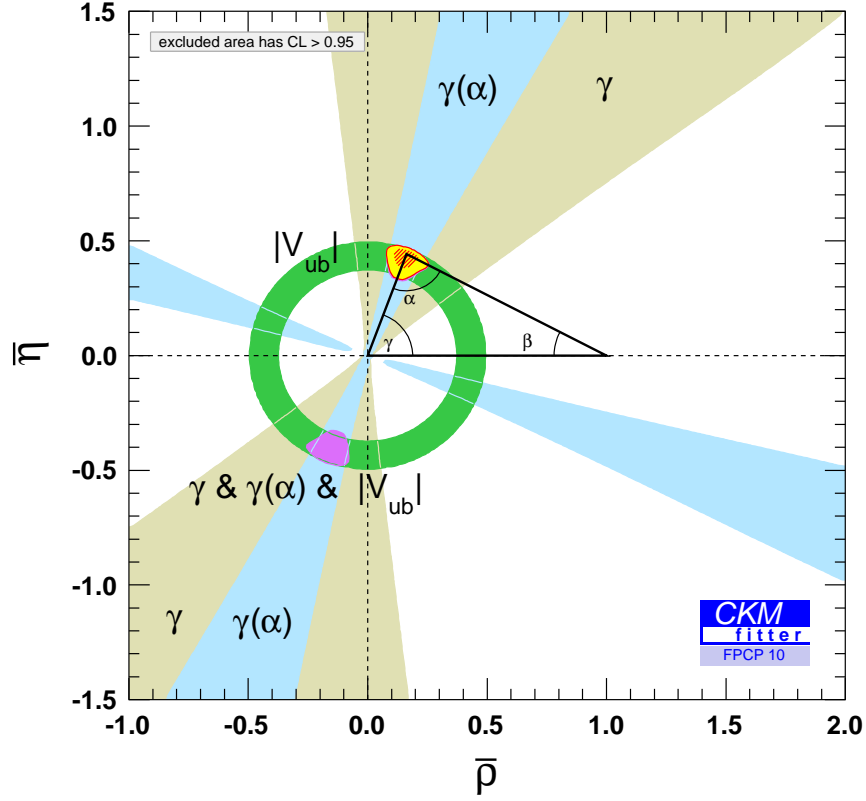


Figure 7: Constraint on the CKM  $(\bar{\rho}, \bar{\eta})$  coordinates, using only the inputs which are not affected by new physics in mixing:  $|V_{ud}|$ ,  $|V_{us}|$ ,  $|V_{cb}|$ ,  $|V_{ub}|$  from semileptonic decays and from  $B \rightarrow \tau\nu$ ,  $\gamma$  (directly and from the combination of  $\alpha - \phi_d^\Delta/2$  and  $\beta + \phi_d^\Delta/2$ ). Regions outside the coloured areas have  $\text{CL} > 95.5\%$ . For the combined fit, two solutions are available: the usual solution corresponds to the yellow area (points with  $\text{CL} < 95.4\%$ , the shaded region corresponding to points with  $\text{CL} < 68.3\%$ ), and the second solution corresponds to the purple region.

and 9 show the results of the global fit for scenario I in the complex  $\Delta_d$  and  $\Delta_s$  planes, respectively. We emphasize that we assume that  $\Delta_d$  and  $\Delta_s$  are taken as independent in this scenario, but that some of the constraints correlate them (such that  $a_{fs}^d$  from the inclusive dimuon asymmetry, and the ratio  $\Delta m_d/\Delta m_s$ ). Therefore the figures should be understood as two-dimensional projections of a single multidimensional fit, and not as independent computations. The constraint from  $\Delta m_d$  in the  $\text{Re}\Delta_d - \text{Im}\Delta_d$  plane shows two allowed ring-like regions. They correspond to the two allowed solutions in the  $\bar{\rho} - \bar{\eta}$  plane when  $a_{fs}^d$  is excluded from the list of inputs. Indeed, in this NP scenario,  $\Delta m_d$  is proportional to the product  $|\Delta_d|^2 \cdot |V_{td}V_{tb}^*|^2$ , where the second factor is different for the two allowed solutions since it is the side of the unitarity triangle relating  $(1, 0)$  and  $(\bar{\rho}, \bar{\eta})$ . The impact of  $a_{fs}^d$  highlights the power of this measurement to exclude a large region of the possible

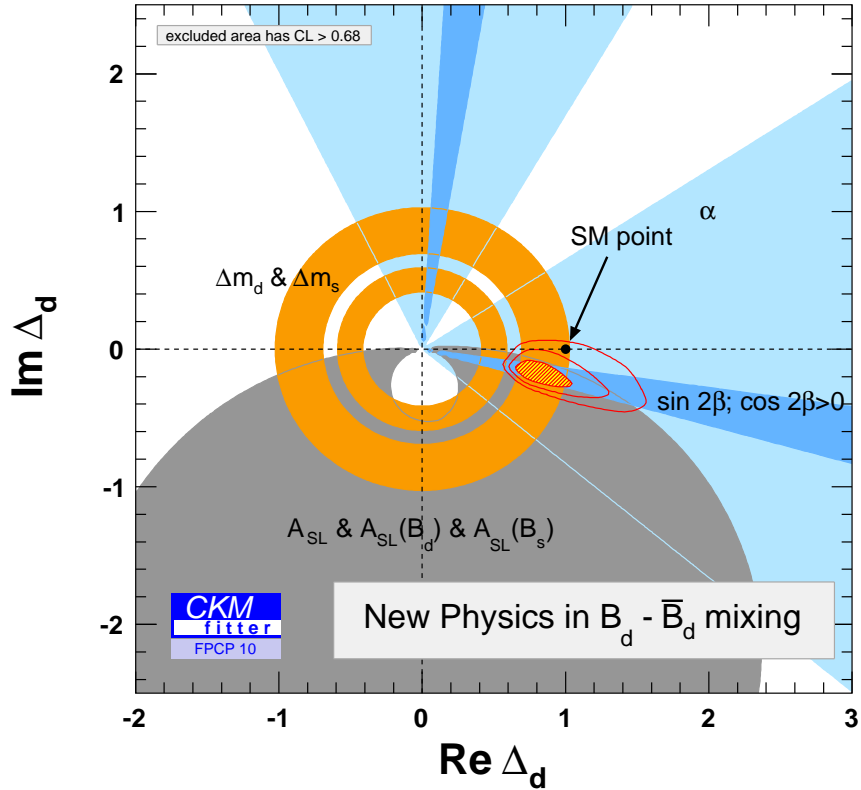


Figure 8: Constraint on the complex parameter  $\Delta_d$  from the fit in scenario I. For the individual constraints the coloured areas represent regions with  $CL < 68.3\%$ . For the combined fit the red area shows the region with  $CL < 68.3\%$  while the two additional contour lines inscribe the regions with  $CL < 95.45\%$ , and  $CL < 99.73\%$ , respectively.

NP parameter space even with a measurement precision of  $O(5 \cdot 10^{-3})$ . In the combined fit the inner ring (which corresponds to the solution for  $\phi_d^\Delta$  in the first quadrant near the  $\text{Im } \Delta_d$  axis) in the complex  $\Delta_d$  plane is disfavoured. This leaves us with an allowed region for  $|\Delta_d|$  which is in agreement with the SM value  $\Delta_d = 1$ , albeit with possible deviations up to 40%. The New Physics phase  $\phi_d^\Delta$ , mainly driven by the  $\mathcal{B}(B \rightarrow \tau\nu)$  vs.  $\sin 2\beta$  correlation, can be as large as  $-12^\circ$  and shows currently a deviation from the Standard Model of  $2.5\sigma$ . It is interesting to note that the combined individual constraint from  $a_{\text{fs}}^d$ ,  $a_{\text{fs}}^s$  and  $a_{\text{fs}}$  also favours a negative New Physics phase  $\phi_{\Delta_d}$ , mainly due to the measured negative  $a_{\text{fs}}^d$  value. When  $\mathcal{B}(B \rightarrow \tau\nu)$  is excluded from the inputs  $\text{Im } \Delta_d$  and hence  $\phi_{\Delta_d}$  is in good agreement with the Standard Model value (see Fig. 11). At the same time the allowed range for  $|\Delta_d|$  is significantly enlarged since  $\mathcal{B}(B \rightarrow \tau\nu)$  helps to reduce the uncertainty on  $\Delta m_d$ : the two rings are enlarged and merge into a single one.

The constraint on  $|\Delta_s|$  from  $\Delta m_s$  is more stringent than that for  $|\Delta_d|$  - thanks to the

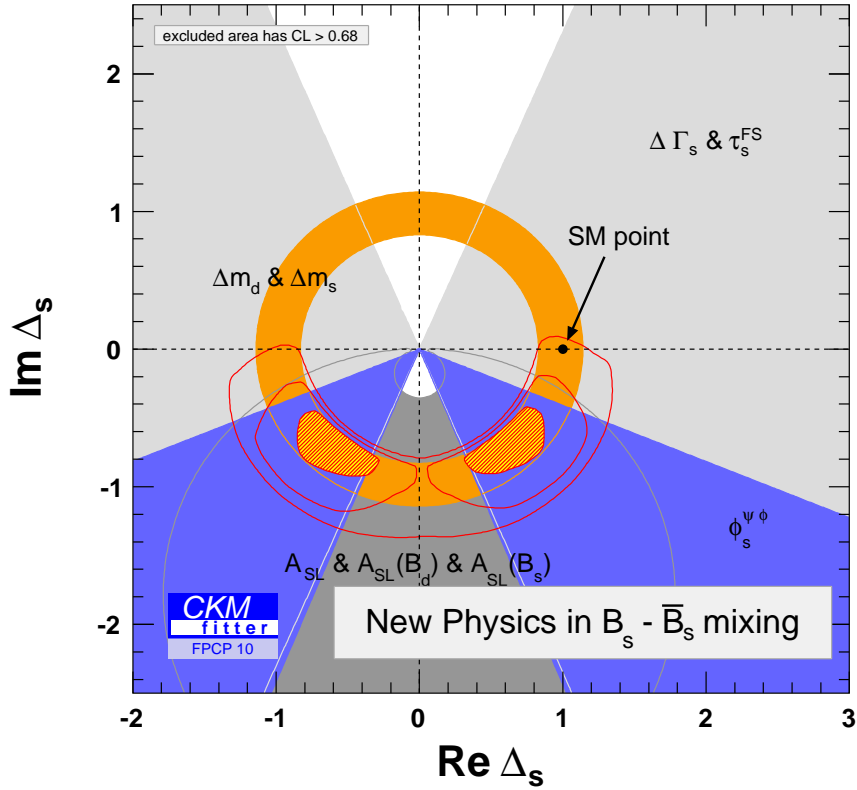


Figure 9: Constraint on the complex parameter  $\Delta_s$  from the fit in scenario I. For the individual constraints the coloured areas represent regions with  $\text{CL} < 68.3\%$ . For the combined fit the red area shows the region with  $\text{CL} < 68.3\%$  while the two additional contour line inscribe the regions with  $\text{CL} < 95.45\%$ , and  $\text{CL} < 99.73\%$ , respectively.

smaller theoretical uncertainty in its prediction compared to  $\Delta m_d$  - and in good agreement with the Standard Model point. It is interesting to note that also for the  $B_s$  system the constraint from  $\mathcal{B}(B \rightarrow \tau\nu)$  plays a non-negligible role: when removing this measurement from the list of inputs the constraint on  $|\Delta_s|$  becomes weaker since this measurement improves the input on the decay constant  $f_{B_s}$  through the SU(3)-breaking parameter  $\xi$  (compare Fig. 12 with Fig. 9). There is evidence for a non-zero NP phase  $\phi_s^\Delta$  at the  $3.1\sigma$  level. This discrepancy is driven by the  $a_{fs}$  from D0 and by the  $\phi_s^\Delta - 2\beta_s$  analyses from Tevatron, but is expected to be somewhat relaxed by the updated measurements [29, 30].

We note also that there is an interesting difference in the allowed size of the NP contribution when comparing the  $B_d$  and the  $B_s$  systems. While in the  $B_s$  system the size of the NP contribution is essentially constrained by the  $\Delta m_s$  measurement alone this is not the case in the  $B_d$  system. Indeed, the theoretical prediction of  $\Delta m_d$  strongly depends on the Wolfenstein parameters  $\bar{\rho}$  and  $\bar{\eta}$  whereas this dependence is very weak for  $\Delta m_s$ .

The constraint on NP in  $B_d$ -mixing relies thus on  $|V_{ub}|$  on one hand and  $\gamma$  on the other hand, the latter being currently dominated by the combination of the  $\sin 2\beta$  and  $\alpha$  measurements which is independent of NP contributions in  $B$ -mixing. The theory prediction for the oscillation frequency  $\Delta m_d$  depends on the quantity  $|\Delta_d| \equiv \sqrt{(\text{Re } \Delta_d)^2 + (\text{Im } \Delta_d)^2}$ . Without a good constraint on  $|\Delta_d|$  from other observables it can only be predicted with a very large uncertainty as observed in Table 9. The only other observables that are sensitive to the modulus of  $\Delta_d$  are  $a_{\text{fs}}^d$  and  $a_{\text{fs}}$  but those are measured with a precision that is significantly above the SM prediction and thus do not constrain very much the range of  $\Delta m_d$  (even though they proved powerful in eliminating the negative  $(\bar{\rho}, \bar{\eta})$  solution) (the same statement holds for  $\Delta m_s$ ).

Tables 8 and 9 show the fit results for various parameters. We also show the result of the fit for observables that have been individually excluded from the fit in order to quantify possible deviations between the individual input values and their fit predictions. Among other things it is interesting to note that the indirect fit prediction for the dimuonic asymmetry  $a_{\text{fs}} = (-42^{+19}_{-18}) \times 10^{-4}$  is a bit smaller in magnitude than the  $D\bar{O}$  measurement  $(-95.7 \pm 25.1 \pm 14.6) \times 10^{-4}$ , and remain more precise in spite of the uncertainties on the theoretical and New Physics parameters. Hence future improvements of this measurement are expected to give crucial information on the underlying physics.

In contrast to the SM fit, our Scenario I relates the  $B_d$  and  $B_s$  anomalies through the correlated determination of the  $\Delta$  parameters. Hence it is particularly interesting to compute the p-values associated with the hypothesis that some specific combination of the  $\Delta$  parameters take their SM value. This is shown in Table 13. We also learn from this table that the Scenario III to be discussed below, is slightly disfavoured by the data when one considers it as a subcase of Scenario I ( $\Delta_d = \Delta_s$ ), in agreement with the third paper of Ref. [32]. Finally as already stressed above, the various evidences against the SM shown in Table 13 will be relaxed when the new TeVatron average of the  $B_s \rightarrow J/\psi\phi$  tagged analysis is available [29, 30]. However a very rough estimate allows us to predict that at least the  $\text{Im}(\Delta_d) = \text{Im}(\Delta_s) = 0$  hypothesis (*i.e.* no CP-violating phase in neither  $B_d$  nor  $B_s$  mixing amplitudes) will remain disfavoured by more than three standard deviations. Indeed although the mixing CP-phase is expected to come back closer to the SM value [29, 30], it remains well compatible with the indirect constraint from the dimuonic asymmetry, as shown by Fig. 10.

| Quantity                                   | central $\pm$ CL $\equiv 1\sigma$                           | $\pm$ CL $\equiv 2\sigma$                                   | $\pm$ CL $\equiv 3\sigma$    |
|--|---|---|------------------------------|
| $A$  | $0.814^{+0.014}_{-0.028}$                                   | $0.814^{+0.023}_{-0.037}$                                   | $0.814^{+0.033}_{-0.046}$    |
| $\lambda$                                  | $0.22511^{+0.00074}_{-0.00075}$                             | $0.2251^{+0.0015}_{-0.0015}$                                | $0.2251^{+0.0022}_{-0.0022}$ |
| $\bar{\rho}$                               | $0.157^{+0.037}_{-0.032}$                                   | $0.157^{+0.071}_{-0.063}$                                   | $0.157^{+0.135}_{-0.096}$    |
| $\bar{\eta}$                               | $0.433^{+0.025}_{-0.025}$                                   | $0.433^{+0.039}_{-0.067}$                                   | $0.433^{+0.052}_{-0.112}$    |
| $\text{Re}(\Delta_d)$                      | $0.742^{+0.206}_{-0.066}$                                   | $0.74^{+0.42}_{-0.11}$                                      | $0.74^{+0.71}_{-0.16}$       |
| $\text{Im}(\Delta_d)$                      | $-0.161^{+0.045}_{-0.081}$                                  | $-0.16^{+0.11}_{-0.15}$                                     | $-0.16^{+0.20}_{-0.25}$      |
| $\phi_d^\Delta$ [deg]                      | $-12.3^{+3.3}_{-3.4}$                                       | $-12.3^{+8.7}_{-5.6}$                                       | $-12.3^{+14.9}_{-7.7}$       |
| $\text{Re}(\Delta_s)$                      | $-0.55^{+0.16}_{-0.19}$<br><i>or</i> $0.55^{+0.21}_{-0.13}$ | $-0.55^{+0.37}_{-0.43}$<br><i>or</i> $0.55^{+0.46}_{-0.35}$ | $-0.55^{+1.84}_{-0.70}$      |
| $\text{Im}(\Delta_s)$                      | $-0.68^{+0.14}_{-0.15}$                                     | $-0.68^{+0.37}_{-0.36}$                                     | $-0.68^{+0.63}_{-0.62}$      |
| $\phi_s^\Delta$ [deg]                      | $-129^{+12}_{-12}$<br><i>or</i> $-51.6^{+14.1}_{-9.4}$      | $-129^{+28}_{-27}$<br><i>or</i> $-52^{+32}_{-25}$           | $-129^{+127}_{-44}$          |
| $f_{B_s}$ [MeV] (!)                        | $280^{+82}_{-36}$   | $280^{+127}_{-61}$  | $280^{+159}_{-88}$           |
| $f_{B_s}/f_{B_d}$ (!)                      | $1.06^{+0.12}_{-0.22}$                                      | $1.06^{+0.30}_{-0.41}$                                      | $1.06^{+0.57}_{-0.48}$       |
| $\widehat{\mathcal{B}}_{B_s}$ (!)          | $2.17^{+0.71}_{-1.00}$                                      | $2.2^{+1.8}_{-1.5}$   | $2.2^{+3.1}_{-2.1}$          |
| $\mathcal{B}_{B_s}/\mathcal{B}_{B_d}$ (!)  | $0.48^{+0.66}_{-0.24}$                                      | $> 0.10$  | $> -0.01$                    |
| $\widetilde{\mathcal{B}}_{S,B_s}(m_b)$ (!) | $3.4^{+2.0}_{-2.9}$   | $3.4^{+5.2}_{-4.4}$   | $3.4^{+9.1}_{-6.1}$          |
| $J$ [ $10^{-5}$ ]                          | $3.73^{+0.15}_{-0.27}$                                      | $3.73^{+0.27}_{-0.63}$                                      | $3.73^{+0.38}_{-1.01}$       |
| $\alpha$ [deg]                             | $82^{+18}_{-12}$  | $82^{+33}_{-22}$  | $82^{+47}_{-31}$             |
| $\beta$ [deg]                              | $26.9^{+1.4}_{-2.0}$  | $26.9^{+2.2}_{-5.1}$  | $26.9^{+3.0}_{-8.6}$         |
| $\gamma$ [deg] (!)                         | $70.0^{+4.3}_{-4.5}$  | $70.0^{+8.5}_{-9.2}$  | $70^{+13}_{-20}$             |

Table 11: Fit results in the New Physics scenario I. The notation ‘(!)’ means that the fit output represents the indirect constraint, *i.e.* the corresponding direct input has been removed from the analysis.

| Quantity   | central $\pm$ CL $\equiv 1\sigma$                                 | $\pm$ CL $\equiv 2\sigma$                         | $\pm$ CL $\equiv 3\sigma$                        |
|--|---|---|--|
| $ V_{ud} (!)$  | $0.97444^{+0.00028}_{-0.00028}$                                   | $0.97444^{+0.00055}_{-0.00056}$                   | $0.97444^{+0.00082}_{-0.00084}$                  |
| $ V_{us} (!)$  | $0.22542^{+0.00095}_{-0.00095}$                                   | $0.2254^{+0.0019}_{-0.0019}$                      | $0.2254^{+0.0028}_{-0.0029}$                     |
| $ V_{ub} (!)$  | $0.00505^{+0.00117}_{-0.00065}$                                   | $0.0051^{+0.0018}_{-0.0012}$                      | $0.0051^{+0.0023}_{-0.0017}$                     |
| $ V_{cd} $   | $0.22498^{+0.00075}_{-0.00075}$                                   | $0.2250^{+0.0015}_{-0.0015}$                      | $0.2250^{+0.0022}_{-0.0022}$                     |
| $ V_{cs} $   | $0.97349^{+0.00021}_{-0.00018}$                                   | $0.97349^{+0.00038}_{-0.00036}$                   | $0.97349^{+0.00056}_{-0.00053}$                  |
| $ V_{cb} (!)$  | $0.0412^{+0.0122}_{-0.0076}$                                      | $0.041^{+0.031}_{-0.019}$                         | $0.041^{+0.045}_{-0.032}$                        |
| $ V_{td} $   | $0.00880^{+0.00036}_{-0.00051}$                                   | $0.00880^{+0.00066}_{-0.00087}$                   | $0.00880^{+0.00097}_{-0.00155}$                  |
| $ V_{ts} $   | $0.04053^{+0.00061}_{-0.00129}$                                   | $0.04053^{+0.00098}_{-0.00167}$                   | $0.0405^{+0.0014}_{-0.0020}$                     |
| $ V_{tb} $   | $0.999140^{+0.000053}_{-0.000026}$                                | $0.999140^{+0.000069}_{-0.000042}$                | $0.999140^{+0.000084}_{-0.000058}$               |
| $\phi_d^\Delta + 2\beta$ [deg] (!)                     | $31^{+15}_{-20}$  | $31^{+34}_{-44}$<br><i>or</i> $-149^{+57}_{-25}$  | $31^{+67}_{-67}$<br><i>or</i> $-149^{+96}_{-31}$ |
| $\phi_d$ [deg]   | $-17.2^{+4.3}_{-5.9}$   | $-17.2^{+10.1}_{-9.6}$                            | $-17^{+17}_{-13}$                                |
| $\phi_s^\Delta - 2\beta_s$ [deg] (!)                   | $-128^{+13}_{-17}$<br><i>or</i> $-58^{+17}_{-14}$                 | $-128^{+34}_{-51}$<br><i>or</i> $-58^{+50}_{-34}$ | $< 40$<br>$> 137$                                |
| $\phi_s$ [deg]   | $-129^{+12}_{-12}$<br><i>or</i> $-51.0^{+13.9}_{-9.8}$            | $-129^{+28}_{-27}$<br><i>or</i> $-51^{+32}_{-25}$ | $-129^{+127}_{-44}$                              |
| $\Delta m_d$ [ $\text{ps}^{-1}$ ] (!)                  | $0.25^{+0.30}_{-0.15}$  | $> 0.03$  |  |
| $\Delta m_s$ [ $\text{ps}^{-1}$ ] (!)                  | $10.5^{+12.0}_{-7.0}$   | $> 0.8$   |  |
| $a_{\text{fs}}$ [ $10^{-4}$ ] (!)                      | $-42^{+19}_{-18}$   | $-42^{+27}_{-26}$                                 | $-42^{+39}_{-32}$                                |
| $a_{\text{fs}}^d$ [ $10^{-4}$ ] (!)                    | $-34.2^{+11.9}_{-6.4}$  | $-34^{+23}_{-12}$                                 | $-34^{+35}_{-17}$                                |
| $a_{\text{fs}}^s$ [ $10^{-4}$ ] (!)                    | $-82^{+31}_{-10}$   | $-82^{+60}_{-21}$                                 | $-82^{+79}_{-28}$                                |
| $\Delta\Gamma_d$ [ $\text{ps}^{-1}$ ] (!)              | $0.00569^{+0.00077}_{-0.00230}$                                   | $0.0057^{+0.0013}_{-0.0033}$                      | $0.0057^{+0.0019}_{-0.0039}$                     |
| $\Delta\Gamma_s$ [ $\text{ps}^{-1}$ ] (!)              | $-0.114^{+0.066}_{-0.034}$<br><i>or</i> $0.126^{+0.026}_{-0.062}$ | $0.126^{+0.051}_{-0.298}$                         | $0.126^{+0.067}_{-0.191}$                        |
| $\mathcal{B}(B \rightarrow \tau\nu)$ [ $10^{-4}$ ] (!) | $1.470^{+0.075}_{-0.404}$   | $1.47^{+0.15}_{-0.86}$                            | $1.47^{+0.23}_{-0.92}$                           |

Table 12: Fit results in the New Physics scenario I. The notation ‘(!)’ means that the fit output represents the indirect constraint, *i.e.* the corresponding direct input has been removed from the analysis.

| Hypothesis   | p-value      |
|--|--------------|
| $\text{Im}(\Delta_d) = 0$ (1D)                       | $2.5 \sigma$ |
| $\text{Im}(\Delta_s) = 0$ (1D)                       | $3.1 \sigma$ |
| $\Delta_d = 1$ (2D)                                  | $2.5 \sigma$ |
| $\Delta_s = 1$ (2D)                                  | $2.7 \sigma$ |
| $\text{Im}(\Delta_d) = \text{Im}(\Delta_s) = 0$ (2D) | $3.8 \sigma$ |
| $\Delta_d = \Delta_s$ (2D)                           | $2.1 \sigma$ |
| $\Delta_d = \Delta_s = 1$ (4D)                       | $3.4 \sigma$ |

Table 13: p-values for various SM hypotheses in the framework of New Physics scenario I, in terms of the number of equivalent standard deviations. These numbers are computed from the  $\chi^2$  difference with and without the hypothesis constraint, interpreted with the appropriate number of degrees of freedom.

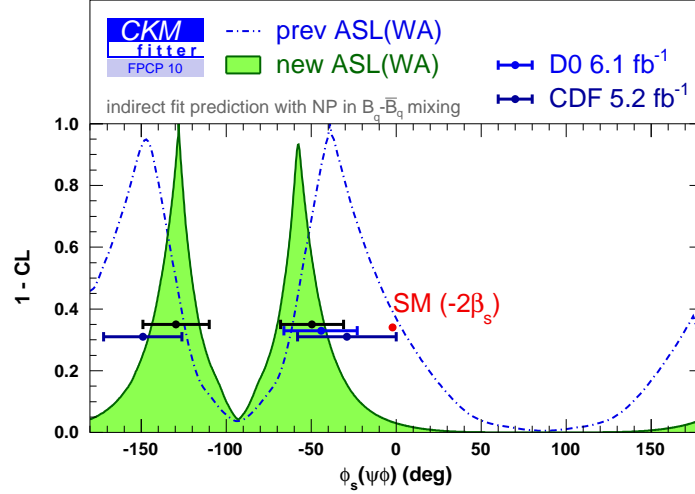


Figure 10: New Physics scenario I. Indirect constraint on the CP phase  $\phi_s^\Delta - 2\beta_s$  as measured in  $B_s \rightarrow J/\psi\phi$ , compared with the direct measurement by the TeVatron measurements: previous world average [134] (in black) and the Summer 2010 CDF and DØ updates [29, 30] (in blue). The dotted line represents the full scenario I fit with the previous world average for  $a_{fs}$ , while the green curve is the update after the DØ evidence for a non zero dimuonic asymmetry.

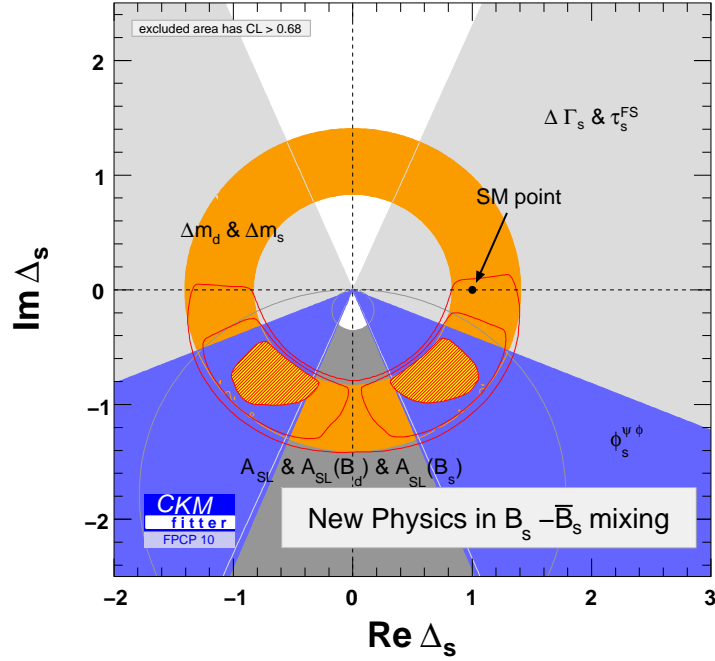


Figure 11: Fit result for the complex parameter  $\Delta_d$  in scenario I when excluding  $\mathcal{B}(B \rightarrow \tau\nu)$  from the list of inputs. For the individual constraints the coloured areas represent regions with  $\text{CL} < 68.3\%$ . For the combined fit the red area shows the region with  $\text{CL} < 68.3\%$  while the contour line inscribes the region with  $\text{CL} < 95.45\%$ .

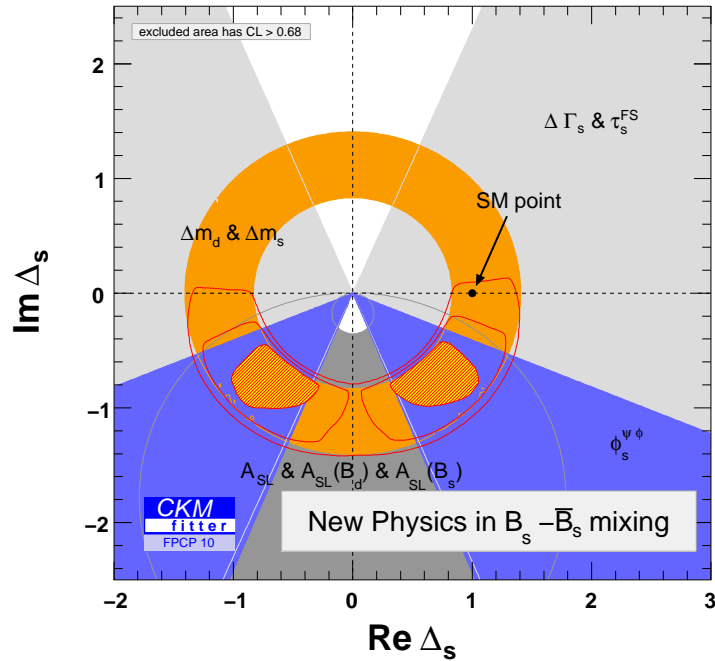


Figure 12: Fit result for the complex parameter  $\Delta_s$  in scenario I when excluding  $\mathcal{B}(B \rightarrow \tau\nu)$  from the list of inputs. For the individual constraints the coloured areas represent regions with  $\text{CL} < 68.3\%$ . For the combined fit the red area shows the region with  $\text{CL} < 68.3\%$  while the contour line inscribes the region with  $\text{CL} < 95.45\%$ .

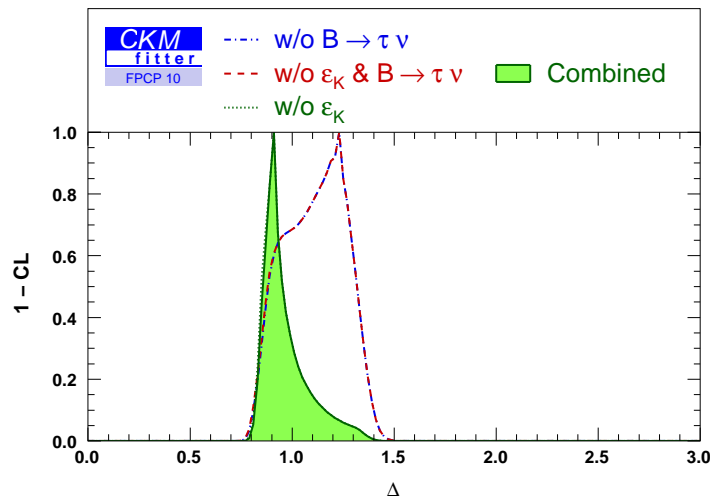


Figure 13: Constraint on the real parameter  $\Delta$  from the fit in scenario II. The red dashed line represents the constraint if only  $B_d$  and  $B_s$  observables are used excluding  $\mathcal{B}(B \rightarrow \tau\nu)$  and  $\epsilon_K$ . When adding  $\epsilon_K$  the constraint is essentially unchanged (blue dotted-dashed line). A significantly stronger constraint is obtained when adding  $\mathcal{B}(B \rightarrow \tau\nu)$  (dotted green). The full constrain when adding both,  $\mathcal{B}(B \rightarrow \tau\nu)$  and  $\epsilon_K$ , is shown in green.

### 4.3 Scenario II: MFV with small bottom–Yukawa coupling

In this section, we discuss the MFV scenario which allows to connect the  $B$  and Kaon sectors. Such a kind of numerical analysis has been first presented in [143]. In this scenario, there is only one additional real NP parameter  $\Delta$ , see Eq. (41). As a consequence, this scenario has difficulties to describe a situation where the data prefer a non-zero NP phase in  $B$ -mixing. Indeed the scenario II hypothesis embedded in scenario I, that is  $\Delta_d = \Delta_s = \Delta$  with  $\text{Im}(\Delta) = 0$ , is disfavoured by 3.5 standard deviations. The quality of the fit does not change when  $\epsilon_K$  is removed from the list of inputs.

Fig. 13 shows the impact of the various constraints on the parameter  $\Delta$ . The constraint is only slightly changed when adding to the  $B$ -meson observables - where  $\mathcal{B}(B \rightarrow \tau\nu)$  has been excluded - the  $\epsilon_K$  constraint. On the other hand, when adding  $\mathcal{B}(B \rightarrow \tau\nu)$ , the constraint gets significantly stronger at the  $1\sigma$  level while at  $2\sigma$  the reduction in the allowed parameter space is modest. In Tables 14 and 15 we further provide the constraints on individual parameters obtained from the combined fit in scenario II as well as predictions for the parameters not used as fit inputs. The compatibility of the parameter  $\Delta$  with one is good, meaning that this New Physics scenario does not describe the data better than the SM, as expected since all discussed anomalies seem to require new CP phases.

| Quantity                                   | central $\pm\text{CL} \equiv 1\sigma$ | $\pm\text{CL} \equiv 2\sigma$ | $\pm\text{CL} \equiv 3\sigma$ |
|--|---------------------------------------|-------------------------------|-------------------------------|
| $A$  | $0.8192^{+0.0093}_{-0.0228}$          | $0.819^{+0.019}_{-0.038}$     | $0.819^{+0.028}_{-0.048}$     |
| $\lambda$                                  | $0.22512^{+0.00075}_{-0.00075}$       | $0.2251^{+0.0015}_{-0.0015}$  | $0.2251^{+0.0022}_{-0.0022}$  |
| $\bar{\rho}$                               | $0.140^{+0.025}_{-0.024}$             | $0.140^{+0.048}_{-0.034}$     | $0.140^{+0.062}_{-0.043}$     |
| $\bar{\eta}$                               | $0.342^{+0.016}_{-0.012}$             | $0.342^{+0.031}_{-0.024}$     | $0.342^{+0.047}_{-0.036}$     |
| $\Delta$                                   | $0.907^{+0.091}_{-0.067}$             | $0.907^{+0.394}_{-0.099}$     | $0.91^{+0.51}_{-0.13}$        |
| $B_K$ (!)                                  | $0.88^{+0.23}_{-0.16}$                | $0.88^{+0.33}_{-0.29}$        | $0.88^{+0.42}_{-0.34}$        |
| $\kappa_\epsilon$ (!)                      | $1.16^{+0.39}_{-0.28}$                | $1.16^{+0.53}_{-0.44}$        | $1.16^{+0.65}_{-0.50}$        |
| $f_{B_s}$ [MeV] (!)                        | $252^{+10}_{-14}$                     | $252^{+19}_{-43}$             | $252^{+29}_{-75}$             |
| $\widehat{\mathcal{B}}_{B_s}$ (!)          | $0.777^{+0.525}_{-0.078}$             | $0.78^{+0.83}_{-0.14}$        | $0.78^{+1.20}_{-0.18}$        |
| $f_{B_s}/f_{B_d}$ (!)                      | $1.198^{+0.057}_{-0.036}$             | $1.198^{+0.108}_{-0.077}$     | $1.20^{+0.15}_{-0.19}$        |
| $\mathcal{B}_{B_s}/\mathcal{B}_{B_d}$ (!)  | $1.153^{+0.075}_{-0.105}$             | $1.15^{+0.15}_{-0.20}$        | $1.15^{+0.23}_{-0.29}$        |
| $\widetilde{\mathcal{B}}_{S,B_s}(m_b)$ (!) | $-1.1^{+1.4}_{-2.0}$                  | $-1.1^{+2.7}_{-3.5}$          | $-1.1^{+4.3}_{-4.8}$          |
| $J$ [ $10^{-5}$ ]                          | $2.98^{+0.15}_{-0.14}$                | $2.98^{+0.30}_{-0.29}$        | $2.98^{+0.45}_{-0.41}$        |
| $\alpha$ [deg] (!)                         | $93.1^{+4.9}_{-5.8}$                  | $93.1^{+7.3}_{-8.1}$          | $93.1^{+9.4}_{-10.0}$         |
| $\beta$ [deg] (!)                          | $28.09^{+0.70}_{-2.43}$               | $28.1^{+1.4}_{-5.4}$          | $28.1^{+2.1}_{-7.7}$          |
| $\gamma$ [deg] (!)                         | $67.6^{+3.8}_{-3.6}$                  | $67.6^{+5.5}_{-7.1}$          | $67.6^{+7.2}_{-9.3}$          |

Table 14: Fit results in the New Physics scenario II. The notation ‘(!)’ means that the fit output represents the indirect constraint, *i.e.* the corresponding direct input has been removed from the analysis.

| Quantity   | central $\pm\text{CL} \equiv 1\sigma$ | $\pm\text{CL} \equiv 2\sigma$      | $\pm\text{CL} \equiv 3\sigma$      |
|--|---------------------------------------|------------------------------------|------------------------------------|
| $ V_{ud} (!)$  | $0.97444^{+0.00028}_{-0.00028}$       | $0.97444^{+0.00055}_{-0.00056}$    | $0.97444^{+0.00082}_{-0.00084}$    |
| $ V_{us} (!)$  | $0.22545^{+0.00095}_{-0.00095}$       | $0.2254^{+0.0019}_{-0.0019}$       | $0.2254^{+0.0028}_{-0.0029}$       |
| $ V_{ub} (!)$  | $0.00354^{+0.00015}_{-0.00014}$       | $0.00354^{+0.00030}_{-0.00031}$    | $0.00354^{+0.00046}_{-0.00046}$    |
| $ V_{cd} $   | $0.22498^{+0.00075}_{-0.00075}$       | $0.2250^{+0.0015}_{-0.0015}$       | $0.2250^{+0.0022}_{-0.0022}$       |
| $ V_{cs} $   | $0.97348^{+0.00017}_{-0.00017}$       | $0.97348^{+0.00035}_{-0.00035}$    | $0.97348^{+0.00052}_{-0.00052}$    |
| $ V_{cb} (!)$  | $0.0490^{+0.0030}_{-0.0075}$          | $0.0490^{+0.0051}_{-0.0099}$       | $0.0490^{+0.0071}_{-0.0119}$       |
| $ V_{td} $   | $0.00865^{+0.00024}_{-0.00025}$       | $0.00865^{+0.00037}_{-0.00059}$    | $0.00865^{+0.00049}_{-0.00081}$    |
| $ V_{ts} $   | $0.04076^{+0.00038}_{-0.00111}$       | $0.04076^{+0.00076}_{-0.00175}$    | $0.0408^{+0.0011}_{-0.0022}$       |
| $ V_{tb} $   | $0.999132^{+0.000046}_{-0.000016}$    | $0.999312^{+0.000072}_{-0.000032}$ | $0.999132^{+0.000088}_{-0.000048}$ |
| $\phi_d$ [deg]   | $-7.7^{+3.5}_{-1.1}$                  | $-7.7^{+4.6}_{-2.2}$               | $-7.7^{+5.3}_{-3.5}$               |
| $\phi_s$ [deg]   | $0.39^{+0.90}_{-1.22}$                | $0.4^{+2.4}_{-2.4}$                | $0.4^{+3.2}_{-3.5}$                |
| $\Delta m_d$ [ps <sup>-1</sup> ] (!)                         | $0.541^{+0.082}_{-0.057}$             | $0.54^{+0.13}_{-0.12}$             | $0.54^{+0.18}_{-0.17}$             |
| $\Delta m_s$ [ps <sup>-1</sup> ] (!)                         | $16.6^{+1.7}_{-1.6}$                  | $16.6^{+3.8}_{-2.7}$               | $16.6^{+8.0}_{-3.7}$               |
| $a_{\text{fs}}$ [10 <sup>-4</sup> ] (!)                      | $-4.0^{+1.3}_{-1.1}$                  | $-4.0^{+3.4}_{-2.8}$               | $-4.0^{+5.0}_{-3.9}$               |
| $a_{\text{fs}}^d$ [10 <sup>-4</sup> ] (!)                    | $-8.3^{+2.6}_{-1.2}$                  | $-8.3^{+4.9}_{-3.2}$               | $-8.3^{+7.1}_{-4.6}$               |
| $a_{\text{fs}}^s$ [10 <sup>-4</sup> ] (!)                    | $0.4^{+1.4}_{-1.2}$                   | $0.4^{+2.7}_{-2.6}$                | $0.4^{+3.6}_{-5.0}$                |
| $\Delta\Gamma_d$ [ps <sup>-1</sup> ] (!)                     | $0.00311^{+0.00150}_{-0.00037}$       | $0.0031^{+0.0021}_{-0.0010}$       | $0.0031^{+0.0026}_{-0.0014}$       |
| $\Delta\Gamma_s$ [ps <sup>-1</sup> ] (!)                     | $0.162^{+0.020}_{-0.067}$             | $0.162^{+0.030}_{-0.091}$          | $0.162^{+0.040}_{-0.108}$          |
| $\mathcal{B}(B \rightarrow \tau\nu)$ [10 <sup>-4</sup> ] (!) | $0.639^{+0.310}_{-0.044}$             | $0.639^{+0.434}_{-0.081}$          | $0.64^{+0.54}_{-0.11}$             |

Table 15: Fit results in the New Physics scenario II. The notation ‘(!)’ means that the fit output represents the indirect constraint, *i.e.* the corresponding direct input has been removed from the analysis.

#### 4.4 Scenario III: Generic MFV

In Fig. 14 we present the result from the combined fit to  $B_d$  and  $B_s$  observables in the complex plane  $\Delta = \Delta_s = \Delta_d$  for the MFV hypothesis allowing for a large bottom Yukawa coupling  $y_b$  (scenario III). In scenario III  $\Delta$  can have a sizable complex component proportional to  $y_b^2$ . One expects that the constraint  $\Delta_s = \Delta_d$  reduces the size of the allowed NP contributions significantly with respect to the general case studied in scenario I. However, our fit result in Fig. 14 still allows for a NP contribution of order  $-20\%$  to  $+40\%$ . The NP phase in this scenario shows evidence for a deviation from the Standard Model since both  $a_{\text{fs}}$  and the  $\phi_s^\Delta$  measurement on the one hand and the discrepancy between  $\sin 2\beta$  measurement and  $\mathcal{B}(B \rightarrow \tau\nu)$  on the other hand, prefer a negative NP phase in  $B_{d,s}$  mixing.

Compared to scenario II this model is in much better agreement with the data regardless of whether one takes into account  $\mathcal{B}(B \rightarrow \tau\nu)$  as an input or not. While the  $B_d$  sector constraints do not allow too large a NP phase, the  $B_s$  sector prefers a large NP phase, though with large errors. As a consequence already discussed above, the quality of the fit in scenario III is significantly less good ( $2.1\sigma$ ) than in scenario I.

| Quantity                                   | central $\pm\text{CL} \equiv 1\sigma$ | $\pm\text{CL} \equiv 2\sigma$ | $\pm\text{CL} \equiv 3\sigma$ |
|--|---------------------------------------|-------------------------------|-------------------------------|
| $A$  | $0.7948^{+0.0286}_{-0.0091}$          | $0.7948^{+0.040}_{-0.018}$    | $0.795^{+0.050}_{-0.027}$     |
| $\lambda$                                  | $0.22506^{+0.00075}_{-0.00075}$       | $0.2251^{+0.0015}_{-0.0015}$  | $0.2251^{+0.0022}_{-0.0022}$  |
| $\bar{\rho}$                               | $0.175^{+0.031}_{-0.019}$             | $0.175^{+0.055}_{-0.033}$     | $0.175^{+0.067}_{-0.051}$     |
| $\bar{\eta}$                               | $0.441^{+0.013}_{-0.021}$             | $0.441^{+0.024}_{-0.051}$     | $0.441^{+0.034}_{-0.090}$     |
| $\text{Re}(\Delta)$                        | $0.886^{+0.141}_{-0.062}$             | $0.886^{+0.399}_{-0.099}$     | $0.886^{+0.49}_{-0.13}$       |
| $\text{Im}(\Delta)$                        | $-0.228^{+0.055}_{-0.051}$            | $-0.23^{+0.11}_{-0.13}$       | $-0.23^{+0.19}_{-0.21}$       |
| $\text{Arg}(\Delta)$ [deg]                 | $-14.4^{+2.9}_{-2.1}$                 | $-14.4^{+6.7}_{-4.2}$         | $-14.4^{+11.9}_{-6.4}$        |
| $\Delta_K^{tt}$                            | $1.01^{+0.40}_{-0.38}$                | $1.01^{+0.52}_{-0.43}$        | $1.01^{+0.69}_{-0.47}$        |
| $f_{B_s}$ [MeV] (!)                        | $270^{+24}_{-25}$                     | $270^{+50}_{-54}$             | $270^{+80}_{-87}$             |
| $\widehat{\mathcal{B}}_{B_s}$ (!)          | $1.37^{+0.34}_{-0.63}$                | $1.4^{+1.1}_{-1.3}$           | $< 3.1$                       |
| $f_{B_s}/f_{B_d}$ (!)                      | $1.210^{+0.067}_{-0.048}$             | $1.21^{+0.12}_{-0.10}$        | $1.21^{+0.17}_{-0.20}$        |
| $\mathcal{B}_{B_s}/\mathcal{B}_{B_d}$ (!)  | $1.171^{+0.091}_{-0.142}$             | $1.17^{+0.18}_{-0.25}$        | $1.17^{+0.28}_{-0.40}$        |
| $\widetilde{\mathcal{B}}_{S,B_s}(m_b)$ (!) | $0.9^{+1.0}_{-1.7}$                   | $0.9^{+3.0}_{-3.7}$           | $0.9^{+5.0}_{-5.1}$           |
| $J$ [ $10^{-5}$ ]                          | $3.62^{+0.18}_{-0.14}$                | $3.62^{+0.29}_{-0.38}$        | $3.62^{+0.39}_{-0.70}$        |
| $\alpha$ [deg] (!)                         | $87.6^{+3.4}_{-5.8}$                  | $87.6^{+5.9}_{-7.5}$          | $87.6^{+9.4}_{-8.9}$          |
| $\beta$ [deg] (!)                          | $27.94^{+0.66}_{-1.56}$               | $27.9^{+1.3}_{-3.7}$          | $27.9^{+2.1}_{-8.1}$          |
| $\gamma$ [deg] (!)                         | $68.4^{+2.3}_{-4.1}$                  | $68.4^{+3.6}_{-7.3}$          | $68.4^{+5.0}_{-8.9}$          |

Table 16: Fit results in the New Physics scenario III. The notation ‘(!)’ means that the fit output represents the indirect constraint, *i.e.* the corresponding direct input has been removed from the analysis.

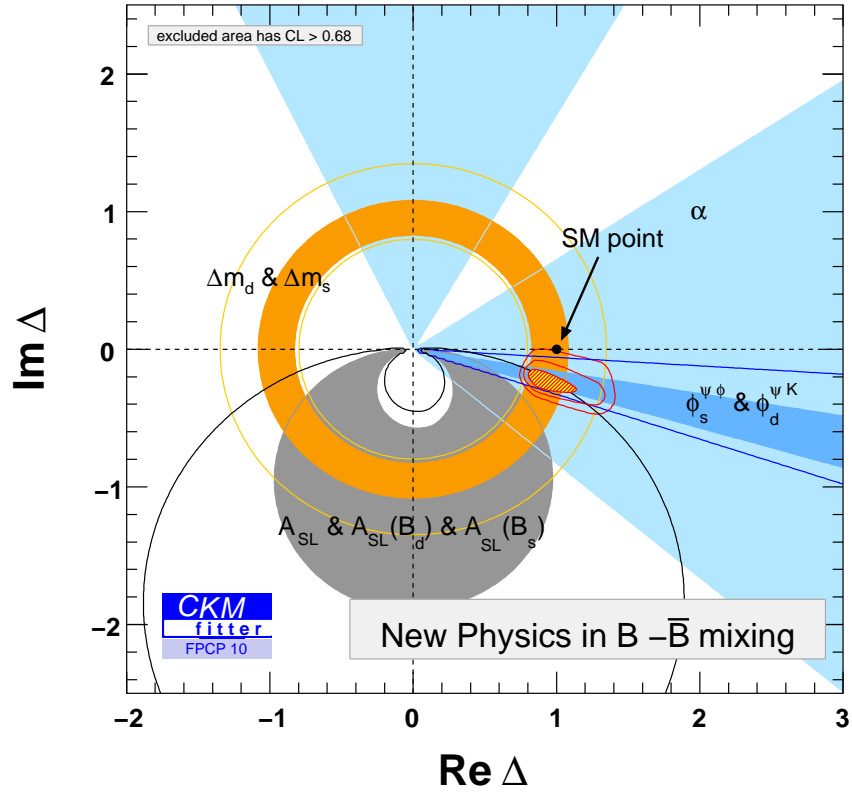


Figure 14: Constraint on the complex parameter  $\Delta \equiv \Delta_d = \Delta_s$  from the fit in scenario III. For the individual constraints the coloured areas represent regions with  $\text{CL} < 68.3\%$ . In addition, a  $\text{CL} < 95.45\%$  contour is shown for the individual constraints obtained from  $\Delta m_d$  and  $\Delta m_s$ , from  $a_{SL}$ ,  $a_{SL}^d$ , and  $a_{SL}^s$ , and from  $\phi_d^{\psi K}$  and  $\phi_s^{\psi\phi}$ . For the combined fit the red area shows the region with  $\text{CL} < 68.3\%$  while the two additional contour lines inscribe the regions with  $\text{CL} < 95.45\%$  and  $\text{CL} < 99.73\%$ , respectively.

| Quantity   | central $\pm\text{CL} \equiv 1\sigma$ | $\pm\text{CL} \equiv 2\sigma$      | $\pm\text{CL} \equiv 3\sigma$                          |
|--|---------------------------------------|------------------------------------|--|
| $ V_{ud} (!)$  | $0.97447^{+0.00028}_{-0.00028}$       | $0.97447^{+0.00055}_{-0.00056}$    | $0.97447^{+0.00082}_{-0.00084}$                        |
| $ V_{us} (!)$  | $0.22535^{+0.00095}_{-0.00095}$       | $0.22535^{+0.0019}_{-0.0019}$      | $0.22535^{+0.0028}_{-0.0029}$                          |
| $ V_{ub} (!)$  | $0.00596^{+0.00049}_{-0.00073}$       | $0.00596^{+0.00090}_{-0.00137}$    | $0.00596^{+0.0013}_{-0.0019}$                          |
| $ V_{cd} $   | $0.22494^{+0.00075}_{-0.00075}$       | $0.2249^{+0.0015}_{-0.0015}$       | $0.2249^{+0.0022}_{-0.0022}$                           |
| $ V_{cs} $   | $0.97354^{+0.00017}_{-0.00017}$       | $0.97354^{+0.00035}_{-0.00036}$    | $0.97354^{+0.00052}_{-0.00055}$                        |
| $ V_{cb} (!)$  | $0.0325^{+0.0035}_{-0.0038}$          | $0.0325^{+0.0092}_{-0.0080}$       | $0.033^{+0.016}_{-0.012}$                              |
| $ V_{td} $   | $0.00848^{+0.00038}_{-0.00031}$       | $0.00848^{+0.00053}_{-0.00057}$    | $0.00848^{+0.00066}_{-0.00071}$                        |
| $ V_{ts} $   | $0.03960^{+0.00136}_{-0.00038}$       | $0.03960^{+0.00184}_{-0.00075}$    | $0.0396^{+0.0022}_{-0.0011}$                           |
| $ V_{tb} $   | $0.999180^{+0.000015}_{-0.000058}$    | $0.999180^{+0.000030}_{-0.000078}$ | $0.999180^{+0.000045}_{-0.000095}$                     |
| $\text{Arg}(\Delta) + 2\beta$ [deg] (!)                      | $32.1^{+6.3}_{-8.8}$                  | $32^{+15}_{-29}$                   | $32^{+26}_{-44}$                                       |
| $\phi_d$ [deg]   | $-21.5^{+3.9}_{-4.0}$                 | $-21.5^{+8.1}_{-7.0}$              | $-21.5^{+13.7}_{-9.8}$<br><i>or</i> $-101^{+21}_{-18}$ |
| $\text{Arg}(\Delta) - 2\beta_s$ [deg] (!)                    | $-16.6^{+3.9}_{-2.5}$                 | $-16.6^{+8.7}_{-5.0}$              | $-16.6^{+15.2}_{-7.4}$                                 |
| $\phi_s$ [deg]   | $-14.0^{+3.0}_{-2.4}$                 | $-14.0^{+7.0}_{-4.9}$              | $-14.0^{+12.2}_{-7.3}$                                 |
| $\Delta m_d$ [ps <sup>-1</sup> ] (!)                         | $0.549^{+0.088}_{-0.076}$             | $0.55^{+0.14}_{-0.14}$             | $0.55^{+0.20}_{-0.20}$                                 |
| $\Delta m_s$ [ps <sup>-1</sup> ] (!)                         | $15.3^{+2.4}_{-1.1}$                  | $15.3^{+4.9}_{-2.2}$               | $15.3^{+8.0}_{-3.1}$                                   |
| $a_{\text{fs}}$ [10 <sup>-4</sup> ] (!)                      | $-21.5^{+6.4}_{-4.0}$                 | $-21.5^{+11.8}_{-8.9}$             | $-22^{+19}_{-15}$                                      |
| $a_{\text{fs}}^d$ [10 <sup>-4</sup> ] (!)                    | $-30.7^{+9.4}_{-4.4}$                 | $-30.7^{+14.4}_{-8.8}$             | $-31^{+21}_{-13}$                                      |
| $a_{\text{fs}}^s$ [10 <sup>-4</sup> ] (!)                    | $-14.2^{+3.5}_{-4.4}$                 | $-14.2^{+7.6}_{-13.3}$             | $-14^{+13}_{-19}$                                      |
| $\Delta\Gamma_d$ [ps <sup>-1</sup> ] (!)                     | $0.00398^{+0.00064}_{-0.00138}$       | $0.0040^{+0.0014}_{-0.0020}$       | $0.0040^{+0.0017}_{-0.0023}$                           |
| $\Delta\Gamma_s$ [ps <sup>-1</sup> ] (!)                     | $0.160^{+0.021}_{-0.065}$             | $0.160^{+0.032}_{-0.089}$          | $0.160^{+0.042}_{-0.107}$                              |
| $\mathcal{B}(B \rightarrow \tau\nu)$ [10 <sup>-4</sup> ] (!) | $1.37^{+0.13}_{-0.39}$                | $1.37^{+0.24}_{-0.63}$             | $1.37^{+0.33}_{-0.80}$                                 |

Table 17: Fit results in the New Physics scenario III. The notation ‘(!)’ means that the fit output represents the indirect constraint, *i.e.* the corresponding direct input has been removed from the analysis.

| Hypothesis                   | p-value      |
|------------------------------|--------------|
| $\text{Im}(\Delta) = 0$ (1D) | $3.4 \sigma$ |
| $\Delta = 1$ (2D)            | $3.1 \sigma$ |

Table 18: p-values for various SM hypotheses in the framework of New Physics scenario III, in terms of the number of equivalent standard deviations. These numbers are computed from the  $\chi^2$  difference with and without the hypothesis constraint, interpreted with the appropriate number of degrees of freedom.

In this scenario, the  $B_d$ - and  $B_s$ -systems decouple from the kaon system and hence the constraint on  $\text{Re}\Delta$  and  $\text{Im}\Delta$  can not be improved by adding  $\epsilon_K$  as this introduces the additional NP parameter  $\Delta_K^{tt}$  in the theoretical prediction for  $\epsilon_K$ . However, when including  $\epsilon_K$  in the fit one is able to constrain  $\Delta_K^{tt}$  from the fitted values of the CKM parameters. The parameter is in agreement with the SM expectation but could differ by more than 40 % from  $\Delta_K^{tt} = 1$ . Similarly to the previous scenarios, one-dimensional results from the fit in scenario III are shown in Tables 16 and 17. Again one sees that in particular the semileptonic asymmetries  $a_{\text{fs}}^d$  and  $a_{\text{fs}}$  are more precisely predicted than the measurements, so that improvements of the data will be extremely instructive.

Finally two tests of the SM are interesting to study within scenario III, and are shown in Table 18. As in scenario I, they show evidence for New Physics, and that scenario III describes the data significantly better than either the SM or scenario II, assuming as before that the improved data on  $B_s \rightarrow J/\psi\phi$  do not change the overall picture dramatically.

## 5 Conclusions

In this paper, we have studied three different scenarios of New Physics in  $\Delta F = 2$  transitions. The complex parameters quantifying the New Physics contributions to  $B_q - \bar{B}_q$  mixing are  $\Delta_q \equiv |\Delta_q| \cdot e^{i\phi_d^\Delta} \equiv M_{12}^q/M_{12}^{\text{SM},q}$ . In  $K - \bar{K}$  mixing three parameters  $\Delta_K^{tt}$ ,  $\Delta_K^{ct}$ , and  $\Delta_K^{cc}$  are needed.

We have first recalled the result of the Standard Model fit using the current available data sets. In the  $B$  system an interesting effect is observed: the inclusion of  $\mathcal{B}(B \rightarrow \tau\nu)$  obtained from a combination of *BABAR* and *Belle*'s measurements deviates from its prediction in the Standard Model fit by  $2.6 \sigma$  which either points to a large statistical fluctuation in the experimental numbers, to a problem in the calculation of the hadronic bag parameter  $\mathcal{B}_{B_d}$  on the Lattice, or to New Physics contributions in  $\sin 2\beta$  and/or in  $B \rightarrow \tau\nu$ . If there were New Physics contributions to  $B_d$  mixing this discrepancy would point to a negative non-vanishing NP phase  $\phi_d^\Delta$ . A second hint for a deviation is observed in the  $B_s - \bar{B}_s$  mixing phase  $2\beta_s$  measured in  $B_s \rightarrow J/\psi\phi$  though the significance is here only around  $2.1 \sigma$ . The largest discrepancy actually comes from the recent improved measurement of the dimuonic asymmetry by the *DØ* collaboration, which is at odds at the  $3.2 \sigma$  level with respect to the indirect fit prediction ( $3.0 \sigma$  when the average with the CDF measurement of the same quantity is made). Furthermore, the correction factor  $\kappa_\epsilon$  [6] in

the theoretical prediction of  $\epsilon_K$  decreases the quality of the Standard Model fit. However, with our inputs (especially the range for  $\hat{\mathcal{B}}_K$  in Tab. 7) and with the conservative Rfit error treatment of theoretical uncertainties used in our fit we do not observe a significant deviation between the measured  $\epsilon_K$  value and its prediction from a Standard Model fit excluding the  $\epsilon_K$  measurement.

In our New Physics scenario I, we have considered uncorrelated NP contributions to  $B_d$ ,  $B_s$  and  $K$  mixing. That is, the complex parameters  $\Delta_d$  and  $\Delta_s$  are allowed to vary independently and the Kaon sector is omitted, since the NP parameters  $\Delta_K^{tt}$ ,  $\Delta_K^{ct}$ , and  $\Delta_K^{cc}$  are unrelated to all other observables entering the fit. The experimental data are well described in this scenario which can accommodate negative NP phases preferred by a) the discrepancy between  $\mathcal{B}(B \rightarrow \tau\nu)$  and  $\sin 2\beta$  both measured at the B-factories *BABAR* and *Belle*, b) the  $2\beta_s$  measurements in  $B_s \rightarrow J/\psi\phi$  at the Tevatron, and c) the dimuon asymmetry  $a_{fs}$  measured by *DØ*. The size of the NP contribution both in  $B_s$ -mixing and  $B_d$ -mixing can be as large as 40 % and the hypothesis of zero new CP phases,  $\phi_d = \phi_s = 0$ , is disfavoured by as much as 3.8 standard deviations in this scenario (see Tab. 13). The large parameter region emphasises that, despite of the success of the *B*-factories and the Tevatron, there is still considerable room for NP in  $B_d$  as well as in  $B_s$  mixing.

In addition, we have considered two Minimal Flavour Violation scenarios. The first MFV scenario, scenario II, corresponds to small bottom Yukawa couplings, leading to  $\Delta_d = \Delta_s = \Delta_K^{tt} = \Delta$  with all NP phases identical to zero,  $\phi_s^\Delta = \phi_d^\Delta = \phi_K^{ij\Delta} = 0$ . This scenario  $\Delta_d = \Delta_s = \Delta_K^{tt} = \Delta$  with vanishing NP phases has been widely studied in the literature. In this scenario, the NP parameter  $\Delta_K^{cc}$  is equal to one to a very good approximation and  $\Delta_K^{ct}$  only deviates by a few percent from one where the deviation can be estimated in terms of  $\Delta_K^{tt}$ . Since in this scenario no NP phases are allowed, the deviations seen in the SM fit are still present. As a consequence, this MFV scenario is currently disfavoured by 3.5 standard deviation, but not totally excluded yet. The NP parameter  $\Delta$  can deviate from one by about +40 % at 95 % C.L.. The constraint gets only slightly relaxed when removing either  $\mathcal{B}(B \rightarrow \tau\nu)$  or  $\epsilon_K$  from the inputs to the fit.

Our scenario III is a generic MFV scenario with large bottom Yukawa coupling and arbitrary new flavour-blind CP phases. In this scenario the Kaon sector is unrelated to the *B*-sector. As in scenario II, one has  $\Delta_d = \Delta_s = \Delta$ , however, this time with a complex parameter  $\Delta$ . The NP parameters in  $\epsilon_K$  are unrelated to  $\Delta$  and  $\epsilon_K$  can be removed from the input list. However, when including  $\epsilon_K$  one is able to constrain the NP parameter  $\Delta_K^{tt}$  which is found to be consistent with the SM value of 1, but can deviate from unity by about  $\pm 40$  %. The fit describes the data significantly better than the SM fit and than the fit in scenario II since the data prefer a negative NP phase in  $B_d$  and in  $B_s$  mixings. The hypothesis of a zero new CP phase,  $\text{Im } \Delta = 0$ , is disfavoured by 3.4 standard deviations (see Tab. 18). As in the other NP scenarios, the allowed size of the NP contribution in  $B_d$  and in  $B_s$  mixing can be as large as +40 %.

The several scenarios discussed here show that we have indeed sensitivity to New Physics in the  $\Delta F = 2$  sector. While the overall picture of current data reveals strong hints for New Physics, the current experimental uncertainties prevent us from excluding the Standard Model, as highlighted by the *p*-values of each hypothesis. It has to be seen how this picture evolves with the improvement of both experimental and theoretical results.

When we completed this study, new results from the Tevatron experiments were given for the measurement of  $\beta_s$ , in better agreement with the Standard Model, which will be included in our analysis once the CDF and DØ collaborations have agreed on a combination of their results. Importantly, more precise measurement of the CP asymmetries in flavour-specific decays,  $a_{\text{fs}}^q$ , from either the Tevatron or the LHC experiments, may become crucial in the future: for the time being the theory-and-data driven fit predictions for  $a_{\text{fs}}^q$  are more precise than the direct measurements, as can be verified by comparing e.g. Tabs. 6 and 12. Hence future more precise data on  $a_{\text{fs}}^q$  could help to discriminate between the Standard Model and different scenarios of New Physics. Meanwhile, our predictions of  $a_{\text{fs}}^d$  in Tabs. 12, 14 and 16 are an important side result of our analyses: They permit a quick extraction of  $a_{\text{fs}}^s$  from future measurements of  $a_{\text{fs}}$  (or  $a_{\text{fs}}^s - a_{\text{fs}}^d$  envisaged by LHCb), which is more accurate than the common use of the experimental value of  $a_{\text{fs}}^d$  listed in Tab. 6.

Significant improvements on the measurement of  $\mathcal{B}(B \rightarrow \tau\nu)$  can only be expected from a Super-B-like electron-positron machine since the *BABAR* and Belle results do already rely on most of the available statistics collected at the B-factories PEP-II and KEKb. Since the theoretical translation of the ratio  $\mathcal{B}(B \rightarrow \tau\nu)/\Delta M_d$  into a constraint on CKM and NP parameters relies on the calculation of the decay constant  $f_{B_d}$  and the bag parameter  $B_d$ , future progress in Lattice QCD calculations is very important. The same remark applies to the hadronic matrix elements entering  $M_{12}^s$  and  $\Gamma_{12}^s$ . We hope that the current exciting experimental situation will stimulate novel activities in lattice gauge theory in this direction.

## ACKNOWLEDGMENTS

We thank D. Becirevic, D. Guadagnoli, L. Lellouch, M. Neubert and N. Uraltsev for stimulating discussions and comments. We would also like to thank the members of the CKMfitter group for their interest and support for the various aspects of this article.

This work was partially supported by the EU Contract No. MRTN-CT-2006-035482, FLAVIANet. The work of UN is supported by the DFG through project C6 of the collective research centre SFB-TR9 and by BMBF grant 05H09VKF.

## A Relationship between $\epsilon_K$ and $K-\bar{K}$ mixing

### A.1 Corrections to the usual $\epsilon_K$ formula

In Sec. 2.2, we have discussed the connection between  $\epsilon_K$  and  $K-\bar{K}$  mixing. The resulting equation, Eq. (25), has been obtained thanks to several approximations (concerning the phase  $\phi_\epsilon$ , neglect of  $\xi$ , computation of  $M_{12}$  from lowest-dimension operators of the effective Hamiltonian). The corrections to these approximations are encoded in the deviation of the factor  $\kappa_\epsilon$  from 1. A series of papers [6, 35, 60, 61] has assessed more precisely the value of this factor in order to account for the terms neglected by the previous approximations.

$\xi \neq 0$  and  $\phi_\epsilon \neq 45^\circ$  imply  $\kappa_\epsilon \neq 1$ , Ref. [6] finds  $\kappa_\epsilon = 0.92 \pm 0.02$ . In Ref. [70] a lattice QCD calculation of  $\text{Im} A_2$  is combined with the experimental value of  $\epsilon'_K/\epsilon_K$  to compute  $\xi$  and finds agreement with Ref. [6] while quoting an even smaller uncertainty:

$\kappa_\epsilon = 0.92 \pm 0.01$ . Finally, correcting for  $\text{Im } M_{12}^K \neq \text{Im } M_{12}^{(6)}$  by including higher-order terms of the operator product expansion leads to  $\kappa_\epsilon = 0.94 \pm 0.02$ . Actually, in the correction factor  $\kappa_\epsilon$ , the three approximations have to be treated in different ways, since they mix uncertainties from experimental and theoretical origins. The correction from  $\phi_\epsilon$  is of experimental nature and can be treated easily.

The correction involving  $\xi$  could be computed by combining the experimental value of  $\text{Re } A_0$  and the theoretical computation of  $\text{Im } A_0$  using the effective Hamiltonian  $H^{|\Delta S|=1}$ . However, the latter is dominated by the matrix element of the QCD penguin in the  $I = 0$  channel  $\langle (\pi\pi)_0 | Q_6 | K \rangle$ , which is poorly known. Here we follow the method of Refs. [6,61,70] which uses  $\epsilon'_K$  to correlate  $\langle (\pi\pi)_0 | Q_6 | K \rangle$  with  $A_2$ . The latter amplitude involves the matrix element of the electroweak penguin  $Q_8$  in the  $I = 2$  channel,  $\langle (\pi\pi)_2 | Q_8 | K \rangle$ , which has been computed using lattice simulations and sum rules. Indeed, one finds [6]

$$\frac{\epsilon'_K}{\epsilon_K} = -\omega \frac{\xi}{\sqrt{2}|\epsilon_K|} (1 - \Omega), \quad \text{with} \quad \omega = \frac{\text{Re}A_2}{\text{Re}A_0}, \quad \Omega = \frac{1}{\omega} \frac{\text{Im}A_2}{\text{Im}A_0}. \quad (58)$$

$\omega = 0.0450$  is obtained from experiment, whereas  $\Omega$  describes the weight of the (imaginary part of the)  $I = 2$  contribution with respect to the  $I = 0$  one.

In practice, a numerical estimate of the contributions from other (subleading) operators than  $Q_6$  and  $Q_8$  in  $H^{|\Delta S|=1}$  has been obtained [59,144,145] under the assumptions that  $\text{Im } A_0$  and  $\text{Im } A_2$  can be computed accurately combining the effective Hamiltonian approach and experimental values for  $\text{Re } A_0$  and  $\text{Re } A_2$ :

$$\frac{\epsilon'_K}{\epsilon_K} = N_0 + N_1 \cdot R_6 + N_2 \cdot R_8, \quad R_6 = R_6[(\epsilon'/\epsilon)_{\text{exp}}, R_8] \quad (59)$$

where  $N_0, N_1, N_2$  are numbers, coming mainly from  $\lambda_t$ , the experimental values for the real parts of  $A_0$  and  $A_2$ , and  $R_6$  and  $R_8$  are rescaled bag parameters. Following the review of ref. [146], the authors of ref. [144] proposed the following conservative range  $R_8 = 1.0 \pm 0.2$  which we will follow. Using  $\epsilon'_K/\epsilon_K = (1.65 \pm 0.26) \cdot 10^{-3}$ , one can use eq.(59) to determine  $\Omega$ , which corresponds to the ratio between the  $I = 2$  and  $I = 0$  contributions to  $\epsilon'_K/\epsilon_K$ . In principle, this would require to split  $N_0$  into two pieces coming respectively from  $I = 0$  and  $I = 2$ , and to assess the size of these contributions following Ref. [59]. A quicker way to obtain a similar estimate consists in computing [145]:

$$\Omega_1 = \frac{N_2 \cdot R_8}{N_0 + N_1 \cdot R_6} \quad \Omega_2 = \frac{N_0 + N_2 \cdot R_8}{N_1 \cdot R_6} \quad (60)$$

where  $\Omega_1$  and  $\Omega_2$  correspond to the (extreme) hypothesis that  $N_0$  is saturated either by either by  $I = 0$  or  $I = 2$  contributions. Eq. (58) can be then used to compute  $\xi$  in either hypotheses, and we will take the spread of the obtained values as a (conservative) systematic uncertainty in the determination of  $\xi$ . A more detailed analysis of the contributions to  $N_0$  would allow us to decrease this systematic uncertainty.

The last correction comes from higher-dimension contributions to  $\text{Im}M_{12}$ . As shown in ref. [60], there are two different corrections at  $d = 8$ , corresponding to the  $\Delta S = 2$   $d = 8$  operators and the double insertion of  $\Delta S = 1$  operators connected by a  $u, c$  loop. The first is expected to be very suppressed compared to the  $d = 6$  contributions, whereas the

second one is essentially dominated by long-distance pion exchanges estimated in Chiral Perturbation Theory for weak processes, leading to:

$$\epsilon_K = \sin \phi_\epsilon e^{i\phi_\epsilon} \left[ \frac{\text{Im}M_{12}^{(6)}}{\Delta M} + \rho \xi \right], \quad \rho = 0.6 \pm 0.3. \quad (61)$$

For our purposes, it will be simpler to combine these corrections with the experimental input for  $\epsilon_K$ :

$$\epsilon_K^{(0)} = \epsilon_K \left( \frac{1}{\sqrt{2} \sin \phi_\epsilon} + \rho \frac{\epsilon'_K}{\epsilon_K} \frac{1}{\omega(1-\Omega)} \right) \equiv \frac{\epsilon_{K,exp}}{\kappa_\epsilon} \quad (62)$$

where  $\epsilon_K^{(0)}$  denote the approximate value of  $\epsilon_K$  in eq. (25) with  $\kappa_\epsilon = 1$ . Depending on the choice of  $\Omega$  (i.e. the respective part of  $I = 0$  and  $I = 2$  contributions in the formula for  $\epsilon'/\epsilon$ ), we get

$$\kappa_\epsilon^{(1)} = 0.943 \pm 0.003(\epsilon'/\epsilon) \pm 0.012(\phi_\epsilon) \pm 0.004(R_8) \pm 0.015(\rho) \quad (63)$$

$$\kappa_\epsilon^{(2)} = 0.940 \pm 0.003(\epsilon'/\epsilon) \pm 0.012(\phi_\epsilon) \pm 0.004(R_8) \pm 0.018(\rho) \quad (64)$$

Combining the first two errors in quadrature for the Gaussian part and the last two errors linearly and taking the spread of the values into the Rfit part, we obtain the estimate

$$\kappa_\epsilon = 0.940 \pm 0.013 \pm 0.023 \quad (65)$$

in good agreement with  $\kappa_\epsilon = 0.94 \pm 0.02$  in ref. [60]. This determination relies on the assumption that  $\epsilon'_K$  is not affected by New Physics.

## A.2 Error budget for $\epsilon_K$

Recently, it has been claimed that there is a discrepancy between the  $\epsilon_K$  constraint and its prediction [5, 6]. With the input values used in our fit and with the Rfit treatment of theoretical uncertainties we do not observe any sizeable discrepancy when comparing the prediction for  $\epsilon_K$  (Table 8) with its measured value (Table 6). This can also be seen in Fig. 3 where the combined fit prefers a region in  $\bar{\rho}$  and  $\bar{\eta}$  that is close to the edge of, though still inside the 95 % CL region of the  $\epsilon_K$  constraint.

As illustrated in Fig. 15 one can obtain a minor discrepancy at 1.2  $\sigma$  if one treats as Gaussian all the parameters involved in Eq. (25) (i.e.,  $|V_{cb}|$ ,  $\mathcal{B}_K$ ,  $\kappa_\epsilon$ , the QCD correction terms  $\eta_{cc,ct,tt}$  and the masses  $\bar{m}_{c,t}$ ), but such a treatment of the systematics remains questionable. Another way of seeing the absence of discrepancy is to compare the prediction for  $\kappa_\epsilon$  and estimates of these quantity. One can see clearly from Fig. 16 that the global fit can cope easily with a value of  $\kappa_\epsilon$  down to 0.9, and that the prediction from the global fit agrees well with the recent estimates of this quantity.

In order to make the comparison of our  $|\epsilon_K|$  analysis with the one of Ref. [70] easier we treat all the errors as Gaussian and calculate the error budget for the fit prediction of  $|\epsilon_K|$ . With our inputs we find

$$\begin{aligned} 10^3 |\epsilon_K| &= 1.911 \pm 0.020|_A \pm 0.021|_\lambda \pm 0.064|_{(\bar{\rho}, \bar{\eta})} \\ &\quad \pm 0.180|_{\mathcal{B}_K} \pm 0.019|_{\text{top}} \pm 0.088|_{\text{charm}} \pm 0.054|_{\kappa_\epsilon} \\ &= 1.91_{-0.24}^{+0.26} \end{aligned} \quad (66)$$

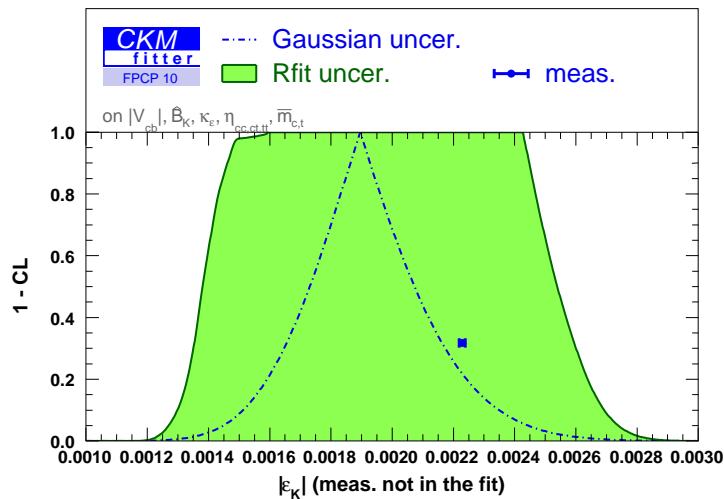


Figure 15: Constraint on  $|\epsilon_K|$  predicted from the global fit, compared to the experimental value. The green curve is obtained with our Rfit treatment of the uncertainties for the parameters entering Eq. (25). The dashed curve is obtained by treating all the errors as Gaussian.

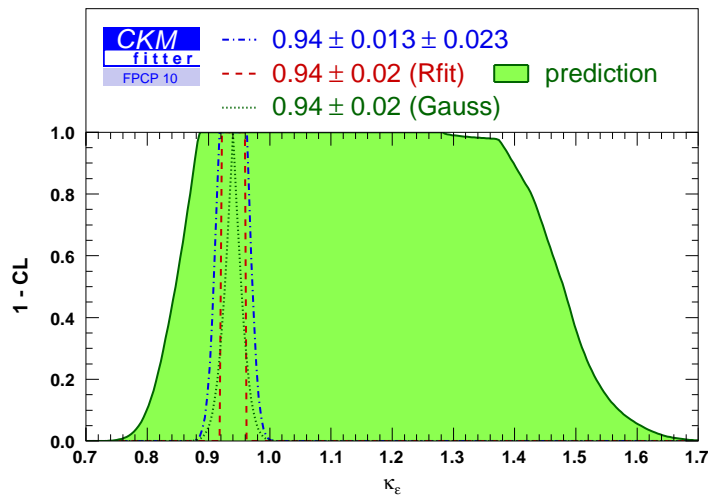


Figure 16: Constraint on  $\kappa_\epsilon$  predicted from the global fit using Eq. (25), compared to three different theoretical inputs  $\kappa_\epsilon = 0.94 \pm 0.02$  with either a Rfit or a Gaussian treatment of the error, or  $\kappa_\epsilon = 0.94 \pm 0.013 \pm 0.023$  corresponding to our own treatment of the uncertainties involved in its evaluation.

which is  $1.2 \sigma$  away from the experimental measurement, while with the inputs of the last

reference in [70] we find

$$\begin{aligned}
 10^3 |\epsilon_K| &= 1.769 \pm 0.019|_A \pm 0.019|_\lambda \pm 0.061|_{(\bar{\rho}, \bar{\eta})} \\
 &\quad \pm 0.062|_{\mathcal{B}_K} \pm 0.018|_{\text{top}} \pm 0.067|_{\text{charm}} \pm 0.033|_{\kappa_\epsilon} \\
 &= 1.77^{+0.18}_{-0.16}
 \end{aligned} \tag{67}$$

which is  $2.4 \sigma$  away from the experimental measurement, in agreement with [70]. Hence we see that the difference between our analysis and Ref. [70] mainly comes from our input for  $\mathcal{B}_K$  that has a larger theoretical error, and from our central value for  $|\epsilon_K|$  that is larger because of the different analysis of the CKM parameters. We thus conclude that the potential anomaly in  $|\epsilon_K|$  cannot yet be precisely quantified independently of the theoretical inputs and therefore deserves further investigations.

## References

- [1] N. Cabibbo, Phys. Rev. Lett. **10**, 531 (1963);  
M. Kobayashi and T. Maskawa, Prog. Theor. Phys. **49**, 652 (1973).
- [2] L. Wolfenstein, Phys. Rev. Lett. **51**, 1945 (1983).
- [3] A. J. Buras, M. E. Lautenbacher and G. Ostermaier, Phys. Rev. D **50**, 3433 (1994), arxiv:hep-ph/9403384].
- [4] R. S. Chivukula and H. Georgi, Phys. Lett. B **188**, 99 (1987);  
L. J. Hall and L. Randall, Phys. Rev. Lett. **65**, 2939 (1990);  
E. Gabrielli and G. F. Giudice, Nucl. Phys. B **433**, 3 (1995), [Erratum-ibid. B **507** (1997) 549], arxiv:hep-lat/9407029;  
A. Ali and D. London, Eur. Phys. J. **C9**, 687 (1999), arxiv:hep-ph/9903535;  
A. J. Buras, P. Gambino, M. Gorbahn, S. Jager and L. Silvestrini, Phys. Lett. B **500**, 161 (2001), arxiv:hep-ph/0007085;  
G. D'Ambrosio, G. F. Giudice, G. Isidori and A. Strumia, Nucl. Phys. B **645**, 155 (2002), arxiv:hep-ph/0207036;  
A. L. Kagan, G. Perez, T. Volansky and J. Zupan, Phys. Rev. D **80**, 076002 (2009), arxiv:0903.1794 [hep-ph]].
- [5] E. Lunghi and A. Soni, Phys. Lett. B **666**, 162 (2008), arxiv:0803.4340 [hep-ph].
- [6] A. J. Buras and D. Guadagnoli, Phys. Rev. D **78**, 033005 (2008), arxiv:0805.3887 [hep-ph].  
A. J. Buras and D. Guadagnoli, Phys. Rev. D **79**, 2009 (053010), arxiv:0901.2056 [hep-ph].
- [7] O. Deschamps (on behalf of the CKMfitter group), talk given at the International Conference for High Energy Physics, July 29 - August 5, 2008, Philadelphia, Pennsylvania.
- [8] M. Beneke, Phys. Lett. B **620**, 143 (2005), arxiv:hep-ph/0505075;  
H. n. Li and S. Mishima, JHEP **0703**, 009 (2007); arxiv:hep-ph/0610120;  
H. n. Li, S. Mishima and A. I. Sanda, Phys. Rev. D **72**, 114005 (2005), arxiv:hep-ph/0508041;  
A. R. Williamson and J. Zupan, Phys. Rev. D **74**, 014003 (2006) [Erratum-ibid. D **74** (2006) 03901], arxiv:hep-ph/0601214;  
J. Zupan, "Predictions for  $\sin 2(\beta/\phi_1)_{eff}$  in  $b \rightarrow s$  penguin dominated modes," *In the Proceedings of 5th Flavor Physics and CP Violation Conference (FPVP 2007), Bled, Slovenia, 12-16 May 2007, pp 012*, arxiv:0707.1323 [hep-ph]; T. Hurth, "Heavy Flavour theory," plenary talk given at the International Conference for High Energy Physics, July 29 - August 5, 2008, Philadelphia, Pennsylvania.

- [9] A. Lenz and U. Nierste, *JHEP* **0706**, 072 (2007), arxiv:hep-ph/0612167.
- [10] T. Moroi, *Phys. Lett. B* **493**, 366 (2000), arxiv:hep-ph/0007328;  
D. Chang, A. Masiero and H. Murayama, *Phys. Rev. D* **67**, 075013 (2003), arxiv:hep-ph/0205111;  
R. Harnik, D. T. Larson, H. Murayama and A. Pierce, *Phys. Rev. D* **69**, 094024 (2004), arxiv:hep-ph/0212180;  
S. Jäger and U. Nierste, *Eur. Phys. J. C* **33**, 256 (2004), arxiv:hep-ph/0312145;  
S. Jäger and U. Nierste, in *Proceedings of the 12th International Conference On Supersymmetry And Unification Of Fundamental Interactions (SUSY 04)*, 17-23 Jun 2004, Tsukuba, Japan, p. 675-678, Ed. K. Hagiwara, J. Kanzaki, N. Okada, arxiv:hep-ph/0410360.
- [11] M. Albrecht, W. Altmannshofer, A. J. Buras, D. Guadagnoli and D. M. Straub, *JHEP* **10**, 055 (2007), arxiv:0707.3954 [hep-ph];  
J. K. Parry and H. h. Zhang, *Nucl. Phys. B* **802**, 63 (2008), arxiv:0710.5443 [hep-ph];  
J. h. Park and M. Yamaguchi, *Phys. Lett. B* **670**, 356 (2009), arxiv:0809.2614 [hep-ph];  
P. Ko, J. h. Park and M. Yamaguchi, *JHEP* **11**, 051 (2008), arxiv:0809.2784 [hep-ph];  
S. Trine, S. Westhoff and S. Wiesenfeldt, *JHEP* **08**, 2 (2009), arxiv:0904.0378 [hep-ph];  
F. Borzumati and T. Yamashita, arxiv:0903.2793 [hep-ph];  
B. Dutta, Y. Mimura and Y. Santoso, arxiv:1007.3696 [hep-ph];  
C. Biggio and L. Calibbi, arxiv::1007.3750 [hep-ph].
- [12] L. Randall and S. f. Su, *Nucl. Phys. B* **540**, 37 (1999), arxiv:hep-ph/9807377;  
P. Ball, S. Khalil and E. Kou, *Phys. Rev. D* **69**, 115011 (2004), arxiv:hep-ph/0311361;  
M. Ciuchini and L. Silvestrini, *Phys. Rev. Lett.* **97**, 021803 (2006), arxiv:hep-ph/0603114;  
M. Endo and S. Mishima, *Phys. Lett. B* **640**, 205 (2006), arxiv:hep-ph/0603251;  
J. Foster, K.-i. Okumura and L. Roszkowski, *Phys. Lett. B* **641**, 452 (2006), arxiv:hep-ph/0604121;  
S. Khalil, *Phys. Rev. D* **74**, 035005 (2006), arxiv:hep-ph/0605021;  
S. Baek, *JHEP* **09**, 077 (2006), arxiv:hep-ph/0605182;  
R. Arnowitt, B. Dutta, B. Hu and S. Oh, *Phys. Lett. B* **641**, 305 (2006), arxiv:hep-ph/0606130;  
R.-M. Wang *et al.*, *High Energy Phys. Nucl. Phys* **31**, 332 (2007), arxiv:hep-ph/0609276;

- W. Altmannshofer, A. J. Buras and D. Guadagnoli, JHEP **11**, 065 (2007), arxiv:hep-ph/0703200;
- S.-L. Chen *et al.*, JHEP **09**, 044 (2007), arxiv:0706.1100 [hep-ph];
- T. Goto, Y. Okada, T. Shindou and M. Tanaka, Phys. Rev. D **77**, 095010 (2008), arxiv:0711.2935 [hep-ph];
- N. Kifune, J. Kubo and A. Lenz, Phys. Rev. D **77**, 076010 (2008), arxiv:0712.0503 [hep-ph];
- P. Ko and J.-h. Park and M. Yamaguchi, Phys. Rev. D **80**, 035019 (2009), arxiv:0809.0705 [hep-ph];
- K. Kawashima, J. Kubo and A. Lenz, Phys. Lett. B **681**, 60 (2009), arxiv:0907.2302 [hep-ph];
- L. L. Everett, J. Jiang, P. G. Langacker and T. Liu, arxiv:0911.5349 [hep-ph];
- J. K. Parry, arxiv:1006.5331 [hep-ph];
- P. Ko and J. h. Park, arxiv:1006.5821 [hep-ph];
- S. F. King, arxiv:1006.5895 [hep-ph];
- J. Kubo and A. Lenz, arxiv:1007.0680 [hep-ph];
- R. M. Wang, Y. G. Xu, M. L. Liu and B. Z. Li, arxiv:1007.2944 [hep-ph].
- [13] A. J. Buras, P. H. Chankowski, J. Rosiek and L. Slawianowska, Phys. Lett. B **546**, 96 (2002), arxiv:hep-ph/0207241;
- A. J. Buras, P. H. Chankowski, J. Rosiek and L. Slawianowska, Nucl. Phys. B **659**, 3 (2003), arxiv:hep-ph/0210145;
- M. S. Carena, A. Menon, R. Noriega-Papaqui, A. Szykman and C. E. M. Wagner, Phys. Rev. D **74**, 015009 (2006), arxiv:hep-ph/0603106;
- S. Trine, arxiv:0710.4955 [hep-ph].
- M. Gorbahn, S. Jager, U. Nierste and S. Trine, arxiv:0901.2065 [hep-ph];
- A. Crivellin and U. Nierste, Phys. Rev. D **81**, 095007 (2010), arxiv:0908.4404 [hep-ph];
- W. Altmannshofer, A. J. Buras, S. Gori, P. Paradisi and D. M. Straub, Nucl. Phys. B **830**, 17 (2010), arxiv:0909.1333 [hep-ph].
- [14] R. Mohanta and A. K. Giri, Phys. Rev. D **76**, 075015 (2007), arxiv:0707.1234 [hep-ph];
- A. Lenz, Phys. Rev. D **76**, 065006 (2007), arxiv:0707.1535 [hep-ph];
- S.-L. Chen *et al.*, Eur.Phys.J. **C59**, 899 (2009), arxiv:0710.3663 [hep-ph];
- C.-H. Chen, C.S. Kim Y.W. and Y. W. Yoon, Phys. Lett. B **671**, 250 (2009), arxiv:0801.0895 [hep-ph];
- J. K. Parry, Phys. Rev. D **78**, 114023 (2008), arxiv:0806.4350 [hep-ph];
- J. K. Parry, Mod.Phys.Lett. **A24**, 1835 (2009), arxiv:0810.0971 [hep-ph].

- [15] L. x. Lu and Z. j. Xiao, *Commun.Theor.Phys.* **47**, 1099 (2007), arxiv:hep-ph/0609279;  
S. L. Chen, N. G. Deshpande, X. G. He, J. Jiang and L. H. Tsai, *Eur. Phys. J.* **C53**, 607 (2008), arxiv:0705.0399 [hep-ph];  
A. S. Joshipura and B. P. Kodrani, *Phys. Lett. B* **670**, 369 (2009), arxiv:0706.0953 [hep-ph];  
E. Lunghi and A. Soni, *JHEP* **09**, 053 (2007), arxiv:0707.0212 [hep-ph];  
A. S. Joshipura and B. P. Kodrani, *Phys. Rev. D* **77**, 96003 (2008), arxiv:0710.3020 [hep-ph];  
A. S. Joshipura and B. P. Kodrani, *Phys. Rev. D* **81**, 035013 (2010), arxiv:0909.0863 [hep-ph];  
B. A. Dobrescu, P. J. Fox and A. Martin, arxiv:1005.4238 [hep-ph];  
M. Jung, A. Pich and P. Tuzon, arxiv:1006.0470 [hep-ph].
- [16] V. Barger, C. W. Chiang, J. Jiang and P. Langacker, *Phys. Lett. B* **596**, 229 (2004), arxiv:hep-ph/0405108;  
X. G. He and G. Valencia, *Phys. Rev. D* **74**, 013011 (2006), arxiv:hep-ph/0605202;  
S. Baek, J. H. Jeon and C. S. Kim, *Phys. Lett. B* **641**, 183 (2006), arxiv:hep-ph/0607113;  
J. M. Cabarcas, D. Gomez Dumm and R. Martinez, *Phys. Rev. D* **77**, 036002 (2008), arxiv:0711.2467 [hep-ph];  
S. Baek, J. H. Jeon and C. S. Kim, *Phys. Lett. B* **664**, 84 (2008), arxiv:0803.0062 [hep-ph];  
C. H. Chen, C. Q. Geng and L. Li, *Phys. Lett. B* **670**, 374 (2009), arxiv:0808.0127 [hep-ph];  
V. Barger, L. L. Everett, J. Jiang, P. Langacker, T. Liu and C. E. M. Wagner, *JHEP* **12**, 48 (2009), arxiv:0906.3745 [hep-ph];  
Q. Chang, X. Q. Li and Y. D. Yang, *JHEP* **02**, 082 (2010), arxiv:0907.4408 [hep-ph];  
C. H. Chen, *Phys. Lett. B* **683**, 160 (2010), arxiv:0911.3479 [hep-ph].
- [17] S. Chang, C. S. Kim and J. Song, *JHEP* **02**, 087 (2007), arxiv:hep-ph/0607313;  
M. Blanke, A. J. Buras, B. Duling, S. Gori and A. Weiler, *JHEP* **03**, 001 (2009), arxiv:0809.1073 [hep-ph];  
M. Bauer, S. Casagrande, U. Haisch and M. Neubert, arxiv:0912.1625 [hep-ph];  
C. Delaunay, O. Gedalia, S. J. Lee and G. Perez, arxiv:1007.0243 [hep-ph].
- [18] A. J. Buras, K. Gemmler and G. Isidori, arxiv:1007.1993 [hep-ph].
- [19] J. P. Lee and K. Y. Lee, arxiv:0809.0751 [hep-ph].

- [20] A. Arhrib and W. S. Hou, *Eur. Phys. J. C* **27**, 555 (2003), arxiv:hep-ph/0211267;  
W. S. Hou, M. Nagashima and A. Soddu, *Phys. Rev. D* **76**, 016004 (2007), arxiv:hep-ph/0610385;  
A. Soni, A. K. Alok, A. Giri, R. Mohanta and S. Nandi, *Phys. Lett. B* **683**, 302 (2010), arxiv:0807.1971 [hep-ph];  
M. Bobrowski, A. Lenz, J. Riedl and J. Rohrwild, *Phys. Rev. D* **79**, 113006 (2009), arxiv:0902.4883 [hep-ph];  
A. Soni, A. K. Alok, A. Giri, R. Mohanta and S. Nandi, arxiv:1002.0595 [hep-ph];  
A. J. Buras, B. Duling, T. Feldmann, T. Heidsieck, C. Promberger and S. Recksiegel, arxiv:1002.2126 [hep-ph];  
W. S. Hou and C. Y. Ma, arxiv:1004.2186 [hep-ph];  
O. Eberhardt, A. Lenz and J. Rohrwild, arxiv:1005.3505 [hep-ph];  
D. Choudhury and D. K. Ghosh, arxiv:1006.2171 [hep-ph].
- [21] J. A. Aguilar-Saavedra, *Phys. Rev. D* **67**, 035003 (2003), [Erratum-ibid. *D* **69** (2004) 099901], arxiv:hep-ph/0210112;  
J. A. Aguilar-Saavedra, F. J. Botella, G. C. Branco and M. Nebot, *Nucl. Phys. B* **706**, 204 (2005), arxiv:hep-ph/0406151;  
F. J. Botella, G. C. Branco and M. Nebot, *Phys. Rev. D* **79**, 096009 (2009), arxiv:0805.3995 [hep-ph];  
R. Mohanta and A. K. Giri, *Phys. Rev. D* **78**, 116002 (2008), arxiv:0812.1077 [hep-ph].
- [22] L. Mercolli and C. Smith, *Nucl. Phys. B* **817** (2009) 1 [arXiv:0902.1949 [hep-ph]].
- [23] M. Blanke, A. J. Buras, D. Guadagnoli and C. Tarantino, *JHEP* **0610**, 003 (2006), arxiv:hep-ph/0604057;  
M. Blanke, A. J. Buras, A. Poschenrieder, C. Tarantino, S. Uhlig and A. Weiler, *JHEP* **0612**, 003 (2006), arxiv:hep-ph/0605214;  
M. Blanke *et al.*, arxiv:0805.4393 [hep-ph];  
M. Blanke, A. J. Buras, B. Duling, S. Recksiegel and C. Tarantino, *Acta Phys. Polon.* **B41**, 657 (2010), arxiv:0906.5454 [hep-ph].
- [24] V. M. Abazov *et al.* [DØ collaboration], *Phys. Rev. Lett.* **97**, 021802 (2006), arxiv:hep-ex/0603029;  
A. Abulencia *et al.* [CDF collaboration], *Phys. Rev. Lett.* **97**, 062003 (2006), arxiv:hep-ex/0606027;  
V. M. Abazov *et al.* [DØ collaboration], Conference Note 5618, <http://www-d0.fnal.gov/Run2Physics/WWW/results/prelim/B/B54/B54.pdf>.

- 
- [25] A. Abulencia *et al.* [CDF collaboration], Phys. Rev. Lett. **97**, 242003 (2006), arxiv:hep-ex/0609040.
- [26] T. Aaltonen *et al.* [CDF collaboration], Phys. Rev. Lett. **100**, 161802 (2008), arxiv:0712.2397 [hep-ex].
- [27] V. M. Abazov *et al.* [DØ collaboration], Phys. Rev. Lett. **101**, 241801 (2008), arxiv:0802.2255 [hep-ex].
- [28] T. Aaltonen *et al.* [CDF collaboration], CDF public note 9458.
- [29] T. Aaltonen *et al.* [CDF collaboration], CDF public note 10206.
- [30] V. M. Abazov *et al.* ([DØ collaboration]), DØ Conference note 6098.
- [31] V. M. Abazov *et al.* ([DØ collaboration]), arxiv:1005.2757 [hep-ex], submitted to Phys. Rev. D;  
V. M. Abazov *et al.* [D0 Collaboration], arxiv:1007.0395 [hep-ex], submitted to Phys. Rev. Lett..
- [32] A. Dighe, A. Kundu and S. Nandi, arxiv:1005.4051 [hep-ph];  
C. H. Chen and G. Faisel, arxiv:1005.4582 [hep-ph];  
Z. Ligeti, M. Papucci, G. Perez and J. Zupan, arxiv:1006.0432 [hep-ph];  
C. W. Bauer and N. D. Dunn, arxiv:1006.1629 [hep-ph];  
N. G. Deshpande, X. G. He and G. Valencia, arxiv:1006.1682 [hep-ph];  
B. Batell and M. Pospelov, arxiv:1006.2127 [hep-ph];  
C. H. Chen, C. Q. Geng and W. Wang, arxiv:1006.5216 [hep-ph];  
Y. Bai and A. E. Nelson, arxiv:1007.0596 [hep-ph];  
K. Blum, Y. Hochberg and Y. Nir, arxiv:1007.1872 [hep-ph];  
A. J. Buras, G. Isidori and P. Paradisi, arxiv::1007.5291 [hep-ph].
- [33] C. Tarantino, arxiv:hep-ph/0702235;  
A. J. Lenz, AIP Conf. Proc. **1026**, 36 (2008), arxiv:0802.0977 [hep-ph]].
- [34] A. Lenz, U. Nierste and G. Ostermaier, Phys. Rev. D **56**, 7228 (1997), arxiv:hep-ph/9706501;  
A. Lenz, arxiv:hep-ph/0011258.
- [35] K. Anikeev *et al.*, Chapters 1.3 and 8.3, arxiv:hep-ph/0201071.
- [36] U. Nierste, “CP asymmetry in flavour-specific B decays,” in *Proceedings of the XXXIXth Rencontres de Moriond, Electroweak Interactions and Unified Theories*, 21-28 Mar 2004, La Thuile, Aosta Valley, Italy, Ed. J. Tran Thanh Van, arxiv:hep-ph/0406300;

- R. N. Cahn and M. P. Worah, Phys. Rev. D **60**, 076006 (1999), arxiv:hep-ph/9904480.
- [37] J. S. Hagelin and M. B. Wise, Nucl. Phys. B **189**, 87 (1981);  
J. S. Hagelin, Nucl. Phys. B **193**, 123 (1981);  
A. J. Buras, W. Slominski and H. Steger, Nucl. Phys. B **245**, 369 (1984);  
E. H. Thorndike, Ann. Rev. Nucl. Part. Sci. **35**, 195 (1985).
- [38] T. Inami and C. S. Lim, Prog. Theor. Phys. **65**, 297 (1981) [Erratum-ibid. **65**, 1772 (1981)].
- [39] A. J. Buras, M. Jamin and P. H. Weisz, Nucl. Phys. B **347**, 491 (1990).
- [40] Ref. [39], with a numerical update according to [9].
- [41] G. Buchalla, A. J. Buras and M. E. Lautenbacher, Rev. Mod. Phys. **68**, 1125 (1996), arxiv:hep-ph/9512380.
- [42] M. Beneke, G. Buchalla, A. Lenz and U. Nierste, Phys. Lett. B **576**, 173 (2003), arxiv:hep-ph/0307344.
- [43] T. Goto, N. Kitazawa, Y. Okada and M. Tanaka, Phys. Rev. D **53**, 6662 (1996), arxiv:hep-ph/9506311.
- [44] The CKMfitter Group (J. Charles *et al.*), Eur. Phys. J. C **41**, 1 (2005), arxiv:hep-ph/0406184; updated at <http://ckmfitter.in2p3.fr/>.
- [45] A.J. Buras, P. Gambino, M. Gorbahn, S. Jäger and L. Silvestrini, Phys. Lett. B **500**, 161 (2001), arxiv:hep-ph/0007085.
- [46] H. Lacker and A. Menzel, JHEP **1007**, 006 (2010), arxiv:1003.4532 [hep-ph].
- [47] J. M. Soares and L. Wolfenstein, for new physics,” Phys. Rev. D **47**, 1021 (1993);  
N. G. Deshpande, B. Dutta and S. Oh, Phys. Rev. Lett. **77**, 4499 (1996), arxiv:hep-ph/9608231;  
J. P. Silva and L. Wolfenstein, Phys. Rev. D **55**, 5331 (1997), arxiv:hep-ph/9610208;  
A. G. Cohen *et al.*, Phys. Rev. Lett. **78**, 2300 (1997), arxiv:hep-ph/9610252;  
Y. Grossman, Y. Nir and M. Worah, Phys. Lett. B **407**, 307 (1997), arxiv:hep-ph/9704287.
- [48] Y. Grossman, Y. Nir and G. Raz, Phys. Rev. Lett. **97**, 151801 (2006), arxiv:hep-ph/0605028.
- [49] S. Laplace, Z. Ligeti, Y. Nir and G. Perez, Phys. Rev. D **65**, 094040 (2002), arxiv:hep-ph/0202010.
- [50] K. Agashe *et al.*, arxiv:hep-ph/0509117.

- 
- [51] Z. Ligeti, M. Papucci and G. Perez, Phys. Rev. Lett. **97**, 101801 (2006), arxiv:hep-ph/0604112.
- [52] P. Ball and R. Fleischer, Eur. Phys. J. C **48**, 413 (2006), arxiv:hep-ph/0604249.
- [53] M. Bobrowski, A. Lenz, J. Riedl and J. Rohrwild, arxiv:0904.3971 [hep-ph];  
M. Bobrowski, A. Lenz, J. Riedl and J. Rohrwild, JHEP **03**, 009 (2010), arxiv:1002.4794 [hep-ph].
- [54] U. Nierste, arxiv:0904.1869 [hep-ph].
- [55] S. Herrlich and U. Nierste, Nucl. Phys. B **419**, 292 (1994), arxiv:hep-ph/9310311; numerical update in [147].
- [56] S. Herrlich and U. Nierste, Phys. Rev. D **52**, 6505 (1995), arxiv:hep-ph/9507262;  
S. Herrlich and U. Nierste, Nucl. Phys. B **476**, 27 (1996), arxiv:hep-ph/9604330; numerical update in [147].
- [57] J. Brod and M. Gorbahn, arxiv:1007.0684 [hep-ph].
- [58] L. L. Chau, Phys. Rept. **95** (1983) 1.
- [59] A. J. Buras, arXiv:hep-ph/0505175.
- [60] A. J. Buras, D. Guadagnoli and G. Isidori, Phys. Lett. B **688**, 309 (2010), arxiv:1002.3612 [hep-ph].
- [61] E. A. Andriyash, G. G. Ovanesyan and M. I. Vysotsky, Phys. Lett. B **599** (2004) 253 arxiv:hep-ph/0310314.
- [62] M. Beneke, G. Buchalla and I. Dunietz, Phys. Rev. D **54**, 4419 (1996), arxiv:hep-ph/9605259;  
M. Beneke, G. Buchalla, C. Greub, A. Lenz and U. Nierste, Phys. Lett. B **459**, 631 (1999), arxiv:hep-ph/9808385;  
M. Ciuchini, E. Franco, V. Lubicz, F. Mescia and C. Tarantino, JHEP **0308**, 031 (2003), arxiv:hep-ph/0308029.
- [63] M. Beneke, G. Buchalla, C. Greub, A. Lenz and U. Nierste, Nucl. Phys. B **639**, 389 (2002), arxiv:hep-ph/0202106.
- [64] I. Dunietz, R. Fleischer and U. Nierste, Phys. Rev. D **63**, 114015 (2001), arxiv:hep-ph/0012219.
- [65] L. J. Hall, R. Rattazzi and U. Sarid, Phys. Rev. D **50**, 7048 (1994), arxiv:hep-ph/9306309;  
R. Hempfling, Phys. Rev. D **49**, 6168 (1994);

- M. Carena, M. Olechowski, S. Pokorski and C. E. M. Wagner, Nucl. Phys. B **426**, 269 (1994), arxiv:hep-ph/9402253;
- T. Blazek, S. Raby and S. Pokorski, Phys. Rev. D **52**, 4151 (1995), arxiv:hep-ph/9504364;
- C. Hamzaoui, M. Pospelov and M. Toharia, Phys. Rev. D **59**, 095005 (1999), arxiv:hep-ph/9807350;
- K. S. Babu and C. F. Kolda, Phys. Rev. Lett. **84**, 228 (2000), arxiv:hep-ph/9909476;
- M. Carena, D. Garcia, U. Nierste and C. E. M. Wagner, Nucl. Phys. B **577**, 88 (2000), arxiv:hep-ph/9912516;
- M. S. Carena, D. Garcia, U. Nierste and C. E. M. Wagner, Phys. Lett. B **499**, 141 (2001), arxiv:hep-ph/0010003;
- G. Degrassi, P. Gambino and G. F. Giudice, JHEP **0012**, 009 (2000), arxiv:hep-ph/0009337;
- G. Isidori and A. Retico, JHEP **0111**, 001 (2001), arxiv:hep-ph/0110121; JHEP **0209**, 063 (2002), arxiv:hep-ph/0208159;
- L. Hofer, U. Nierste and D. Scherer, JHEP **0910** (2009) 081, arxiv:0907.5408 [hep-ph].
- [66] S. Baek and P. Ko, Phys. Rev. Lett. **83**, 488 (1999), arxiv:hep-ph/9812229.
- [67] V.M. Abazov *et al.* [DØ collaboration], Conference Note 5906, <http://www-d0.fnal.gov/Run2Physics/WWW/results/prelim/B/B56/B56.pdf>;
- T. Aaltonen *et al.* [CDF collaboration], Phys. Rev. Lett. **100**, 101802 (2008), arxiv:0712.1708 [hep/ex];
- T. Aaltonen *et al.* [CDF collaboration], Public Note 9892, [http://www-cdf.fnal.gov/physics/new/bottom/090813.blessed-Bsd2mumu//bsmumupub3.7fb\\_v01.pdf](http://www-cdf.fnal.gov/physics/new/bottom/090813.blessed-Bsd2mumu//bsmumupub3.7fb_v01.pdf).
- [68] The CKMfitter Group (A. Höcker *et al.*), Eur. Phys. J. **C**, 21 (225)2001, arxiv:hep-ph/0104062.
- [69] V. Lubicz and C. Tarantino, Nuovo Cim. **123B** (2008) 674, arxiv:0807.4605 [hep-lat].
- [70] J. Laiho, E. Lunghi and R. S. Van de Water, Phys. Rev. D **81**, 034503 (2010), arxiv:0910.2928 [hep-ph]; J. Laiho, talk given at the Flavour Physics and CP Violation Conference, May 25-29, 2010 (Torino - Italy); E. Lunghi, talk given at the Flavour Physics and CP Violation Conference, May 25-29, 2010 (Torino - Italy).
- [71] A. Ali Khan *et al.* [CP-PACS Collaboration], heavy quarks,” Phys. Rev. D **64**, 054504 (2001), arxiv:hep-lat/0103020.
- [72] C. Bernard *et al.* [MILC Collaboration], Phys. Rev. D **66**, 094501 (2002), arxiv:hep-lat/0206016.

- 
- [73] S. Aoki et al. [JLQCD Collaboration], Phys. Rev. Lett. **91**, 212001 (2003), arxiv:hep-ph/0307039.
- [74] M. Wingate, C. T. H. Davies, A. Gray, G. P. Lepage and J. Shigemitsu, Phys. Rev. Lett. **92**, 162001 (2004), arxiv:hep-ph/0311130.
- [75] C. Bernard et al. [Fermilab Lattice, MILC and HPQCD Collaborations], PoS LAT2008 , 278 (2008), arxiv:0904.1895 [hep-lat].
- [76] E. Gamiz, C. T. H. Davies, G. P. Lepage, J. Shigemitsu and M. Wingate [HPQCD Collaboration], Phys. Rev. D **80** (2009) 014503, arxiv:0902.1815 [hep-lat].
- [77] M. Jamin and B. O. Lange, Phys. Rev. D **65**, 056005 (2002), arxiv:hep-ph/0108135.
- [78] C. Bernard *et al.*, PoS **LATTICE2008** (2008) 278, arxiv:0904.1895 [hep-lat].
- [79] E. Dalgic et al., Phys. Rev. D **76**, 011501 (2007), arxiv:hep-lat/0610104.
- [80] D. J. Antonio et al. [RBC Collaboration and UKQCD Collaboration], Phys. Rev. Lett. **100**, 032001 (2008), arxiv:hep-ph/0702042.
- [81] C. Aubin, J. Laiho and R. S. Van de Water, Phys. Rev. D **81**, 014507 (2010), arxiv:0905.3947[hep-lat].
- [82] S. Aoki et al. [JLQCD Collaboration], Phys. Rev. D **77**, 094503 (2008), arxiv:0801.4186[hep-lat].
- [83] E. Gamiz, S. Collins, C. T. H. Davies, G. P. Lepage, J. Shigemitsu and M. Wingate [HPQCD Collaboration and UKQCD Collaboration], Phys. Rev. D **73**, 114502 (2006), arxiv:hep-lat/0603023.
- [84] C. Albertus et al. [RBC and UKQCD Collaborations], PoS LAT2007 , 376 (2007).
- [85] E. Blucher *et al.*, in: Proceedings of the CKM 2005 Workshop (WG1), UC San Diego, 15-18 March 2005, arxiv:hep-ph/0512039.
- [86] C. Amsler *et al.* [Particle Data Group], Physics Letters B667, 1 (2008) Phys. Lett. B **667**, 1 (2008) and 2009 partial update for the 2010 edition Cut-off date for this update was January 15, 2009.
- [87] J. C. Hardy and I. S. Towner, Phys. Rev. D **79** (2009) 055502 arxiv:0812.1202 [nucl-ex].
- [88] M. Antonelli *et al.* [FlaviaNet Workshop on Kaon Decays Collaboration], arxiv:0801.1817 [hep-ph].
- [89] P. A. Boyle *et al.* (RBC and UKQCD collaborations), arxiv:hep-lat/0702026; P. A. Boyle *et al.*, Phys. Rev. Lett. **100**, 141601 (2008), arxiv:0710.5136 [hep-lat].

- 
- [90] E. Barberio *et al.* [Heavy Flavour Averaging Group], arxiv:0808.1297 [hep-ex] and online update at <http://www.slac.stanford.edu/xorg/hfag>, updated PDG 2010, respectively, End of Year 2009.
- [91] C. Bernard *et al.*, Phys. Rev. D **78**, 094505 (2008), [Phys. Rev. D **79**, 014506 (2009)], arxiv:0808.2519 [hep-lat].
- [92] A. Sirlin, Nucl. Phys. B **196** (1982) 83.
- [93] M. Okamoto *et al.*, Nucl. Phys. Proc. Suppl. **140**, 461 (2005); arxiv:hep-lat/0409116.
- [94] E. Gulez *et al.* [HPQCD collaboration], Phys. Rev. D **73**, 074502 (2006), arxiv:hep-lat/0601021, [Erratum-ibid. **D**, 75 (119906)2007].
- [95] P. Ball and R. Zwicky, Phys. Rev. D **71**, 014015 (2005), arxiv:hep-ph/0406232.
- [96] B. O. Lange, M. Neubert and G. Paz, Phys. Rev. D **72**, 073006 (2005), arxiv:hep-ph/0504071.
- [97] M. Neubert, private communications
- [98] K. Ikado *et al.* (Belle collaboration), Phys. Rev. Lett. **97**, 251802 (2006), arxiv:hep-ex/0604018.
- [99] I. Adachi *et al.* (Belle collaboration), arxiv:0809.3834 [hep-ex].
- [100] B. Aubert *et al.* (BABAR collaboration), Phys. Rev. D **77**, 011107(R) (2008), arxiv:0708.2260 [hep-ex].
- [101] B. Aubert *et al.* (BABAR collaboration), Phys. Rev. D **81**, 051101 (2010), arxiv:0809.4027 [hep-ex].
- [102] J. Charles, Phys. Rev. D **59** (1999) 054007 [arXiv:hep-ph/9806468].
- [103] M. Gronau and D. London, Phys. Lett. B **253** (1991) 483; M. Gronau and D. Wyler, Phys. Lett. B **265** (1991) 172.
- [104] D. Atwood, I. Dunietz and A. Soni, Phys. Rev. Lett. **78** (1997) 3257, arxiv:hep-ph/9612433.
- [105] A. Giri, Y. Grossman, A. Soffer and J. Zupan, Phys. Rev. D **68**, 054018 (2003), arxiv:hep-ph/0303187.
- [106] K. Trabelsi, “Measurement(s) of  $\gamma/\phi_3$ ”, Talk presented at the the CKM08 workshop, 9-13 September 2008, Roma, Italy.
- [107] Tevatron Electroweak Working Group, 2008.
- [108] U. Langenfeld, S. O. Moch and P. Uwer, arxiv:1006.0097 [hep-ph].

- [109] J. Abdallah *et al.* [DELPHI collaboration], Eur. Phys. J. C **28**, 155 (2003), arxiv:hep-ex/0303032;  
B. Aubert *et al.* [BABAR collaboration], Phys. Rev. D **70**, 012007 (2004), arxiv:hep-ex/0403002.
- [110] B. Aubert *et al.* [BABAR collaboration], Phys. Rev. Lett. **92**, 181801 (2004), arxiv:hep-ex/0311037.
- [111] CLEO collaboration, Phys. Rev. Lett. **71**, 1680 (1993),  
Phys. Lett. B **490**, 36 (2000), arxiv:hep-ex/0005013;  
Phys. Rev. Lett. **86**, 5000 (2001), arxiv:hep-ex/0101006;  
B. Aubert *et al.* [BABAR collaboration], Phys. Rev. Lett. **96**, 251802 (2006), arxiv:hep-ex/0603053; contributed to 33rd International Conference on High Energy Physics (ICHEP 06), Moscow, Russia, 26 Jul - 2 Aug 2006, arxiv:hep-ex/0607091;  
E. Nakano *et al.* [Belle collaboration], Phys. Rev. D **73**, 112002 (2006), arxiv:hep-ex/0505017.
- [112] H. Boos, T. Mannel and J. Reuter, Phys. Rev. D **70** (2004) 036006, arxiv:hep-ph/0403085.
- [113] Y. Grossman, A. Kagan and Z. Ligeti, Phys. Lett. B **538**, 327 (2002), arxiv:hep-ph/0204212.
- [114] H.-n. Li and S. Mishima, JHEP **0703**, 009 (2007), arxiv:hep-ph/0610120.
- [115] M. Ciuchini, M. Pierini and L. Silvestrini, Phys. Rev. Lett. **95**, 221804 (2005), arxiv:hep-ph/0507290.
- [116] S. Faller, M. Jung, R. Fleischer and T. Mannel, Phys. Rev. D **79** (2009) 014030, arxiv:0809.0842 [hep-ph].
- [117] H. Lacker (for the BABAR and Belle collaboration), Nucl. Phys. Proc. Suppl. **170**, 14 (2007), arxiv:hep-ex/0702038.
- [118] M. Gronau and D. London, Phys. Rev. Lett. **65**, 3381 (1990).
- [119] J. Charles *et al.*, arxiv:hep-ph/0607246.
- [120] A. E. Snyder and H. R. Quinn, Phys. Rev. D **48**, 2139 (1993).
- [121] B. Aubert *et al.* (BABAR collaboration) Phys. Rev. Lett. **102**, 141802 (2009), arxiv:0901.3522.
- [122] E. Barberio *et al.* [Heavy Flavour Averaging Group], arxiv:0808.1297 [hep-ex] and online update at <http://www.slac.stanford.edu/xorg/hfag>, updated FPCP09 2009, respectively, Summer 2009.

- [123] E. Barberio *et al.* [Heavy Flavour Averaging Group], arxiv:0808.1297 [hep-ex] and online update at <http://www.slac.stanford.edu/xorg/hfag>, updated Summer 2008.
- [124] Public Note 9015 (2007).
- [125] V. Abazov *et al.* [DØ collaboration], submitted to Phys. Rev. Letters, Fermilab-Pub-09-140-E, arxiv:0904.3907 [hep-ex].
- [126] D. Becirevic, V. Gimenez, G. Martinelli, M. Papinutto and J. Reyes, JHEP **0204**, 025 (2002), arxiv:hep-lat/0110091.
- [127] V. M. Abazov *et al.* ([DØ collaboration]), Phys. Rev. D **74**, 092001 (2006), arxiv:hep-ex/0609014.
- [128] V. M. Abazov *et al.* ([DØ collaboration]), Phys. Rev. D **76**, 057101 (2007), arxiv:hep-ex/0702030.
- [129] E. Barberio *et al.* [Heavy Flavour Averaging Group], arxiv:0808.1297 [hep-ex] and online update at <http://www.slac.stanford.edu/xorg/hfag>, updated PDG 2009.
- [130] V. M. Abazov *et al.* [DØ collaboration], Phys. Rev. Lett. **98**, 121801 (2007), arxiv:hep-ex/0701012.
- [131] T. Aaltonen *et al.* [CDF collaboration], Phys. Rev. Lett. **100**, 121803 (2008), arxiv:0712.2348 [hep-ex].
- [132] M. Bona *et al.* [UTfit Collaboration], PMC Phys. **A3**, 6 (2009), arxiv:0803.0659 [hep-ph].
- [133] J. Charles (on behalf of the CKMfitter group), Nucl. Phys. B (Proc. Suppl.) **185** (2008) 17.
- [134] G. Punzi, PoS E **PS-HEP2009** (2009) 022, arxiv:1001.4886 [hep-ex]. See also the combination page at [http://tevbwg.fnal.gov/results/Summer2009\\_betas/](http://tevbwg.fnal.gov/results/Summer2009_betas/).
- [135] S. Eidelman *et al.* [Particle Data Group], Phys. Lett. B **592**, 1 (2004).
- [136] O. Buchmüller and H. Flächer, Phys. Rev. D **73**, 073008 (2006), arxiv:hep-ph/0507253; Lepton Photon 2007 update at [http://www.slac.stanford.edu/xorg/hfag/semi/LP07/gbl\\$\\\_fits/kinetic/lp07-update.pdf](http://www.slac.stanford.edu/xorg/hfag/semi/LP07/gbl$\_fits/kinetic/lp07-update.pdf).
- [137] J. H. Kühn and M. Steinhauser, Nucl. Phys. B **619**, 588 (2001) [Erratum-ibid. B **640**, 415 (2002)], arxiv:hep-ph/0109084.
- [138] A. H. Hoang and M. Jamin, Phys. Lett. B **594**, 127 (2004), arxiv:hep-ph/0403083.
- [139] J. H. Kuhn, M. Steinhauser and C. Sturm, Nucl. Phys. B **778**, 192 (2007); arxiv:hep-ph/0702103.

- 
- [140] M. Steinhauser, arxiv:0809.1925 [hep-ph].
- [141] M. Bona *et al.* (UTfit collaboration), Phys. Rev. Lett. **97**, 151803 (2006), arxiv:hep-ph/0605213.
- [142] M. Bona *et al.* (UTfit collaboration), JHEP **0803**, 049 (2008), arxiv:0707.0636 [hep-ph].
- [143] M. Bona *et al.* (UTfit collaboration), JHEP 0603, 080 (2006).
- [144] A. J. Buras and M. Jamin, JHEP **0401**, 048 (2004) arxiv:hep-ph/0306217.
- [145] D. Guadagnoli, private communication.
- [146] V. Cirigliano, J. F. Donoghue, E. Golowich and K. Maltman, Phys. Lett. B **555** (2003) 71, arxiv:hep-ph/0211420.
- [147] M. Battaglia *et al.*, CERN-2003-002, Cern Yellow Report, Based on the Workshop on CKM Unitarity Triangle (CERN 2002-2003), Geneva, Switzerland, 13-16 Feb 2002, arxiv:hep-ph/0304132.